Applied Catalysis B: Environmental 340 (2024) 123241

Contents lists available at ScienceDirect

Applied Catalysis B: Environmental

journal homepage: www.elsevier.com/locate/apcatb

A review on exhaust gas after-treatment of lean-burn natural gas engines – From fundamentals to application

Patrick Lott [a,*], Maria Casapu [a], Jan-Dierk Grunwaldt [a,b], Olaf Deutschmann [a,b]

[a] Institute for Chemical Technology and Polymer Chemistry (ITCP), Karlsruhe Institute of Technology (KIT), Engesserstr. 20, 76131 Karlsruhe, Germany
[b] Institute of Catalysis Research and Technology (IKFT), Karlsruhe Institute of Technology (KIT), Hermann-von-Helmholtz-Platz 1, 76344 Eggenstein-Leopoldshafen, Germany

ARTICLE INFO

Keywords:
Emission control
Formaldehyde oxidation
Methane oxidation
Natural gas engine
Selective catalytic reduction

ABSTRACT

Modern lean-operated internal combustion engines running on natural gas, biogas or methane produced from wind or solar energy are highly fuel-efficient and can greatly contribute to securing energy supply, e.g. by mitigating fluctuations in the power grid. Although only comparably low emission levels form during combustion, a highly optimized emission control system is required that converts pollutants over a wide range of operation conditions. In this context, this review article pinpoints the main challenges during methane and formaldehyde oxidation as well as selective catalytic reduction of nitric oxides. The impact of catalyst formulation and operation conditions on catalytic activity and selectivity as well as the combination of several technologies for emission abatement is critically discussed. Additionally, recent experimental and theory-based progress and developments are assessed, allowing coverage of all time and length scales relevant in emission control, i.e. ranging from mechanistic and fundamental insights including atomic-level phenomena to full-scale applications.

1. Introduction

Carbon-based fossil resources are the foundation of our modern society. Particularly the widespread use of liquid hydrocarbons as a fuel for combustion engines, both in the mobile sector and in stationary applications, results in the emission of enormous amounts of carbon dioxide (CO_2). Since the greenhouse gas CO_2 represents the primary reason for global warming, science, economy, and politics strive for developing measures and technologies that allow for a substantial reduction of greenhouse gas emissions. Ambitious aspirations such as Europe's and Germany's goal to achieve net-zero greenhouse gas emissions by 2050 and 2045, respectively, [1,2] are already vitalizing the technological competition for the most suitable approaches to redesign our worldwide energy system. Although electrification enjoys great popularity in this context, the transition towards a fully electrified energy system requires significant investments and – equally important – time for realization, particularly with regard to materials and infrastructure. Current state-of-the-art battery capacities are mostly insufficient for heavy-duty applications in both the on-road and off-road sector. At the same time, the electricity grids worldwide are not yet able to cope with the electrical load that accompanies electrification of all industry and energy sectors. Despite manifold political efforts, the share of well-established renewable energy sources grows too slow and retards the necessary energy transition. Hence, a diversified energy system with

Abbreviations: ASC, Ammonia slip catalyst; CNG, Compressed natural gas; DFT, Density functional theory; DOC, Diesel oxidation catalyst; DPF, Diesel particulate filter; DRIFTS, Diffuse reflectance infrared Fourier-transform spectroscopy; EDXS, Energy dispersive X-ray spectroscopy; EELS, Electron energy-loss spectroscopy; EGR, Exhaust gas recirculation; EPMA, Electron probe microanalysis; EU, European Union; HCs, Hydrocarbons; IR, Infrared; LEED, Low-energy electron diffraction; MARI, Most abundant reaction intermediate; ME-XAS, Modulation excitation X-ray absorption spectroscopy; NMHCs, Non-methane hydrocarbons; PM, Particulate matter; PtG, Power-to-gas; ReaxFF, Reactive force-field; SCR, Selective catalytic reduction; SNMSI, Strong noble metal support interactions; SRP, Short reducing pulses; TEM, Transmission electron microscopy; TGA, Thermogravimetric analysis; THC, Total hydrocarbons; TPD, Temperature-programmed desorption; TP-NAP-XPS, Temperature-programmed near-ambient pressure X-ray photoelectron spectroscopy; TPR, Temperature-programmed reduction; TPRS, Temperature-programmed reaction spectroscopy; TWC, Three-way catalyst; VOCs, Volatile organic compounds; WDXS, Wavelength-dispersive X-ray spectroscopy; WHTC, World harmonized transient cycle; XANES, X-ray near-edge structure; XAS, X-ray absorption spectroscopy; XPS, X-ray photoelectron spectroscopy; XRD, X-ray diffraction.

* Corresponding author.
E-mail address: patrick.lott@kit.edu (P. Lott).

https://doi.org/10.1016/j.apcatb.2023.123241
Received 25 May 2023; Received in revised form 24 August 2023; Accepted 28 August 2023
Available online 30 August 2023

complementary technologies is expected for the next decades, i.e. a growing electrification of the light-duty sector, whereas the heavy-duty and marine sector still rely on hydrocarbon-based fuels that exhibit a high energy density and advantageous emission characteristics.

In this context, transition technologies such as natural gas engines, whose widespread application is influenced by many factors that are illustrated in schematic Fig. 1, might offer an immediate opportunity to mitigate the climate change. Due to the large natural gas resources that are potentially still available worldwide, gas engines are nowadays widely used in mobile applications like marine ships and heavy-duty vehicles or in combined heat and power plants for energy production, since they are not only highly efficient but can also easily be ramped up and down, hereby mitigating fluctuations in the energy grid whenever renewable sources lack temporarily. Hence, it is generally assumed that the relevance of gas engines will remain high in the foreseeable future especially in the context of power generation. Since natural gas consists mostly of methane (CH_4) that exhibits the highest hydrogen-to-carbon ratio of all hydrocarbons, CO_2 emissions can be decreased by up to 35% when replacing conventional diesel fuel by natural gas [3]. Particularly lean-burn gas engines have a high engine efficiency and emit only comparably low levels of unburnt hydrocarbons (HCs), nitrogen oxides (NO_x), toxic carbon monoxide (CO), and particulate matter (PM). All these aspects make gas engines highly attractive for usage in mobile and stationary applications alike. Moreover, future prospects are good as well. A continuous replacement of the currently mostly fossil natural gas by sustainable methane obtained from anaerobic digestion of organic matter ("biogas") [4–7] or by power-to-gas (PtG) processes [8–12] will further benefit the overall carbon balance and may provide a reliable and entirely carbon-neutral methane source in the future. In a diversified future energy system such sustainably produced bio-methane can play a key role, in particular under consideration of the great potential of using methane as a chemical energy carrier that can exploit the enormous energy storage potential of the existing gas grid and infrastructure. Moreover, the combination of PtG processes and combined heat and power plants can be an invaluable cornerstone for a stable energy system, since methane can be produced and stored during periods of excess energy from renewable sources like wind and solar, whereas methane can be used for energy and heat generation if other energy sources are scarce.[8,12,13].

Although gas engines have better emission characteristics compared to gasoline or diesel engines, meeting the upcoming ultra-low emission standards in the near future requires highly efficient and durable catalytic converters, which are a prerequisite for the widespread usage of gas engines [14]. The more and more stringent legislation initiated major research efforts in academia and industry, both aiming at finding holistic solutions that ultimately allow for near-zero pollutant emissions. For instance, although in many countries specific methane emission limits have not been formulated in the past, tightening legislation can be expected for both mobile and non-road applications in the near future, which is mainly motivated by the more than 20 times stronger greenhouse potential of CH_4 compared to CO_2 (100-year metrics) [15]. While a single oxidation catalyst that converts unburnt hydrocarbons was often sufficient for meeting past emission limits, tightening regulations also call for dedicated NO_x control measures, e.g. by selective catalytic reduction (SCR). Such additional measures increase the complexity of the exhaust gas after-treatment system and do not only raise the probability of secondary emissions formed in the exhaust tailpipe, but also increase the costs. Hence, future exhaust gas after-treatment systems require a sophisticated overall system design that ensures a harmonious interaction of different technologies at a multitude of engine operation points and over a wide range of conditions, and at the same time accounts for economic considerations, i.e. cost-efficiency [16,17].

In addition to the fact that the global efforts for environmental protection made emission control a vibrant area of heterogeneous catalysis research for decades, the ongoing methodological progress and tightening environmental legislation during recent years resulted in a wide variety of highly relevant scientific studies. This review summarizes the different aspects important for the catalytic exhaust gas after-treatment of lean-operated gas engines, namely methane oxidation, abatement of formaldehyde emissions, and NO_x reduction as well as technical aspects such as pre-turbine applications. In this context, we highlight current challenges and present concepts for tackling these hurdles. By starting from fundamentals and outlining their significance for full-size applications, both synergies and limitations of the different technologies are identified. Herein, the entire range of time and length scales that are relevant in emission control are covered, for instance mechanistic considerations on an atomic level as well as heat and mass transport phenomena in technical converters. In addition to a comprehensive phenomenological description, we also present current progress and developments regarding a wide variety of theoretical and experimental techniques that are suitable for profound investigations for all kinds of phenomena in heterogenous catalysis in general and in the field of emission control in particular. This holistic approach serves the community twofold. First, our review aims at providing guidance on the currently applied after-treatment concepts for lean-burn natural gas engines and second, it intends to stimulate future research in the field that allows further improvement of existing catalyst technologies.

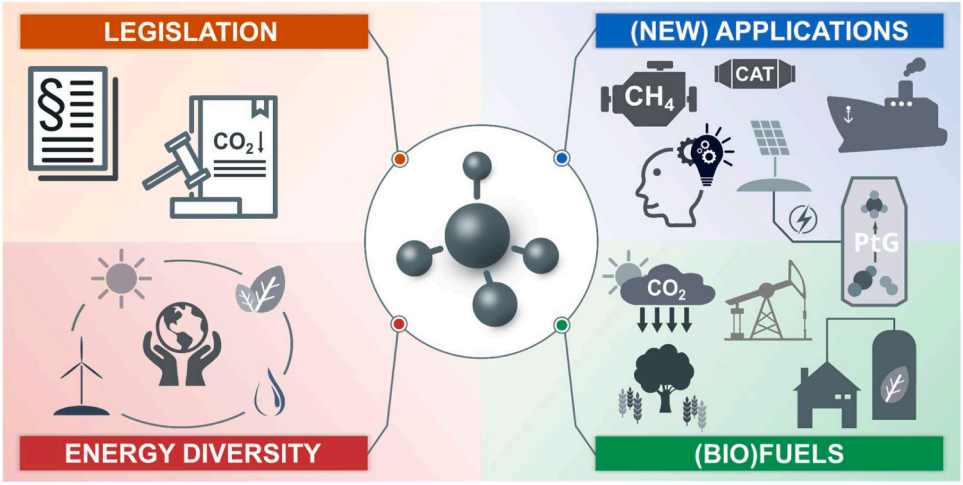

Fig. 1. Factors influencing the widespread application of methane as fuel.

2. Emissions of natural gas engines and emission control concepts

The operational point of natural gas engines, which is typically either stoichiometric or lean with respect to the air-to-fuel ratio [18,19], influences both the combustion process itself and the engine-out raw emissions. The possibility of using a three-way catalyst (TWC) for exhaust gas after-treatment, which is well-established for analogously operated gasoline engines [20,21], represents the main advantage of stoichiometric operation. The TWC reliably converts non-methane hydrocarbons (NMHCs), CO, and NO_x emissions evolving from the engine in considerable amounts [22–24] and keeps the exhaust gas after-treatment system compact. Such a configuration is of particular relevance for mobile applications that exhibit only limited dimensions. However, the efficiency of current TWCs is limited with regard to the oxidation of methane, as the symmetric and rather stable C–H bonds (approximately 440 kJ mol^{-1}) [25–27] make the CH_4 molecule comparably inert and difficult to activate, particularly in the low-temperature regime [28]. Moreover, commonly applied measures like thermal management by means of exhaust gas recirculation (EGR) decrease the temperature during combustion and consequently also the exhaust gas temperature [22,28]. While this temperature diminishment results in significantly reduced NO_x formation rates in the combustion chamber and lowers the thermal stress, low temperatures further impede methane conversion over a TWC.

Lean operation, on the other hand, reduces the heat loss, decreases fuel consumption, and maximizes engine efficiency, which results in significantly lower CO_2 emissions. As large-scale applications benefit notably from these characteristics, applications such as combined heat and power plants for energy production are commonly operated with lean-burn gas engines. Moreover, lean conditions also significantly reduce NO_x raw emissions compared to stoichiometric operation. However, an additional catalytic component is still required in this case for NO_x removal.

Lean-burn gas engines typically exhibit an exhaust gas temperature of less than 500–550 °C and an exhaust gas composition that is similar to the values summarized in Table 1 [29–31]. Note, that the values given in Table 1 represent an average gas composition, which however can strongly vary depending on the specific engine and its operation mode, i.e. during transient operation in mobile applications, versus a more constant exhaust gas composition for stationary applications.

Hydrocarbon (HC) emissions originate from incomplete combustion in the engine combustion chamber, with unburnt methane as main challenge. Additionally, partial combustion in cold zones of the combustion chamber can result in the formation of formaldehyde (HCHO) [32,33]. Due to its neurotoxicity, hematotoxicity, reproductive toxicity, and genotoxicity, formaldehyde does not only cause acute and chronic health effects such as irritation and poisoning [34], but was also classified as potentially carcinogenic substance by the European Union (EU) [35]. Consequently, the expected ultra-low emission standards in the near future necessitate particular attention in the context of emission control [36]. Although engine operation measures like variations of load, swirl, compression ratio, air-to-fuel ratio, top land crevice or ignition timing offer potential for minimizing formaldehyde formation rates, this often happens at the expense of other parameters like thermal efficiency or emission of other pollutants such as NO_x [33,37,38]. To some extent, gas engines also emit particulate matter that either emerges from unburnt hydrocarbons or from the direct contact between combustion flame and lube oil in the combustion chamber. The latter causes a partial combustion of oil that leads to emission of hydrocarbons and oil ash, which contains elements like calcium, magnesium, zinc, phosphorous or sulfur [39–41]. Overall, particulate matter emissions are similar to those of diesel engines equipped with a diesel particulate filter (DPF) and are therefore very low [42–45]. Furthermore, the relatively low combustion temperatures during lean engine operation cause only moderate NO_x levels [46] that are typically slightly lower than for diesel engines [42], as NO_x is mainly formed via the high-temperature reaction between oxygen and nitrogen according to the Zeldovich mechanism [47]. This advantageous emission performance allowed past emission limits to be met with a single oxidation catalyst that converted CO and hydrocarbons.

With respect to the catalytic after-treatment system, the removal of hydrocarbons and CO usually requires oxidation catalysts that contain expensive noble metals like platinum (Pt), palladium (Pd), and rhodium (Rh), which are typically supported on alumina (Al_2O_3) or ceria-zirconia mixed oxides (CeO_2-ZrO_2). While platinum exhibits a fairly high activity for methane conversion under stoichiometric conditions, palladium is clearly more active in a lean exhaust stream [29,48,49]. Identification and preservation of the active noble metal species, inhibition of the catalyst by typical exhaust components such as water, and catalyst poisoning by sulfur compounds that are present in the exhaust have been subject to numerous scientific studies in the past, as a comprehensive knowledge on all of these aspects is vital for a long-term operation of the catalyst. Additionally, new exhaust system concepts were introduced to enhance the performance of methane oxidation catalysts, as for instance their pre-turbine location where the exhaust stream exhibits higher temperatures than in the downstream tailpipe and where higher pressure can be utilized for pollutant reduction [50–52]. Moreover, Pt-based catalysts show a superior activity for converting formaldehyde, which is the most critical pollutant with regard to health considerations, hence highly optimized catalytic converters are necessary to comply with the diffusion-limitation of the HCHO oxidation reaction [53].

The removal of NO_x emissions from lean-burn engines is generally achieved with V-W-Ti- or Fe/Cu-zeolite-based catalysts via selective catalytic reduction with ammonia (NH_3) as reductant. While in stationary applications the direct usage of hazardous NH_3 is common, safety considerations impede the usage of pure NH_3 in mobile applications. Instead, NH_3 is generated from an aqueous urea solution that releases NH_3 during a two-step thermal and catalytic decomposition. This process requires a careful tailpipe and operation design that is capable of coping with the highly transient conditions in the exhaust. Particularly the formation of deposits from urea derivatives and decomposition products needs to be avoided, as this does not only lower the NH_3 selectivity and its homogeneous distribution, but can also cause a clogging of the tailpipe [54–60]. State-of-the-art SCR catalysts can facilitate the decomposition of urea and its by-products [61–66], and advanced dosing and mixing units can reduce urea deposit formation by ensuring a homogeneous distribution of the urea-water solution and its mixing with the gas phase [67,68]. Despite the availability of such well-established technologies, their implementation into after-treatment systems for gas engines entails new challenges due to the differences in gas atmosphere compared to the diesel engine exhaust for which the SCR has originally been developed and tuned. Also in this case, both an in-depth understanding and a further optimization are mandatory. Herein, advanced characterization methods and multiscale modeling represent powerful tools for the emission control research community

Table 1
Typical exhaust gas composition of lean-burn natural gas engines (balanced by N_2).

Species	O_2	CO_2	H_2O	CH_4	HCHO	CO	NMHC	NO	NO_2	SO_2
	[vol.-%]			[ppm]						
Conc.	10	6	12	500–3500	50–120	500	250	120	30	< 5

[69].

In the following sections we aim at addressing the different catalyst technologies applied for the exhaust gas after-treatment of natural gas engines, in particular pinpointing recent advances in their fundamental understanding and in microkinetic and reactor modeling. Furthermore, the systems used as well as advanced operation procedures are discussed. Finally, we illustrate the benefits of in situ and *operando* characterization for deriving robust structure-activity relationships, which can be directly used for modeling and rational catalyst design.

3. Methane oxidation over palladium-based catalysts

The catalytic conversion of methane slippage is considered as the greatest challenge in emission reduction from natural gas engine exhausts. With a C-H bond dissociation enthalpy of approximately 440 kJ mol^{-1} [25–27], the methane molecule with its tetrahedral symmetry is the most stable alkane and therefore most difficult to activate at low temperatures, even over noble metal-based heterogeneous catalysts [70,71]. A wide variety of catalyst formulations has been evaluated in the past, but despite promising advances in cost-efficient non-precious metal-based catalysts were reported, e.g. spinel and perovskite structures or mixed oxides [72–74], these materials are often combined with noble metal species [75–77]. It is generally agreed that the low-temperature activity of palladium-based catalysts for the total oxidation of methane under lean conditions outperforms that of any other material [29,48,78–83]. Therefore, this section lays focus on palladium-based catalysts. Under oxygen-rich conditions, mainly the total oxidation (Eq. 1) takes place and undesired side reactions are negligible. On the contrary, stoichiometric and under-stoichiometric air-to-fuel ratios due to varying engine operation parameters or major changes of the catalyst morphology, e.g. caused by sintering as a consequence of catalyst degradation during long-term application, can lead to an increased formation of by-products like carbon monoxide (CO) or hydrogen (H_2) via partial oxidation, steam reforming or water gas shift reactions (Eqs. 2 – 5) [84–86].

$$CH_4 + 2\,O_2 \rightarrow CO_2 + 2\,H_2O \quad (1)$$

$$2\,CH_4 + O_2 \rightarrow 2\,CO + 4\,H_2 \quad (2)$$

$$CH_4 + H_2O \rightarrow CO + 3\,H_2 \quad (3)$$

$$2\,H_2 + O_2 \rightarrow 2\,H_2O \quad (4)$$

$$CO + H_2O \rightleftharpoons CO_2 + H_2 \quad (5)$$

Moreover, as emphasized in the scheme in Fig. 2, methane oxidation over palladium-based catalysts is a complex process involving several phenomena. The following subsections will pinpoint the present scientific questions and challenges illustrated in Fig. 2, namely the structure and nature of the catalytically most active structures including the oxidation state and the particle morphology, the inhibition of the oxidation reaction by water, and catalyst deactivation due to sulfur poisoning. In addition to an overview on fundamental phenomena, we also point out their implications for modern catalytic converters and operation procedures, and the challenges that come with real-world applications, which substantially raises the complexity as various heterogeneous processes take place simultaneously and thereby influence each other. These different heterogeneous processes can only be understood and fully exploited in real-world applications when applying state-of-the-art and emerging experimental techniques that are capable of resolving spatial and temporal temperature and concentration profiles in the gas phase, the interphase, and inside the bulk material along with microkinetic models that comprehensively describe the gas-surface reactions [69].

3.1. The active structure or the fundamental Pd/PdO dilemma

Although palladium catalysts have been subject to numerous scientific studies for decades, there has been a lively scientific debate on the nature of the most active species: metallic palladium (Pd) or palladium oxide (PdO). The debate on the active species is of high significance, as variations of the electronic state of Pd go along with changes of the reaction mechanism. In this context, three different mechanisms of CH_4 activation and conversion have been proposed. Note that since the most important intermediate species can vary depending on the catalyst formulation or the operation conditions, the set of reaction equations and reaction schemes presented in the following is not generally valid but rather serves as one representative description for each mechanism. In addition, only the forward reactions that result in the decomposition of CH_4 are given in Eqs. 6 – 27, however, under some reaction conditions these can also proceed in reverse direction.

First, methane conversion was suggested to take place via an Eley-Rideal mechanism, with the dissociative adsorption of oxygen on free surface sites (denoted as * in the reaction equations below) of the noble metal (Eq. 6), the direct reaction of methane from the gas phase with preadsorbed oxygen species (Eq. 7), and finally the desorption of the reaction products (Eqs. 13, 15) as key steps. Studies that specifically evaluate the suitability of the Eley-Rideal mechanism for describing CH_4 oxidation over Pd/PdO are rare [87–91]. In fact, to the best of our

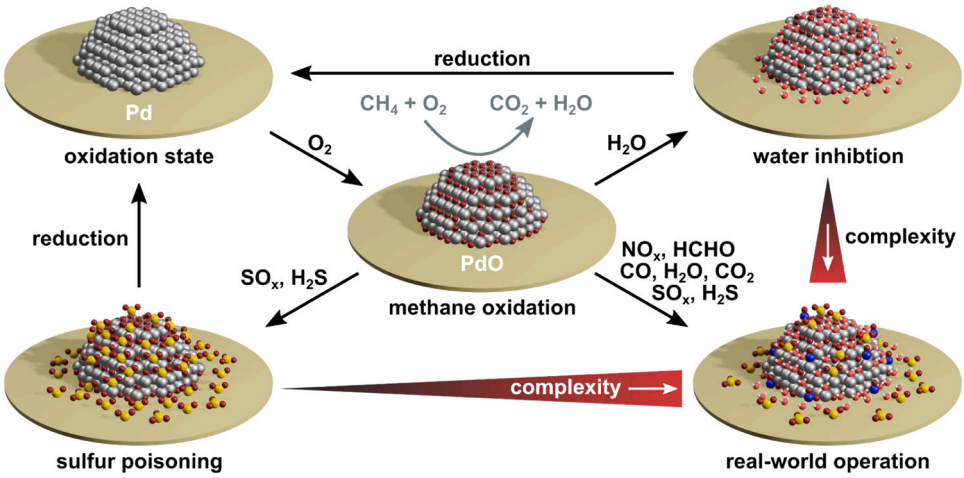

Fig. 2. Factors influencing the activity, stability, deactivation, and reactivation of palladium-based methane oxidation catalysts. The illustration emphasizes how the complexity increases by transformation of the defined PdO system (in the middle) by reduction, poisoning by sulfur species (here simplified by SO_x and H_2S), and inhibition by water.

knowledge, only two studies claim the Eley-Rideal mechanism as the most accurate description of CH_4 oxidation over palladium-based samples [87,88].

$$O_2 + 2\,* \rightarrow 2\,O* \quad (6)$$

$$CH_4 + O* + * \rightarrow CH_3* + OH* \quad (7)$$

$$CH_3* + O* \rightarrow CH_2OH* + * \quad (8)$$

$$CH_2OH* + O* \rightarrow CH_2O* + OH* \quad (9)$$

$$CH_2O* + O* \rightarrow CHO* + OH* \quad (10)$$

$$CHO* + O* \rightarrow CO* + OH* \quad (11)$$

$$CO* + O* \rightarrow CO_2* + * \quad (12)$$

$$CO_2* \rightarrow CO_2 + * \quad (13)$$

$$OH* + OH* \rightarrow H_2O* + O* \quad (14)$$

$$H_2O* \rightarrow H_2O + * \quad (15)$$

Second, several studies assume that under specific operation conditions Pd/PdO-catalyzed CH_4 oxidation proceeds via a Langmuir-Hinshelwood mechanism [90,92,93], during which at first both methane and oxygen adsorb on the catalyst surface (Eqs. 16, 17) and then react with each other (Eq. 18) via several intermediate species (Eqs. 19 – 23) to finally form CO_2 (Eq. 24) and H_2O (Eq. 26).

$$CH_4 + * \rightarrow CH_4* \quad (16)$$

$$O_2 + 2\,* \rightarrow 2\,O* \quad (17)$$

$$CH_4* + O* \rightarrow CH_3* + OH* \quad (18)$$

$$CH_3* + O* \rightarrow CH_2OH* + * \quad (19)$$

$$CH_2OH* + O* \rightarrow CH_2O* + OH* \quad (20)$$

$$CH_2O* + O* \rightarrow CHO* + OH* \quad (21)$$

$$CHO* + * \rightarrow C* + OH* \quad (22)$$

$$C* + O* \rightarrow CO* + * \quad (23)$$

$$CO* + O* \rightarrow CO_2* + * \quad (24)$$

$$CO_2* \rightarrow CO_2 + * \quad (25)$$

$$OH* + OH* \rightarrow H_2O* + O* \quad (26)$$

$$H_2O* \rightarrow H_2O + * \quad (27)$$

Third, the total oxidation of methane was suggested to proceed via a Mars-van-Krevelen mechanism [94], which in addition to experimental evidence [95–97] was proposed based on kinetic modeling that typically results in very good accordance with experimental activity data under the assumption of a redox-cycle [89,91,98,99]. Herein, CH_4 is adsorbed on the PdO surface and then reacts with lattice oxygen from PdO via varying intermediate species to yield CO_2 and H_2O. In a next step, oxygen from the gas phase recovers the lattice oxygen vacancies. Fig. 3 depicts a mean-field extended microkinetic model [99] developed based on first-principles density functional theory (DFT) derived kinetic data [100] that describes CH_4 oxidation over a PdO(101) surface fairly well and that considers the dissociative CH_4 adsorption over coordinatively unsaturated Pd-O site-pairs as the rate controlling step.

The mechanism of methane oxidation over palladium was suggested to be temperature-dependent and sensitive to the Pd oxidation state [101]. Since the exposure of supported palladium catalysts to an oxygen-rich gas mixture at moderate temperature typically results in a fully oxidized catalyst sample with quasi-exclusive presence of PdO [102–104], the Mars-van-Krevelen mechanism is commonly considered as the most plausible one under lean conditions and at moderate

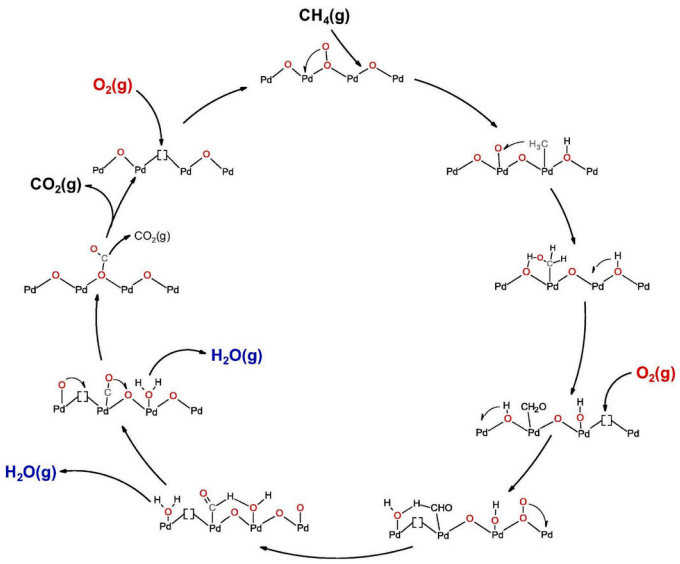

Fig. 3. Cyclic Mars-van-Krevelen redox mechanism for CH_4 oxidation over PdO (101) in a water-free gas feed between 200 °C and 400 °C. Reprinted with permission from ref. [99]. Copyright 2018 Elsevier.

temperatures. In contrast, at low oxygen concentrations in the gas mixture, the Langmuir-Hinshelwood mechanism may be more suitable for describing the oxidation of CH_4 over (oxygen-covered) metallic palladium surfaces at higher temperatures, as suggested by Ciuparu et al. [48]. This mechanism was assigned also if the PdO surface is covered by strong adsorbents such hydroxyl groups, as reported by Velin et al. [93]. At this point it is also worth noticing that the experimental setup itself may bias the kinetic data. Although recommendations on reliable kinetic measurements are beyond the scope of this review article, we would like to refer to the work by Groppi et al. [105–107] as an example for a suitable approach. In their work, the authors used a structured annular reactor that consists of an inner ceramic tube coated with a thin catalyst layer and an external quartz tube that is placed co-axially, which allows for isothermal operation and most importantly minimizes the impact of diffusion phenomena on the kinetic measurements. Since CH_4 conversion over Pd/PdO is typically a fast process, diffusion limitations caused by an inappropriate experimental setup can be detrimental for deriving kinetics. Thorough kinetic insights into CH_4 oxidation in the high-temperature regime gained by this approach, for instance, resulted in a Langmuir-Hinshelwood-like model that describes the experimental data fairly well [106].

To investigate the dynamic behavior of the Pd/PdO-system in detail, Farrauto et al. [108] investigated palladium oxide supported on alumina by means of thermogravimetric analysis (TGA). The authors report that a temperature increase to 750–850 °C initiates a transformation of palladium oxide into metallic palladium and propose that this process starts from small, highly dispersed particles and ultimately results in the formation of large metallic Pd particles. Upon cooling down, the reoxidation rate exhibits a pronounced hysteresis behavior and PdO formation takes place at approximately 600 °C. Based on the corresponding catalytic activity data for methane conversion, Farrauto et al. [108] considered metallic Pd rather inactive for methane oxidation, whereas PdO was suggested as active species. Subsequently, McCarty [109] attributed the hysteresis observed during methane conversion to the high activation energy for the reduction of oxygen chemisorbed on metallic Pd, and to a lower reoxidation rate of metallic palladium in comparison to PdO decomposition. Moreover, based on Raman spectroscopy and temperature-programmed experiments, Carstens et al. [110] suggested that the reducibility of PdO is strongly influenced by the particle morphology, which can be either crystalline or amorphous. These findings are in line with earlier observations suggesting that the

reconstruction of palladium oxide crystallites governs high catalytic activity [111]. Similarly, Datye et al. [112] reported the formation of an amorphous PdO top layer, which passivates the noble metal particle surface and inhibits bulk oxidation. Fundamental studies on the reoxidation of palladium particles during heating support this hypothesis: After chemisorption of oxygen on the palladium surface at ambient temperature, increasing temperatures lead to migration of oxygen into the metallic surface layers, which culminates in bulk oxidation above 350 °C [113,114]. In addition, Datye et al. [112] reported extensive surface roughening by bulk oxide formation, which may originate from the lower interfacial tension of PdO compared to metallic Pd that results in the generation of pits on the Pd/PdO crystallites to decrease the free energy of the system [115,116]. These findings supplement results by Ruckenstein and Chen [117], who reported changes in size and shape upon alternating heating of Pd crystallites in O_2 and H_2, and by Burch and Urbano [118], who attributed varying catalytic activity to different catalyst morphologies. DFT calculations explain these phenomena by a higher dissociation barrier for the $CH_4 \rightarrow CH_3 + H$ reaction over a flat palladium surface, whereas the energy for bond splitting is reduced over kinks and steps [119].

In order to directly probe the state of the noble metal during catalyst pretreatment and reaction, *operando* X-ray absorption spectroscopy (XAS) and X-ray diffraction (XRD) investigations were conducted by Grunwaldt et al. [102] for Pd/ZrO_2, which provided further insights into the pronounced changes of the structure of the noble metal particles and their oxidation state during the heating and cooling cycle. Apart from the clearly observable autoreduction of PdO above 850 °C and its reoxidation below 500 °C, these results point to an influence of the particle size, which along with changes of oxidation state and morphology causes the peculiar hysteresis during methane oxidation. Notably, the reduction causes sintering of the particles, however, reoxidation does not result in full redispersion of the PdO, which leads to deactivation [102,112,120]. In fact, the strong particle size dependency of methane oxidation over PdO, which is illustrated in Fig. 4, is now a well-known effect and the structural changes and their impact on the catalytic activity have recently been incorporated in an appropriate microkinetic model [99]. Several studies correlated an increasing particle size with increasing catalytic activity and attributed this behavior to the Pd-O bond strength, which diminishes for larger particles [96,121].

The role of the Pd-O bond strength is particularly relevant when assuming a Mars-van-Krevelen mechanism [94] for methane oxidation, since this is as described above a redox mechanism that involves oxygen from the PdO lattice for conversion of adsorbed methane molecules into CO_2 and H_2O [96,99,122–124]. Compared to larger particles, Castellazzi et al. [125] found a lower reducibility for small and highly dispersed PdO clusters supported on alumina. These findings suggest that a rational and accurate adjustment of the noble metal particle size can tune the Pd-O bond strength, which ultimately allows enhancing the catalytic performance.

Although it is consensus that tuning the oxidation state of the noble metal can be a feasible option for optimizing the catalyst performance, the nature of the most active catalyst state has been subject of an intensive debate. Especially studies assuming a Mars-van-Krevelen redox mechanism surmise PdO as mandatory active species for methane oxidation [96,99,122–124]. By investigating the thermal history of the catalyst and the pretreatment effect prior to activity tests, Burch and Urbano [118] observed catalytic methane conversion only over PdO, whereas metallic palladium did not exhibit catalytic activity. On the other hand, several other studies observed methane conversion taking place over metallic palladium [112,126–128] or over mixed Pd and PdO phases or over PdO_x surface sites [129–136]. While a mild reduction pretreatment generates metallic palladium to a certain extent [133,137–140], X-ray photoelectron spectroscopy (XPS) and electron energy-loss spectroscopy (EELS) data by Hoflund et al. [141] indicate the reformation of PdO during exposure to a lean atmosphere. These apparent contradictions underscore the high complexity of these palladium-based catalysts and especially of the assigned reaction. Although the explanations for the observed activity strongly vary, more recent studies tried to correlate the different findings.

Density functional calculations by Broclawik et al. [142] suggest that although palladium dimers favor methane activation and C-H bond scission, a PdO-methyl-hydrogen complex forms during the course of methane decomposition. Based on DFT, Hellman et al. [133] similarly link a low activation energy for dissociative adsorption of CH_4 to under-coordinated Pd sites in PdO(101) particles or to metallic surfaces. Subsequent DFT studies refine this hypothesis and consider the close proximity of an oxygen atom located below the coordinatively unsaturated Pd atom in a two-layer PdO(101) film as a crucial factor governing efficient methane dissociation [134]. Hence, although the catalyst might contain metallic palladium, the presence of PdO_x seems to be mandatory. Assessing the mechanism with a combination of DFT calculations as well as kinetic and isotopic methods allowed Chin et al. [124] to combine this apparent contradiction on a fundamental level. As illustrated in Fig. 5, bare Pd cluster surfaces activate the C-H bond scission via oxidative addition, whereas PdO clusters cause hydrogen abstraction via σ-bond metathesis through a $(H_3C^{\delta-}\cdots Pd_{ox}\cdots H^{\delta+}\cdots O_{ox})^{\ddagger}$ four-center transition state. The last path seems to be the favored reaction pathway at higher oxygen concentrations, since the activation energy is minimized and, therefore, turnover rates for methane conversion are

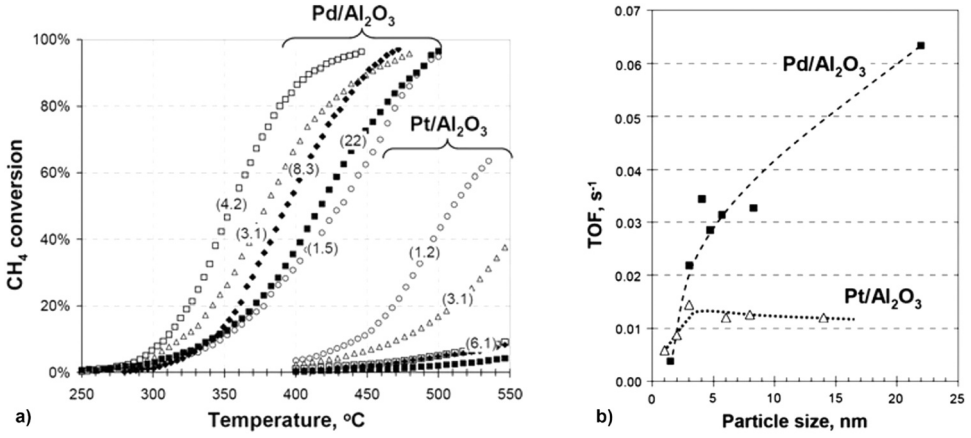

Fig. 4. a) Varying light-off behavior of Pd/Al_2O_3 and Pt/Al_2O_3 with different noble metal particle sizes (given in parentheses) and b) dependence of turnover frequency (TOF) in CH_4 conversion on the noble metal particle size over Pd/Al_2O_3 at 320 °C and Pt/Al_2O_3 at 430 °C. Adapted with permission from ref. [121]. Copyright 2002 Springer Nature.

maximized. A recent study on the dynamic evolution of methane oxidation over Pd(111) and PdO(101) surfaces using reactive force-field molecular dynamics is in line with such first-principle electronic structure calculations [143]. In addition, the study emphasizes that lattice oxygen is more active compared to oxygen that is chemisorbed on metallic palladium, which is in accordance with experimental findings [103].

3.2. The support material and its influence on the catalytic activity

The support material can tremendously influence the redox properties, oxidation state, and catalytic activity of palladium catalysts. While alumina-supported catalysts served as the main subject of research for decades, a variety of other metal oxides like ceria, zirconia, and ceria-zirconia [83], but also multicomponent materials such as $Ce_xZr_{1-x}O_2$-Al_2O_3 [144] are considered as promising support materials. Moreover, as summarized in recent reviews by Mortensen et al. [145] and Chen et al. [146], zeolite structures attract increasing interest since their properties can be controlled rather well via the structure and composition chosen during synthesis, hereby also influencing the active palladium sites [147,148]. Losch et al. [149], for instance, prepared a mesoporous Pd-loaded zeolite and varied the Si/Al-ratio to find an optimum hydrophobic/hydrophilic character that enhances the water tolerance of the catalyst. Also catalyst formulations based on a ZSM-5 structure with palladium loading showed competitive activity and sintering-resistance, as reported by Petrov et al. [150,151]. Although such encouraging results emphasize the great potential of zeolite-supported palladium catalysts for complete methane oxidation, to date the same challenges as for catalysts supported on metal oxides remain and interactions and synergies between the noble metal and the support need to be optimized.

In this regard, particularly palladium supported on ceria has lately been in the focus, since ceria is able to strongly interact with the noble metal particles (so-called strong noble metal support interactions, SNMSI) and exhibits excellent redox properties [152]. Colussi et al. [153], for instance, report an enhanced methane conversion of nano-faceted Pd-O sites in Pd-Ce surface superstructures and explain this phenomenon by labile undercoordinated surface O atoms at the interface of a Pd-O moiety. Similarly, Cargnello et al. [154] synthesized modular Pd@CeO_2 subunits supported on functionalized, hydrophobic Al_2O_3, which did not only result in catalysts that are sintering-resistant up to 800 °C, but also enabled complete methane combustion already at 400 °C. In order to explain their observations, the authors speculate about mechanical stress and a high degree of disorder in the ceria-shell causing high oxygen mobility and increased reducibility, respectively. In addition, the authors attribute the high conversion to highly reactive Pd sites at the Pd-Ce interface, which is in analogy to findings in the context of CO oxidation over Pd/CeO_2 reporting that in the low-temperature regime the oxidation reaction takes place predominantly at the highly active Pd-O-Ce interface [155,156]. Moreover, this hypothesis is in line with combined DFT and reactive force-field (ReaxFF) simulations on the interface of Pd clusters supported on ceria conducted by Senftle et al. [157], which revealed low methane activation barriers for Pd sites at the interface due to dynamic changes of the Pd state from Pd^{4+} to Pd^{2+} that was reported to drive C-H bond activation.

The iterative DFT/ReaxFF workflow summarized in schematic Fig. 6 represents a very powerful combination of tools that allows for theoretical consideration of thermodynamic stability and catalytic activity. With respect to complex noble metal-support interactions, these tools are capable of describing the underlying physical and chemical elementary processes in detail. Supplemented by detailed experimental insights, the ongoing progress in simulation and modeling of heterogeneous chemical reactions on the microscopic scale can contribute to a rational development of novel materials and processes [69].

Further exploitation of the unique properties of ceria can be achieved by tuning the morphology of the support material. By comparing the methane oxidation activity over Pd-based catalysts supported on CeO_2 that was calcined at different temperatures prior to the addition of Pd, Lee et al. [158] found a promotion of methane oxidation for catalysts that were supported on ceria calcined at high temperatures of 800 °C and 950 °C. In contrast, the use of supports that were calcined at 500 °C and 650 °C resulted in lower CH_4 conversion. This observation was explained by fewer defects in the surface of the ceria lattice, which the authors believe enhances the reducibility of the support and results in an active participation of surface ceria oxygen in the catalytic activity. Possibly, a lower concentration of support defects prevents an incorporation of palladium in the ceria lattice as Pd^{4+} ions. Such species were reported to be inactive for CH_4 oxidation by Chen et al. [159], who investigated the impact of metal-support interactions by loading PdO nanoparticles onto octahedrons, cubes, and rods of nanocrystalline ceria and found the highest activity for Pd^{2+} species that were supported on the octahedral ceria support in the form of PdO.

As an additional parameter, the acid-base properties of the support material were identified to crucially affect the methane combustion activity [160,161], and, as discussed later, the resistance to water inhibition and sulfur poisoning. Moderate support acidity was found to maximize methane oxidation rates over palladium-based catalysts, whereas basic supports such as MgO diminish methane conversion. In particular, XAS studies and temperature programmed experiments by Yoshida et al. [160] point to a stabilization of the PdO phase over MgO, which could hamper the Mars-van-Krevelen redox mechanism that involves PdO lattice oxygen. Moreover, Willis et al. [161] suggested that also the adsorption of CO_2 takes place on MgO, hereby suppressing methane adsorption and activation. While basic support materials like

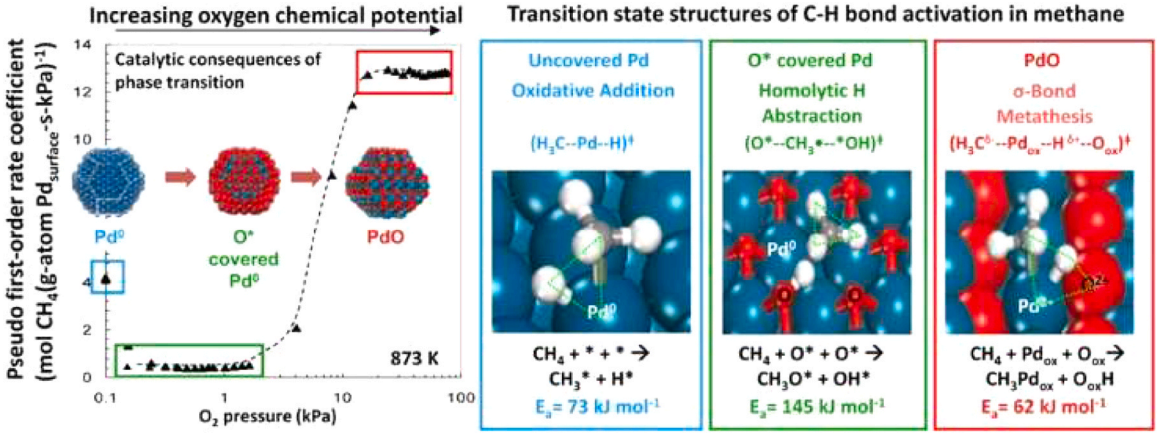

Fig. 5. Consequence of the Pd-PdO phase transition for methane activation. Reprinted with permission from ref. [124]. Copyright 2013 American Chemical Society.

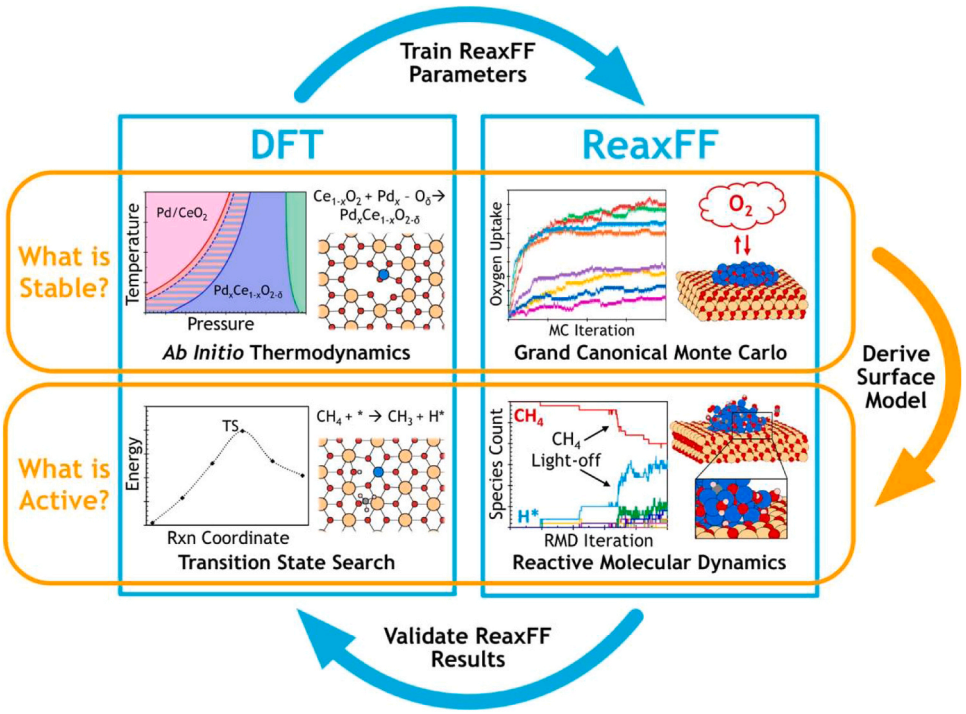

Fig. 6. Combined DFT/ReaxFF workflow for investigating the stability and activity of an oxide-supported metal catalyst. Reprinted with permission from ref. [157]. Copyright 2017 American Chemical Society.

MgO exhibited a substantially lower activity for CH_4 oxidation, similar reaction rates were found over inert (SiO_2), acidic (Al_2O_3), and redox-active ($Ce_{0.8}Zr_{0.2}O_2$) support materials [161], as illustrated in Fig. 7a. In order to deconvolute the effect of the support material, Murata et al. [162] correlated the turnover frequency (TOF) for methane combustion and the standard formation enthalpy ($\Delta_f H^0_{M\text{-}O}$) of the metal oxide support and obtained a volcano plot (Fig. 7b). In line with previous studies, the authors were able to control the palladium oxidation state by utilizing the noble metal-support interactions. Particularly Al_2O_3, CeO_2, and ZrO_2 have been identified as suitable supports for palladium-based methane oxidation catalysts, since their moderate oxide formation enthalpy ensures an optimal reducibility of the PdO particles during catalytic methane activation. In contrast, too low formation enthalpies cause a lack of active PdO sites, whereas too high enthalpies impede the participation of lattice oxygen in the redox mechanism.

These fundamental insights on the noble metal structure and support effects provide guidance for designing novel catalyst formulations and allow enhancing the catalytic activity of methane oxidation catalysts by rational process control. For instance, Pd/Al_2O_3 catalyst samples that were mildly reduced prior to a dynamic light-off test exhibited a higher hydrocarbon oxidation activity compared to fully oxidized samples [103,128]. Taking the information summarized above into account, several phenomena account for this activity boost. An optimal oxidation state and a moderate particle size weaken the Pd-O bond, hereby ensuring sufficient oxygen provision from the PdO lattice [96,121,125, 140,163]. In addition, the particle morphology can undergo changes during reductive treatment, particularly if this goes along with temperature variations [112,117,118], resulting in a change of the surface roughness, and also surface adsorbates can be removed by pretreating

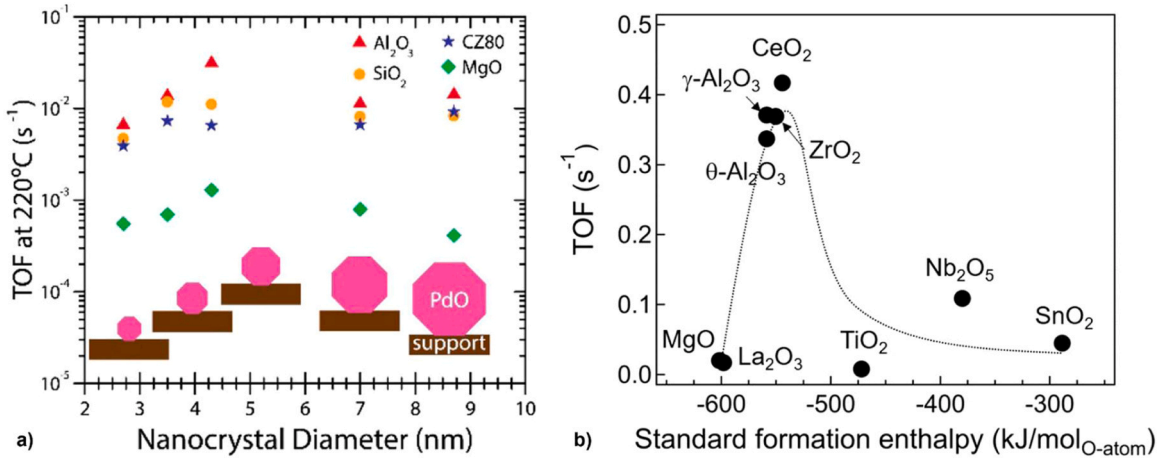

Fig. 7. a) TOFs for Pd-catalyzed CH_4 oxidation at 220 °C versus the nanocrystal diameter for different support materials. Adapted with permission from ref. [161]. Copyright 2017 American Chemical Society. b) Turnover frequencies (TOFs) for Pd-catalyzed CH_4 oxidation at 300 °C against the standard formation enthalpy of the metal oxide support (Pd-particle size of 7 nm). Adapted with permission from ref. [162]. Copyright 2019 American Chemical Society.

the catalysts at elevated temperatures, e.g. as high as 475 °C [164]. Notably, adsorbates do not only include reactants and reaction products, e.g. H_2O, but also species such as NO or SO_x that originate from the exhaust gas stream. While under typical working conditions CO_2 plays a negligible role with respect to competition for active sites on the surface of the catalyst [163,165,166], the following sections demonstrate that steam and sulfur species pose major challenges for palladium-based methane oxidation catalysts.

3.3. Water inhibition

Water represents an unavoidable exhaust gas component, which acts as a strong inhibitor for methane conversion and causes continuous deactivation of palladium catalysts, especially in the low-temperature regime [167,168]. Water does not only originate from the combustion process in the engine, but also forms during catalytic methane conversion. Hence, with reaction time on stream self-inhibition will cause deactivation even in the absence of external water [52]. On a molecular level, diffuse reflectance infrared Fourier-transform spectroscopy (DRIFTS) revealed a pronounced hydroxyl accumulation on the catalyst surface [93,169]. Since these hydroxyls block catalytically active surface sites that could otherwise catalyze methane C-H bond activation, raising water vapor concentrations progressively cause a drop of the overall methane conversion rate over palladium catalysts, as depicted in Fig. 8.

With respect to reaction kinetics, power law models suggest a clear difference between lean methane oxidation over Pd/Al_2O_3 under "dry" and "wet" conditions: Ribeiro et al. [171] determined an apparent activation energy of 85 kJ mol^{-1} for water-free conditions, whereas van Giezen et al. [172] reported 151 kJ mol^{-1} for a steam-containing gas stream. Notably, Burch et al. [165] point to a strong temperature dependency of water inhibition, with diminishing inhibitory effects at temperatures above 450 °C. Ciuparu and Pfefferle [167] did not only confirm these findings, but also found the inhibition to be dependent on the water concentration, which is also visible in the data shown in Fig. 8. Commonly, microkinetic modeling attributes more pronounced inhibition to higher water concentrations, since the surface coverage with hydroxyl groups decreases the surface site accessibility, which is crucial for methane adsorption and activation over PdO [170]. In this respect, hydroxyl functional groups formed during the catalytic reaction impact the catalyst even stronger than external water, possibly due to the close proximity between noble metal sites and water that facilitates immediate blockage of sites [169,173]. In addition to mere adsorption, speculations about a reaction between H_2O and palladium oxide leading to the formation of $Pd(OH)_2$, which is considered inactive for methane oxidation [174–177], have been confirmed by means of in situ XAS studies at the Pd K and L edges [178] and by modulation excitation X-ray absorption spectroscopy (ME-XAS) combined with XAS spectra simulations [179] for alumina-supported catalysts. $Pd(OH)_2$ formation represents an even stronger inhibition mechanism than simple surface coverage with hydroxyl functionalities as it results in the formation of an actual chemical compound with an ionic structure instead of comparably weakly chemisorbed surface adsorbates. Ambient pressure XPS experiments by Li et al. [180] corroborate the formation of $Pd(OH)_2$ upon water exposure as top layer of a Pd foil and underscore that beyond inhibition of methane adsorption, a $Pd(OH)_2$ layer also suppresses the migration of oxygen from bulk PdO to the surface, i.e. for filling oxygen vacancies. By combining DRIFTS and energy-dispersive XAS measurements, Velin et al. [93] concluded that water addition hampers the redox dynamics of the palladium oxide particles, hereby preventing the contribution of lattice oxygen to the methane oxidation reaction. Based on their results, the authors also speculate about a shift of the methane oxidation mechanism from the Mars-van-Krevelen mechanism with a lattice oxygen contribution under dry conditions to a slower Langmuir-Hinshelwood mechanism with chemisorbed oxygen under wet conditions.

Since water itself is an omnipresent factor during methane oxidation, a wide variety of measures for overcoming water inhibition has been evaluated in the past. As hydroxyl accumulation was found on both, the noble metal and the support material, namely alumina [169], a variation of the support material can be expected to account for improvement [181]. As demonstrated by Murata et al. [182], already a change of the alumina crystalline phase can mitigate the inhibition by H_2O. As shown by the turnover frequency plotted in Fig. 9, $Pd/\alpha\text{-}Al_2O_3$ outperforms $Pd/\theta\text{-}Al_2O_3$ or the most commonly studied $Pd/\gamma\text{-}Al_2O_3$ catalyst. In addition to the particle size dependency already discussed in Section 3.1, the authors report that the hydrophobic nature of $\alpha\text{-}Al_2O_3$, which was uncovered by means of temperature-programmed desorption (TPD) of H_2O and infrared (IR) measurements, allows for more pronounced adsorption-desorption dynamics of OH/H_2O species.

Particularly in the context of dynamic operation, materials like ceria, zirconia or mixed oxides of these are widely used in the field of emission control, i.e. for three-way catalysis, as these materials exhibit a high oxygen storage capacity and a pronounced oxygen mobility [154,162,183]. Consequently, also methane oxidation catalysts could benefit from their advantageous properties, e.g. by diminishing the water inhibition effect. Strong noble metal-support interactions (SNMSI) allow for an oxygen exchange between the palladium oxide particles and the support

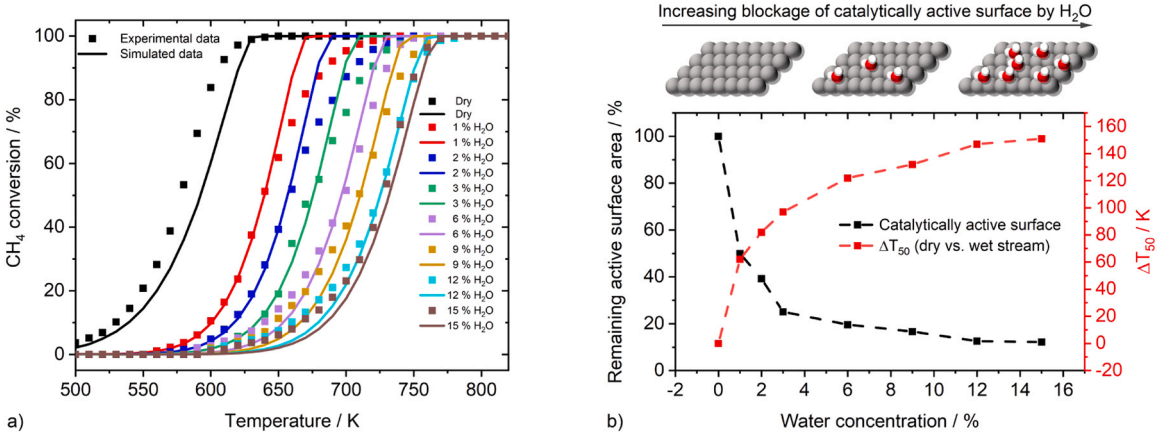

Fig. 8. a) Inhibition of methane conversion with increasing water levels in the feed gas as observed during experimental light-off measurements (square symbols) and as described by a microkinetic model (solid lines) that takes the blockage of active surface sites by H_2O as an 'inhibition factor' into account (b). Adapted with permission from ref. [170] under the terms and conditions of the Creative Commons Attribution (CC BY 4.0) license (http://creativecommons.org/licenses/by/4.0/). Copyright 2020 by the authors. Licensee MDPI, Basel, Switzerland.

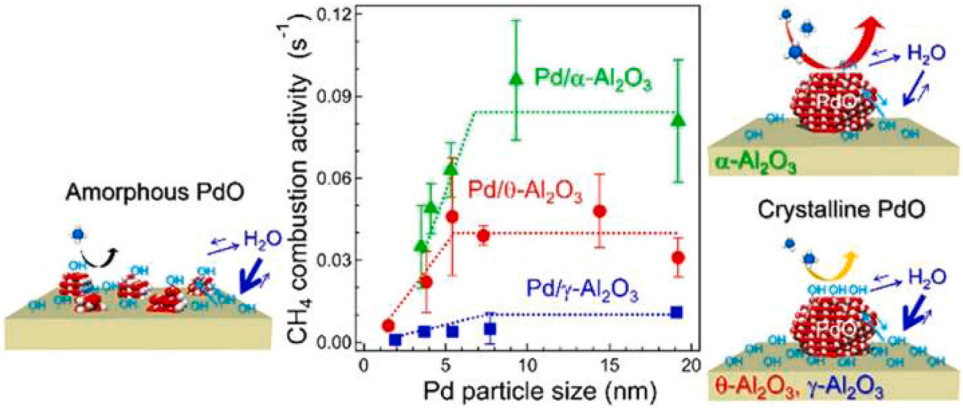

Fig. 9. Dependence of the TOF on the Pd particle size and on the alumina phase during CH_4 oxidation in humid reaction atmosphere. Reprinted with permission from ref. [182]. Copyright 2020 American Chemical Society.

material, as systematically investigated by Ciuparu et al. [173] for zirconia- and ceria-zirconia-supported palladium oxide. Oxygen originating from the PdO lattice that was used for CH_4 activation leaves vacancies, which can either be refilled with oxygen from the gas phase, from the support material or with hydroxyl groups. While the latter possibility causes catalyst deactivation, the provision of oxygen atoms from support materials with high oxygen mobility could represent an effective measure to increase the water tolerance of the catalyst, as it influences the dynamic behavior of hydroxyl groups and potentially decreases their number on the active sites of the catalyst [154,169,173]. Similarly, Barrett et al. [178] proposed tin oxide (SnO_2) as an alternative support for alumina, and attributed the higher activity of Pd/SnO_2 to the dehydroxylation ability of SnO_2 that allows extracting hydroxyls from the palladium particles. Although support materials with high oxygen mobility can reduce the inhibitory effect of water, a complete suppression of the negative impact by water has been unsuccessful so far. Despite their overall lower hydrophobicity in comparison to alumina-supported materials [184], the presence of hydroxyl groups on ceria-based catalysts, for instance, was found to inhibit oxygen exchange from the support to the noble metal, hereby preventing efficient reoxidation of palladium particles [185].

Hence, in addition to finding water-tolerant catalyst formulations, research efforts have focused on the removal of hydroxyl groups. Kikuchi et al. [168] and Escandón et al. [186] report that water inhibition is an at least partially reversible process for a relatively wide variety of catalyst formulations. Already a simple temporary removal of steam from the gas stream engendered a recovery of active sites and a regain of catalytic activity. A more efficient desorption of hydroxyl groups in particular and surface adsorbates in general can be induced by reductive treatment of deactivated palladium catalysts, e.g. as demonstrated by Arosio et al. [187] over a Pd/CeO_2/Al_2O_3 catalyst. Reducing conditions – even if applied in a time range of few seconds – do not only facilitate desorption of surface species but also reduce palladium particles [103,138,150,187–189]. In this respect, the dynamic redox chemistry of Pd-PdO influences the catalytic activity, as discussed in the previous sections, and influences also the inhibition and poisoning tendency. During their experimental investigations of a Pd crystal, Nyberg and Uvdal [190] observed hydroxyl formation solely on palladium surfaces covered with oxygen, but not on metallic palladium. Obviously, metallic palladium is less prone to water inhibition, which is indicated also by the activity boost observed after prereducing palladium catalysts as already discussed in detail in the previous section [48,103,125,138]. The fact that reoxidation of metallic palladium particles is a fast process only at the Pd nanoparticle surface leads to a delay in the onset of water inhibition since achieving an equilibrium between PdO, surface hydroxyls, and $Pd(OH)_2$ requires time. However, as long as the surface is not completely covered with hydroxyls, the negative inhibitory effect of water is not fully developed. This behavior calls for the use of dopants that are less sensitive to H_2O and benefit the most active phase of palladium. Herein, a variety of studies reported a beneficial effect of platinum addition with respect to activity, stability, and tolerance towards inhibiting and poisonous species [191–196]. These aspects are illustrated in Fig. 10 that shows light-off curves over mono- and bimetallic catalysts and the positive influence of Pt-addition to palladium.

Albeit Pt-Pd alloying is a well-established approach for diminishing deactivation and water inhibition, the optimal noble metal ratio and the underlying phenomena are still under debate. It is consensus that Pt-only catalysts show poor activity for lean methane conversion [199] (Fig. 4, Fig. 10), however, different bimetallic compositions were suggested for gaining superior durability and activity, with Pt:Pd molar ratios ranging from 0.1 to 0.5 [193,195,196]. Narui et al. [193] attributed the improved durability to the close contact between the two noble metals that prevents migration, coalescence, and sintering of alumina-supported particles, whereas monometallic palladium particles exhibited a strong sintering tendency. Subsequent research strongly supports this hypothesis [200] and speculates about a Pd-Pt alloy domain that is less prone to water inhibition than monometallic PdO domains [201]. In addition, DFT calculations by Hou et al. [202] suggest that the platinum directly intervenes in the reaction mechanism by increasing the availability of electrons on the noble metal surface, hereby weakening the bonding of intermediates. Moreover, it was claimed that platinum is capable of stabilizing the metallic palladium oxidation state [128,196,200], which is considered less prone for hydroxylation and hereby may offer a possibility for reducing water inhibition. Surface science studies on Pd and Pd-Pt foils by Large et al. [203,204] using temperature-programmed near-ambient pressure X-ray photoelectron spectroscopy (TP-NAP-XPS) revealed that Pt addition inhibits the oxidation of Pd under stoichiometric and lean excess-oxygen conditions, but also uncovered a significant restructuring of the bimetallic alloy upon exposure to reaction gases, i.e. resulting in Pt migration towards the bulk. Analogous to bimetallic foils, also bimetallic Pd-Pt particles can undergo significant changes during hydrothermal aging and during exposure to reactive gas mixtures even at temperatures as low as 400–550 °C, namely restructuring, de-alloying, and segregation [205–208]. Notably, Goodman et al. [206] claim that the segregation of a PdO phase in close contact to a bimetallic Pd-Pt phase accounts for high activity and stability. Similarly, Yang et al. [209] recently reported that PdO-shell-Pt-core clusters, as illustrated in Fig. 11, whose formation is induced by an oxidizing atmosphere, benefit methane conversion and particularly increase the water resistance of the catalyst. Last but not least, Divins et al. [210] found that also the support material is a decisive factor and attributed high catalytic activity and robustness of Pt-Pd/CeO_2 catalysts to the formation of PdO_x-Ce species whose

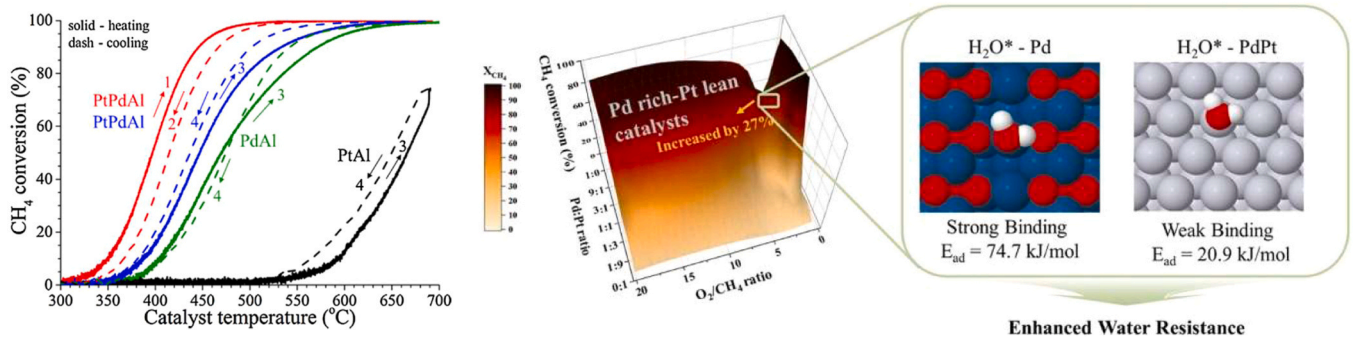

Fig. 10. Left: Methane conversion over mono- and bimetallic methane oxidation catalysts supported on alumina. Reprinted with permission from ref. [197]. Copyright 2018 Elsevier. Right: Impact of Pt addition on the noble metal-water interaction. Reprinted with permission from ref. [198]. Copyright 2022 Elsevier.

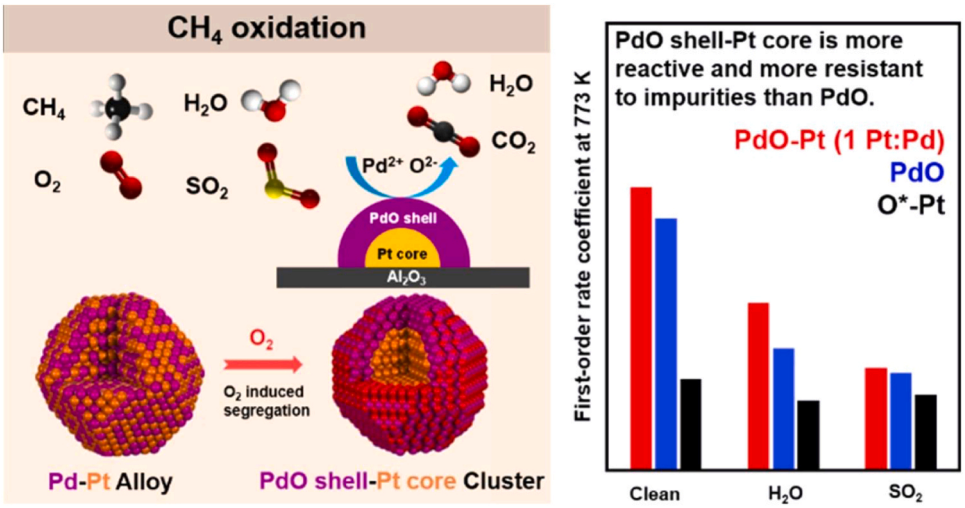

Fig. 11. Illustration of the active structure of bimetallic Pd-Pt particles. Reprinted with permission from ref. [209]. Copyright 2021 Elsevier.

intimate contact with Pt-Pd/PdO structures represents a unique nanostructure that can only be created by an optimized mechanochemical milling preparation strategy.

Furthermore, experimental data by Hurtado et al. [211] and Gremminger et al. [166] point to a mitigation of the inhibitory effect of water in the presence of nitrogen-containing inorganic gas phase species such as NO_x. As shown in Fig. 12, the Pd-Pt/Al_2O_3 catalyst tested by Gremminger et al. [166] suffered continuous deactivation in the presence of 12 vol.-% steam, whereas the addition of 120 ppm NO and 30 ppm NO_2 stabilized the catalytic conversion for 100 h of operation.

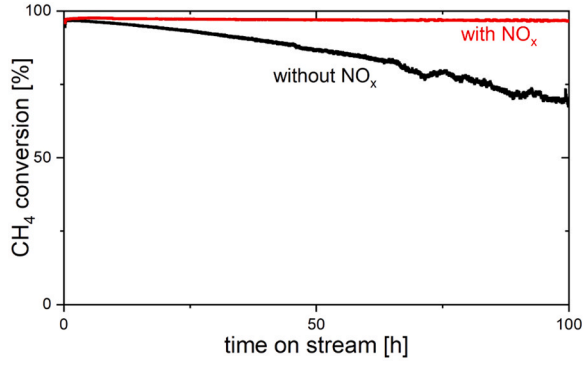

Fig. 12. CH_4 conversion over a Pd-Pt/Al_2O_3 catalyst versus reaction time on stream in the absence and presence of NO_x. Adapted with permission from ref. [166]. Copyright 2015 Elsevier.

Similarly, also NH_3 was reported to benefit methane oxidation [211], presumably because the noble metal species catalyze ammonia oxidation toward NO_x [212]. This is remarkable, since similar to water, also NO was reported to block the active noble metal sites, hereby suppressing methane oxidation [213]. By conducting experiments with monometallic palladium and bimetallic Pd-Pt catalysts in a feed gas containing H_2O and NO, Sadokhina et al. [213] investigated the NO_x-H_2O interplay in more detail. Based on their experimental observations, the authors speculate about a reaction of inactive surface hydroxyls with NO resulting in the formation of active HNO_2 species that reduce the negative impact of water. In this respect, Boubnov et al. [179] studied the reversible inhibitory effects of H_2O and NO by ME-XAS and DRIFTS for monometallic Pd/Al_2O_3 and bimetallic Pd-Pt/Al_2O_3 catalysts. The authors found that both water and NO interact with the Pd particle surface as well as with the Al_2O_3 support, with water leading to a pronounced decrease in formate production, which was identified as intermediate during complete methane oxidation.

3.4. Sulfur poisoning and catalyst regeneration

Sulfur species such as H_2S or SO_x represent some of the most detrimental catalyst poisons throughout heterogeneous catalysis, since sulfur does not only physisorb or chemisorb on the catalyst surface, but commonly reacts with the active (noble) metal and the support material, hereby causing severe catalyst degradation and deactivation [214]. Although the sulfur content of unprocessed natural gas strongly depends on its origin and ranges from few ppm up to 1 vol.-% of H_2S [215–217],

only low sulfur concentrations are present after purification (approximately 1 ppm H_2S or SO_x). Despite this very low sulfur level, exposure at low exhaust temperatures accounts for accumulation of significant sulfur amounts and concomitant deactivation of palladium-based methane oxidation catalysts [218–221]. As illustrated in Fig. 13, the presence of 5 ppm SO_2 causes a pronounced and rapid activity drop at temperatures from 400 °C to 500 °C.

As revealed by IR spectroscopy and XPS studies, the presence of sulfur species under humid lean conditions favors the formation of Pd-SO_x compounds, i.e. primarily $PdSO_4$, which are inactive for methane activation [223–225]. Complementary XAS and energy dispersive X-ray spectroscopy (EDXS) measurements of Pd-Pt/Al_2O_3 and Pd-Pt/CeO_2-ZrO_2-Y_2O_3-La_2O_3 catalysts, which were poisoned for 15 h at 450 °C and 500 °C in a reaction gas mixture containing 5 ppm SO_2, provided information on the $PdSO_4$ amounts and sulfur content of the noble metal particles, respectively, hereby suggesting a predominant surface poisoning [222]. Analogously, DFT predicts surface poisoning rather than bulk $PdSO_4$ formation and indicates that particularly the simultaneous presence of both surface hydroxyls and sulfates causes poor catalyst performance [226]. In contrast, platinum suffers less deactivation and its combination with palladium has been demonstrated as a feasible approach for obtaining more sulfur-tolerant catalysts [219,220,227]. Based on a first-principles thermodynamics study, Sharma et al. [228] demonstrated that under lean conditions palladium shows a significantly higher tendency to form surface oxide layers compared to platinum. The authors identified the amount of oxidized metal surface as major factor governing the sulfation behavior of the two noble metals, as they found a remarkably higher SO_3-to-surface oxide binding strength for palladium oxide than for platinum. In this respect, it is important to note that sulfur species undergo stepwise oxidation over noble metal species, as shown for sulfur poisoning of a Pt/Al_2O_3 catalyst by Hamzehlouyan et al. [229,230]: Oxidation catalysts transform sulfur species first into SO_2 and subsequently into more detrimental SO_3. Oxygen-precovered Pt(111) surfaces, which likely occur in oxidation catalysts operated in the exhaust tailpipe of lean-burn gas engines, accelerate SO_4 formation [231]. Ultimately, the presence of water enables formation of H_2SO_4, which efficiently reacts with both the support material and the noble metal, and consequently has the most dramatic impact on catalyst degradation [230].

As revealed in a series of systematic studies by Wilburn and Epling [227,232–234] on mono- and bimetallic Pd-Pt catalysts supported on alumina, sulfur poisoning strongly depends on noble metal particle size, noble metal loading, temperature of exposure, and noble metal particle composition. While small particles and high palladium loading facilitate the formation of thermally stable alumina sulfates, larger particle sizes and high platinum contents benefit the formation of less stable species that decompose at lower temperature [227,233].

Hence, in addition to the noble metal poisoning, the catalyst support is as well affected during SO_2 exposure. Due to its ability to form surface and bulk aluminum sulfites and sulfates, alumina acts as a sulfur trap that delays the poisoning process and partially protects the noble metal from complete deactivation [197,219,229,235]. Herein, sulfur species are adsorbed, oxidized, and transferred to the support, which according to Hu and Williams [236] can result in accommodation of more than 80% of the adsorbed sulfur in the alumina support. Similarly, support materials like CeO_2, ZrO_2 or mixed oxides of these can also form surface and bulk sulfites and sulfates [237–241]. This spillover of sulfur species from the active phase to the support or even the direct reaction of SO_2 with the metal oxide is more efficient at higher temperatures, hence the catalytic activity remains longer and on a higher level compared to the typical low-temperature conditions in lean-burn gas engine exhaust tailpipes [222,225]. While the exposure of Al_2O_3 and CeO_2 thin films to SO_2 predominantly results in sulfite (SO_3^{2-}) formation at temperatures below 200 °C, temperatures of 300–400 °C under lean-burn gas engine conditions favor the formation of more stable sulfates (SO_4^{2-}) on the support [242,243]. In contrast, less sulfating or non-sulfating supports like Ti- and Si-doped alumina [244–246] or SiO_2-based materials result in significantly faster activity drops due to direct noble metal poisoning [219,247]. On the other hand, catalysts with less sulfating supports ease the release of sulfur species [248], which is a crucial aspect for regeneration considerations. Hence, optimizing the ratio of different components in mixed oxide supports, e.g. as demonstrated by Venezia et al. [249] for Pd supported on TiO_2-doped SiO_2, can increase the SO_2 tolerance. More recently, Lin et al. [250] chose a similar approach and doped alumina with a variety of elements. As depicted in Fig. 14, the authors found a correlation between the sulfur uptake and the surface acidity/basicity. Among the tested catalysts, Pd/Zr-Al_2O_3 was identified as most active for CH_4 oxidation both in the presence of SO_2 and after regeneration.

Although optimized catalyst formulations facilitate the regeneration of sulfur poisoned catalysts, the release of sulfur requires considerable changes of the reaction conditions, namely temperature and gas composition. Excess oxygen, as typically present in the exhaust of lean-burn gas engines, stabilizes sulfates and sulfites and impedes their decomposition at moderate temperatures [251]. In a lean or inert gas stream, full decomposition of bulk sulfates of aluminum, cerium, zirconium or lanthanum, which are commonly used in catalysts for emission control, requires temperatures above 750 °C [222]. In contrast, rich conditions benefit catalyst regeneration at lower temperatures by promoting not only the reduction of palladium sulfate, but also of support-related surface and bulk sulfates [187,218,252–256]. As suggested by Arosio et al. [255], rich pulses at 600 °C can adequately restore the catalytic activity of sulfur-poisoned Pd/Al_2O_3, whereas lower temperatures only allow for partial recovery. Bimetallic Pd-Pt catalysts with high Pt loading show a lower tendency to form sulfates at low temperature during SO_2 poisoning and form a larger amount of species

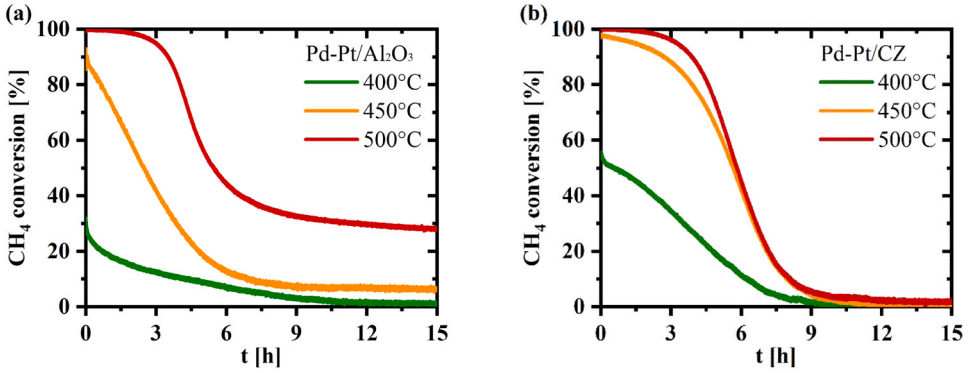

Fig. 13. Impact of SO_2 on the performance of a Pd-Pt/Al_2O_3 (a) and of a Pd-Pt/CeO_2-ZrO_2 (b) methane oxidation catalyst. Reprinted with permission from ref. [222]. Copyright 2020 Elsevier.

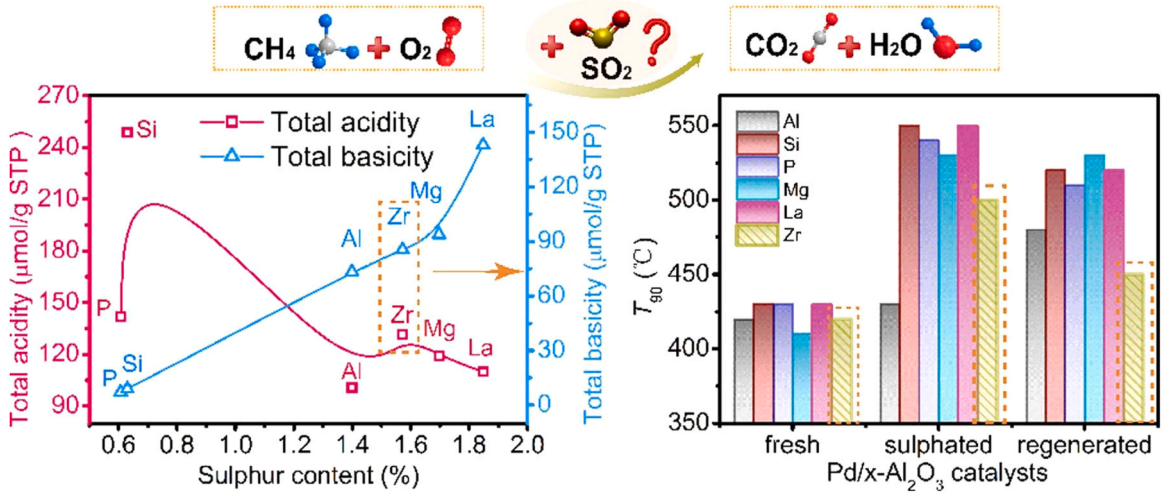

Fig. 14. Correlation of acidity/basicity of the support material with the sulfur content after sulfation and the temperature of 90% CH_4 conversion over palladium catalysts supported on doped alumina. Reprinted with permission from ref. [250]. Copyright 2022 Elsevier.

with low decomposition and desorption temperatures than bimetallic catalysts with high Pd content [234]. However, the overall regeneration efficiency during temperature-programmed reduction (TPR) or desorption (TPD) is lower and the sintering during the regeneration is more pronounced for Pd-Pt catalysts with high Pt loading [232,233]. Irrespective of the noble metal type or loading, rich regeneration at mild temperatures typically does not efficiently remove all S-containing species formed on the catalyst support. Remaining sulfates such as $Al_2(SO_4)_3$ can cause a re-poisoning of the active noble metal species [257]. Similarly, also ceria-containing catalysts remain poisoned to some extent, exhibiting a dynamic transformation during lean-rich cycling, with $Ce_2(SO_4)_3$ as predominant species in the presence of excess oxygen [238,239] and Ce_2O_2S during reducing periods [239,240]. Nevertheless, replacing alumina by ceria-zirconia as support material can reduce the sulfur spillover tendency and hereby mitigates the need for full decomposition and desorption of sulfur compounds on the catalyst [221,258], which is a particularly vital aspect for the long-term operation of methane oxidation catalysts.

With respect to the noble metal state under dynamic poisoning and regeneration cycles, recent studies reported the formation of several phases depending on the reaction conditions. For elucidating the effect of reductive treatment on sulfur-poisoned palladium species, Nissinen et al. [259] used powder XRD for investigating a model 4 wt.-% $PdSO_4/Al_2O_3$ catalyst. While the decomposition of $PdSO_4$ in inert atmosphere yielded metallic palladium, the authors observed a transformation of $PdSO_4$ into Pd_4S upon exposure to a H_2-containing gas atmosphere. Notably, Pd_4S formation has previously been reported in the context of Pd-based hydrogen purification membranes and was found to form during a reaction between H_2S and metallic palladium [260]. Similarly, PdS formation was found during rich regeneration by means of XAS measurements [222,258], which was explained by the reaction between the noble metal and sulfur-containing species like SO_2, COS, CS_2, and H_2S that evolve during the reductive regeneration of sulfur poisoned Pd-Pt methane oxidation catalysts [222]. Furthermore, during continuous heating in a reductive gas atmosphere, in situ XAS revealed the gradual transformation of $PdSO_4$ species to metallic palladium around 200 °C, followed by the formation of PdS, which remained stable in a considerable amount up to 750 °C under rich conditions [222]. In contrast, excess oxygen transforms PdS immediately into PdO [258], possibly due to the formation and immediate spillover of SO_2 and SO_3 species to the support. This restoration of the active PdO species is accompanied by the regain of the catalytic activity. Notably, these results underscore that in situ and *operando* spectroscopic studies of the catalyst structure under reaction conditions can be of great help for identifying the appropriate conditions for catalyst regeneration.

3.5. *Poisoning by metals and phosphorous*

As underscored by the large number of scientific studies dealing with sulfur poisoning, it is consensus that sulfur is the most relevant catalyst poison for methane oxidation catalysts. However, apart from sulfur there are also other trace compounds in the engine exhaust that can cause catalyst deactivation, namely phosphorous (P), silicon (Si), iron (Fe), nickel (Ni), zinc (Zn), lead (Pb), calcium (Ca), or magnesium (Mg) [20,214,261–264]. Among these species that can originate from lubricants, the fuel itself, or in the case of iron from the engine and exhaust tailpipe parts, phosphorous and silicon are of major concern. In contrast, the significance of other species dropped in the past years, primarily due to advances in lubricant design allowing the replacement of harmful substances by less critical ones. Although the majority of studies addressing metal and phosphorous poisoning were conducted for diesel oxidation catalysts, the phenomena can essentially directly be transferred to methane oxidation catalysts in natural gas engine exhausts, since in both cases the exhaust gas is lean and the oxidation catalyst is frequently based on the noble metals Pd and Pt. Similarly, a number of findings from studies on TWC deactivation are also relevant for methane oxidation catalysts and are therefore discussed in the following.

Phosphorous is a common additive in lubricating oils and can react with ceria and alumina in the catalyst washcoat, thereby forming phosphates such as $CePO_4$ and $AlPO_4$ [20,262,265–267], but can also react with other contaminants such as Ca or Zn to form $Ca_3(PO_4)_2$ or $Zn_2P_2O_7$, respectively [262,268,269]. In contrast to other species such as sodium (Na) or potassium (K), which are frequently found evenly distributed throughout the entire catalyst washcoat [270,271], P seems to accumulate predominantly at the inlet zone of the catalyst sample and on the washcoat surface [262,272–276]. The reaction of the washcoat with P and the P-containing deposits can not only result in the formation of an overlayer that decreases the surface area and masks or blocks active sites and noble metal particles, respectively, but can also reduce the oxygen storage capacity, change the redox properties, and influence the interactions between the noble metal and the support [267,269,272,277–280]. Notably, the P-induced (approximately 2.5 wt.-% P) decrease of the noble metal reducibility was recently reported to strongly affect NO oxidation over an engine-aged $Pt-Pd/Al_2O_3$ diesel oxidation catalyst (Pt:Pd ratio of approximately 5:2), whereas CO and HC oxidation remained mostly unaffected [280]. Moreover, in situ X-ray absorption near edge structure (XANES) measurements of P-poisoned 1.2 wt.-% Pt-Pd bimetallic oxidation catalysts (Pt:Pd mass ratio of 3:1) by Bergman

et al. [271] uncovered that the co-localization of phosphorous and the noble metal decreases the reducibility of the catalytically active material and hereby influences the conversion of pollutants.

The continuous replacement of fossil natural gas by sustainable biomethane increases the relevance of Si poisoning. While the levels in farm biogas are comparably low, especially sewage and landfill digester gases that are sources of biomethane and that enjoy growing popularity contain significant amounts of organic silicon compounds, typically in the form of siloxanes [281–284]. These cannot only damage the combustion engine due to the formation of solid Si-based deposits [285], but can also accumulate in the catalyst. It is well known that Si from biogas can act as a strong catalyst poison for a variety of reactions and processes, e.g. during catalytic dry reforming [286] and steam reforming [287] of biogas over Ni-based catalysts. However, so far only few studies in the field of emission control investigated the distribution of Si in catalytic converters. Rokosz et al. [262] investigated catalysts from high mileage taxis, namely monolithic Pd-based catalysts exhibiting a two-layer washcoat with ceria as a bottom layer and alumina as a top layer by means of electron probe microanalysis (EPMA) combined with wavelength-dispersive X-ray spectroscopy (WDXS). The authors found a thin layer of silicon on the washcoat, which was covered by another overlayer consisting of engine oil-related contaminants like P, Ca, Zn, and Mg. It was assumed that silicone elastomer engine sealants that out-gas early in the life of the vehicle caused the deposition of silica or silicates. Analogously, Winkler et al. [264] found Si deposits on an engine-aged DOC mainly between the washcoat and the P- and Zn-containing contaminant overlayer; as a consequence of the poisoning, the activity for NO and propene conversion was substantially shifted to higher temperatures. In the same study, an EDXS analysis of a vehicle-aged TWC uncovered an island-like, non-uniform distribution of Si that strongly resembled the distribution of Ca and Mg on the TWC, but with an only minor effect on CH_4 conversion [264].

Regarding regeneration, washing of deactivated catalysts with weak acid solutions such as acetic acid [288], citric acid [289–292], and oxalic acid seems to be a promising approach to remove P, S, Ca, and Zn [262,292,293]. When washing Pd/Rh-based TWCs containing 1.9 wt.-% P for 30 min in an oxalic acid solution (followed by a distilled water rinse), Darr et al. [293] were able to remove approximately 82% of P, whereas only 54% were removed when using a citric acid washing solution and essentially no P removal was achieved with acetic acid. In contrast, the results by Angelidis et al. [288] suggest that the regeneration works also with mild acetic acid as long as the leaching conditions such as acid concentration, solution feed rate, and temperature are optimized. However, frequently only a partial regain of the catalytic activity can be achieved and contaminant traces remain on the catalyst even after acidic washing [293,294]. Equally important, the acidic treatment can induce changes of the physicochemical properties of cordierite substrates [295] that can be considered irreversible. Therefore, weak acids should be preferred over stronger acids whenever possible.

All in all, the most effective measure to avoid poisoning by metals and phosphorous is to completely avoid these species in the exhaust or at least to keep their levels as low as possible. While a careful choice of lubricating oil is a direct engine-related measure, the purification of (bio)gas can particularly help alleviating sulfur and silicon poisoning. In this regard, a variety of promising techniques that mostly rely on efficient absorbers or adsorbers for removing sulfur species and siloxanes from biogas have been developed [7,296–300]. Since phosphorous can hardly be avoided completely, innovative washcoat technologies are necessary to mitigate P-poisoning [301]. For instance, a controlled modification of the support with phosphorous during catalyst synthesis can enhance the P-tolerance of noble metal-based oxidation catalysts. As recently demonstrated by Zhang et al. [302], Pd supported on a phosphate-modified alumina maintains the catalytic activity under conditions relevant to stoichiometrically operated natural gas engines. In addition, Jianjun et al. [303] observed a stabilization of palladium in its active PdO form, which they suggested is due to the electronic interaction between the Pd particles and the P additive.

3.6. Implications for modern catalytic converters and operation procedures

The previous sections, which provide an overview on fundamental aspects of palladium-based methane oxidation catalysts, emphasize that both activity and durability heavily depend on manifold factors like catalyst formulation, noble metal state, gas composition, and temperature. Since with transient engine operation also catalysts can undergo highly dynamic changes, tracking the state of the active sites is a prerequisite for further developing catalytic converters and for tuning the operation conditions to ensure long-lasting and efficient methane conversion. Besides applying high-temperature regeneration procedures once the activity decreased considerably, more recent studies showed that periodic regeneration under milder conditions is a promising approach for maintaining a high methane conversion. Reductive pulsing on a regular basis can alleviate the severe yet reversible water inhibition on palladium-based catalysts and does not only ensure high CH_4 conversion during long-term operation as first demonstrated by Ciuparu et al. [138] and later confirmed by Petrov et al. [150], but also represents an efficient in situ activation strategy for Pd-based catalysts. During and after reductive pulsing, Karinshak et al. [188] reported a higher activity compared to that of a fully oxidized catalyst and explained this observation by a threefold effect. First, rich conditions remove surface adsorbates such as hydroxyls from the catalyst, which restores surface sites making them available for adsorption of reagents. Second, at least at the noble metal surface short phases of oxygen deficiency facilitate the reduction of PdO to metallic Pd, which is less prone to adsorption of hydroxyl species. However, this is just an interim state, as Pd can rapidly reoxidize to surface PdO once the operation switches back to lean conditions. And third, catalysts are dynamic, particularly under dynamic oxidation-reduction cycles. Hence, reductive pulsing can influence the noble metal particle size and morphology, hereby amplifying phenomena like surface roughening and slight particle sintering, which can ultimately promote methane conversion over Pd-based catalysts. By means of *operando* XAS data during dynamic operation of a Pd/Al_2O_3 catalyst by applying short reducing pulses (SRP), Franken et al. [189] confirmed these findings and demonstrated the suitability of reducing pulses for reactivating Pd/Al_2O_3 samples that have been subject to harsh thermal aging at 800 °C for 60 h or to hydrothermal aging at 600 °C for 24 h. Fig. 15 summarizes the great potential of transferring insights gained by comprehensive testing and characterization to application-relevant real-world conditions. Similar oxidizing/reducing pulses were previously used to tune the noble metal particle size and state, and thus the performance of diesel oxidation catalysts [304].

Analogously, the periodic reductive treatment is a feasible strategy to overcome catalyst deactivation caused by sulfur species. Engine test bench runs conducted under lean conditions for a $Pd\text{-}Pt/CeO_2\text{-}ZrO_2$ catalyst by Gremminger et al. [221] demonstrate the feasibility of short reducing pulses on a regular basis for maintaining sufficient methane conversion at a moderate exhaust temperature of approximately 450 °C in the presence of 0.3 ppm SO_2 (Fig. 16). Similarly, during continuous engine operation at 550 °C under lean conditions, Lehtoranta et al. [305] report regeneration by switching the engine driving mode to stoichiometric conditions for several minutes per day as a suitable approach for preserving the catalytic activity of a Pd-Pt methane oxidation catalyst in a gas stream containing 0.5 ppm SO_2. Notably, the bimetallic oxidation catalyst ensures formaldehyde conversion rates of more than 95%, irrespective of the aging state of the catalyst [221]. This underscores that for the abatement of HCHO emissions diffusion limitation as discussed below (cf. Section 4) is the decisive factor rather than catalyst deactivation.

Exploiting interactions between real-world exhaust gas components can open up additional opportunities for diminishing undesired

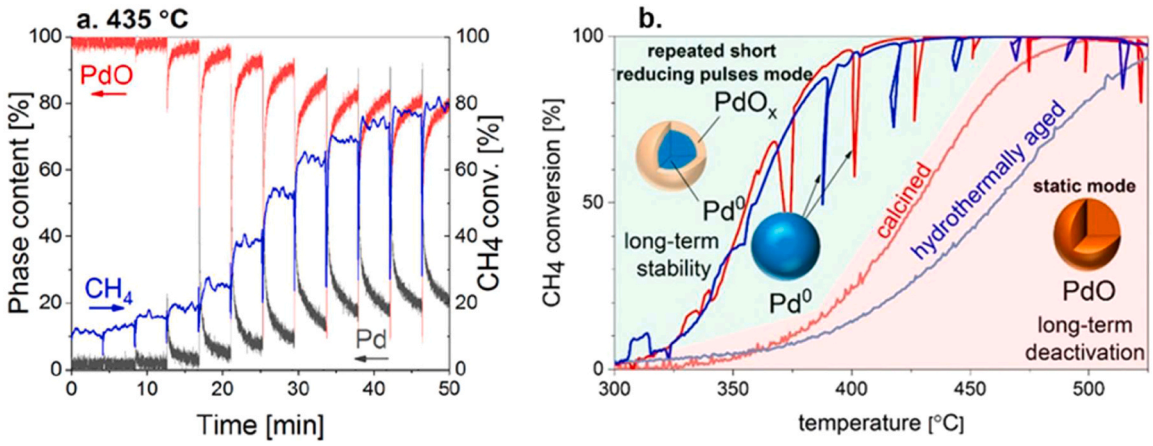

Fig. 15. a) Methane conversion and phase content of Pd/Al_2O_3 as followed by *operando* XAS during dynamic operation and b) comparative light-off measurements under static and dynamic conditions with reductive pulsing equalizing hydrothermal aging. Adapted with permission from ref. [189]. Copyright 2021 American Chemical Society.

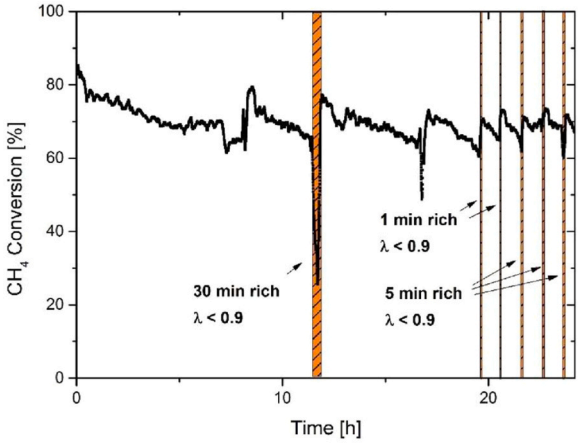

Fig. 16. CH_4 conversion as function of time over a monolithic $Pd\text{-}Pt/CeO_2\text{-}ZrO_2$ catalyst operated behind a natural gas engine running at $\lambda = 1.68$ (2680 ppm CH_4, 660 ppm CO, 7.5 vol.-% CO_2, 7.7 vol.-% O_2, approximately 0.3 ppm S-species) with temporary switches to $\lambda < 1$. Reprinted with permission from ref. [221]. Copyright 2017 Elsevier.

deactivation effects. While the presence of steam was found to intensify sulfur poisoning compared to a dry gas stream [223,224], the presence of water vapor in a reductive gas mixture facilitates desulfation of poisoned noble metal catalysts. Steam did not only reduce the onset temperature of sulfur desorption [306], but also increased the total amount of desorbed sulfur species, hereby restoring the catalytic activity more efficiently than a dry oxygen-free gas mixture [222]. Possible explanations range from a lower desorption energy in the presence of water, since support-related sulfates in the form of $(Al_3O_3)SO$ can react with water and form $(Al_2O_2)SO(OH)$ [307], to a steam reforming reaction between methane and water that results in the formation of H_2 species, which ultimately contribute to a surface regeneration via H_2S release [222].

With respect to the gas atmosphere, several recent studies report a lower SO_2-induced deactivation rate of Pd-Pt methane oxidation catalysts if NO_x is present in the gas stream [197,258,308]. Sadokhina et al. [197] suggest that under these conditions an increased tendency of surface sulfite formation and a lower sulfate formation rate are encountered. Similarly, Auvinen et al. [308] propose a strong competition for active sites among SO_2 and NO_x. Noble metal sites temporarily blocked by NO_x could enforce a spillover of SO_x to the support, hereby leading to $Al_2(SO_4)_3$ formation instead of catalytically inactive $PdSO_4$.

Despite these promising observations on the effect of the gas mixture composition, the results point to the need for more fundamental insights into these processes for a rational usage. In this regard, studies that consider different length- and time-scales are of special value. A series of studies on CO oxidation over Pt/CeO_2 catalysts, which is frequently used as a model system for investigating catalyst dynamics, profoundly demonstrated the feasibility of exploiting dynamic operation conditions for maximizing the catalyst performance in lab-scale setups, i.e. as achieved by well-defined temporary lean-rich cycling that offers an elegant way for tuning the particle size, structure, and oxidation state of oxidation catalysts [304,309–312]. Notably, spatiotemporal insights from IR thermography and spatially resolved XAS measurements on model-like powder catalysts could recently be transferred to realistic monolithic samples [313]. Herein, spatial profiling (also known as SpaciMS or SpaciPro [188,314,315]) allowed the presence of different reaction zones and noble metal particle size gradients along the monolithic oxidation catalyst to be uncovered, which may ultimately be the basis for generating highly efficient reaction zones for a variety of pollutants along a single catalyst.

3.7. Alternative design options for the exhaust gas after-treatment architecture

Apart from the endeavor to optimize conventional catalyst formulations and operation procedures, also additional technical elements in the tailpipe design have been proposed for ensuring high and long-lasting methane conversion. Kinnunen et al. [316] demonstrated the potential of combining existing technologies by placing a traditional Pd-Rh three-way catalyst upstream of a methane oxidation catalyst. The TWC with its at least temporary good sulfur storage ability did not only increase the sulfur tolerance of the overall catalyst system during lean operation, but also produced reducing agents under rich conditions, hereby promoting the regeneration of the downstream Pd-Pt methane oxidation catalyst. Similarly, also an upstream diesel oxidation catalyst (DOC) can substantially increase the catalytic methane conversion performance and durability [317]. While this approach provides impressive results at a model-like synthetic gas test bench with respect to methane conversion, secondary emissions due to the formation of undesired by-products like N_2O or NH_3, particularly during regenerative periods, represent a major challenge [317]. Hence, a careful control of the exhaust gas composition and regeneration timing is necessary to minimize secondary emissions. Current EURO VI emission legislation for a lean-operated natural gas engine [318], for instance, can be met by a well-harmonized after-treatment system. Notably, the upcoming EURO VII regulations [319,320] will add even more complexity to the tailpipe

design and operation procedures, since the emission limits will also comprise exhaust species that remained unregulated so far. Particularly avoiding the formation of the strong greenhouse gas N_2O, which does not only form during regeneration of the aforementioned catalyst system [317], but which can also form over Pd-Pt oxidation catalysts as a consequence of interactions between hydrocarbons and NO_x [321,322], is crucial.

In search of an efficient and low-cost method for CH_4 reduction, Keenan et al. [323] suggested the use of ozone (O_3) rather than oxygen for oxidizing methane, resulting in up to 60% CH_4 conversion at 220 °C over an iron-containing zeolite (Fe-BEA). Although the gas composition of 200 ppm CH_4, 150 ppm CO, and only 3 vol.-% H_2O contains unrealistic low methane and water levels, the concept of exploiting ozone as an enabler for low-temperature methane oxidation appears interesting, particularly for stationary large-bore engines. More recently, Yasumura et al. [324] exploited a computer-based automated reaction route mapping to design main-group element-based catalysts containing Si and Al for low-temperature CH_4 combustion with O_3. The developed proton-type beta zeolite was demonstrated to be water- and sulfur-tolerant and was found more active than a 5 wt.-% Pd/Al_2O_3 benchmark catalyst at temperatures between approximately 100 °C and 300 °C, whereas at higher temperatures the Pd-based catalyst was more active. When considering an upscaling to real-world applications, the ozone generation itself needs to be embedded into a holistic process design, since in addition to the energy consumption for ozone generation, also NO_x formation needs to be minimized by choosing a suitable generator design [325].

4. Formaldehyde emission control

Removal of formaldehyde is important not only because its high reactivity can lead to ozone formation [326], but especially due to its classification as carcinogenic and toxic compound [35,327]. In addition to indoor sources, the outdoor emission of formaldehyde and other carbonyl compounds due to industrialization, increased mobility, and energy consumption has become of major environmental concern [328]. Recent studies show that formaldehyde emissions potentially can be generated from both conventional and renewable fuels used for transportation and in power plants for energy production [329–332]. In the following the formation and catalytic conversion of formaldehyde is discussed in detail for natural gas applications.

4.1. Formaldehyde formation

Despite formaldehyde being suggested as an intermediate compound during methane combustion, its formation as a product is not thermodynamically favored during homogeneous combustion of premixed CH_4-air mixtures under lean conditions (<1 ppb, [333,334]). Hence, the presence of this partial oxidation product in the exhaust of most natural gas engines (over 50 ppm [334,335]) indicates that other factors contribute to HCHO generation. According to Mitchell and Olsen [32], formaldehyde formed in the upstream part is consumed in the downstream region of a self-propagating flame leading to no emissions. At the same time, the authors claim that partial oxidation at sufficiently low temperatures to prevent further conversion could lead to formaldehyde emissions, as for instance present at cold walls, crevices [334], or cold regions of the flame (400 – 800 K, [33]) due to incomplete fuel-air mixing zones. Several studies have shown that the engine type and operating parameters such as air-to-fuel ratio, ignition timing, compression ratio, and engine speed can significantly affect formaldehyde emissions [33,37,336]. When completely switching a dual-fuel marine engine from diesel fuel to natural gas, a remarkable reduction of PM, NO_x, and CO_2 concentrations was detected of about 93%, 92%, and 18%, respectively [337]. However, this occurred along with a simultaneous increase in formaldehyde and carbon monoxide emissions by factors of 6 and 4, respectively, and CH_4 increased from less than 0.002 g/kWh to 11.5 g/kWh. Similarly, Zavala et al. [338] reported formaldehyde emissions of up to 9 g/kWh, depending on the operation mode (reactivity-controlled compression ignition or conventional dual-fuel combustion) for a dual-fueled natural gas-diesel engine equipped with a dual-loop EGR system. With respect to the air-to-fuel ratio, Bauer and Wachtmeister [33] showed a clear increase in HCHO emissions at higher lambda values that correspond to leaner conditions. Furthermore, Van Roekel et al. [339] found that implementing an exhaust gas recirculation system to a stoichiometric natural gas engine results in higher formaldehyde emissions due to the lower combustion temperatures.

Fuel composition has as well an effect not only on the formaldehyde concentration in the exhaust gases but also on the formation of further aldehydes and ketones. By sampling the exhaust gases of vehicles operated exclusively on natural gas and of dual-fueled vehicles running on natural gas or gasohol/alcohol/diesel, Correa and Arbilla [340] correlated the increase of formaldehyde emissions with the increased use of compressed natural gas. Moreover, when using biomethane containing 98.69 vol.-% CH_4 and 1.31 vol.-% CO_2 for a stoichiometric natural gas engine, Lee et al. [331] found higher concentrations of formaldehyde and acetaldehyde in the engine-out gas stream in comparison to the values measured for the corresponding engine fueled with compressed natural gas (CNG; 91.33 vol.-% CH_4, 8.45 vol.-% C_2-C_5-species, 0.22 vol.-% N-species). Investigations by Karavalakis et al. [341,342] on the influence of high methane and/or high Wobbe number fuels on the emissions of lean-burn and stoichiometric natural gas heavy-duty vehicles showed that fuels with lower methane content and lean-burn vehicles produce higher aldehyde emissions, but for all vehicles tested formaldehyde was the aldehyde emitted most, followed by acetaldehyde. The authors assigned the formation of formaldehyde not only to methane but also to ethane presence. The formation of formaldehyde as a by-product of hydrocarbon oxidation was reported to occur even over NH_3-SCR catalysts, as previously observed for V_2O_5-based [343–346] as well as for Fe-zeolite and Cu-zeolite catalysts [347,348]. For all emission cases, finding a catalyst formulation suitable to remove formaldehyde over a broad temperature range is mandatory.

4.2. Oxidation catalysts and reaction mechanism

As formaldehyde is emitted also by various household and industrial indoor pollution sources, its removal by complete oxidation according to Eq. 28 at low temperatures has been highly desired in recent years [349–357].

$$HCHO + O_2 \rightarrow CO_2 + H_2O \quad (28)$$

Numerous non-noble metal and noble metal-based catalysts have been reported, which are discussed in detail in the review papers by Yusuf et al. [358] and Guo et al. [359]. Among the non-noble metals, Mn, Co, Ce, Sn, and their combination were considered as suitable catalysts; among the noble metals, Au, Ag, Pt, Pd, and Rh on various supports were investigated at low temperatures. While the majority of these catalysts was mostly studied under simplified reaction conditions, a number of studies was conducted also for combustion engine applications running on liquid [42,336,360–364] or gaseous [38,42,340,343,360,365,366] fuels that considered HCHO as relevant pollutant.

Mehne and Kureti investigated commercial α-Fe_2O_3 catalysts with respect to their activity for CH_4 and HCHO conversion [335]. Despite the poor performance for methane oxidation, these catalysts showed a promising activity for formaldehyde conversion above 300 °C via a reaction mechanism involving OH surface groups, which was confirmed by tests on a stationary biomethane engine. In contrast, the participation of support lattice O was suggested to contribute to formaldehyde oxidation for a Mn-doped CeO_2 catalyst upon formaldehyde adsorption and C-H bond cleavage in a Mars-van-Krevelen mechanism [367,368]. This does not exclude O_2 adsorption at ceria-oxygen-vacancy/defect

sites next to Mn, leading to a Langmuir-Hinshelwood-like mechanism according to DFT calculations [368].

The possibility of using NH_3-SCR catalysts for 2-way SCRonDPF applications [369–371] represented one of the driving forces for investigating the activity of this class of catalysts for hydrocarbon removal, including also formaldehyde oxidation. In a study of Zheng et al. [344], it was shown that a promising formaldehyde conversion can be achieved with a conventional V_2O_5-WO_3-TiO_2 catalyst. However, the oxidation process is not highly selective towards CO_2 formation and leads to CO emissions. Additionally, through a reaction involving NH_3, formaldehyde is converted also to highly toxic HCN [372], as discussed in detail in the following sections.

For further increasing the formaldehyde oxidation to CO_2 and H_2O at lower temperatures and under more demanding reaction conditions, noble metal-based catalysts seem to be the most suitable systems, especially when platinum is chosen as active component [373–375]. When comparing a series of noble metal catalysts supported on TiO_2, Zhang and He [375] found Pt/TiO_2 as the most efficient in comparison to Rh-, Pd-, and Au-based samples, converting formaldehyde already at room temperature in a model gas mixture containing 100 ppm HCHO and 20 vol.-% O_2 in balance He. A simplified mechanistic scheme was proposed based on DRIFTS measurements with dioxymethylene, formate, and adsorbed CO species as reaction intermediates for HCHO oxidation, and with the conversion of formate to adsorbed CO as the rate determining step. Based on results from XPS and kinetic performance tests, Huang et al. [351] claimed that metallic platinum rather than PtO_x results in high HCHO conversion rates over Pt/TiO_2, which is supported by later investigations on similar Pt catalysts by means of XAS measurements [246]. McCabe and McCready [376] proposed formaldehyde decomposition via dissociative adsorption on platinum sites leading to hydrogen abstraction from HCHO and a subsequent reaction with oxygen adsorbed on the surface. Similarly, a surface science study by Attard et al. [377] combining low-energy electron diffraction (LEED), XPS, and temperature-programmed reaction spectroscopy (TPRS) reports a HCHO split into hydrogen atoms and CO over a clean Pt(110) surface, whereas the presence of surface oxygen changes the mechanism. Particularly in a highly lean atmosphere (excess oxygen), microkinetic modeling suggests HCHO decomposition via an oxygen-assisted mechanism, in which surface oxygen acts as the most abundant reaction intermediate (MARI) and CO is oxidized via a Langmuir-Hinshelwood mechanism [378,379]. These possible reaction paths were summarized by Torkashvand et al. [379] (shown here in Fig. 17) and were included in a numerical model based on 30 elementary-like-steps among six gas phase and ten surface species.

The formaldehyde oxidation mechanism on the Pt/TiO_2(101) surface was further investigated by Li et al. [380] using DFT calculations. For this system containing highly dispersed Pt atoms, the dehydrogenation of formaldehyde is suggested to occur at Pt-5cTi (5-fold-coordinated titanium atoms) bridged sites with the reaction pathway in the presence of oxygen including HCHO → HCOOH → HCOO → CO_2 as intermediates.

Replacing TiO_2 with another support may lead to variations in Pt

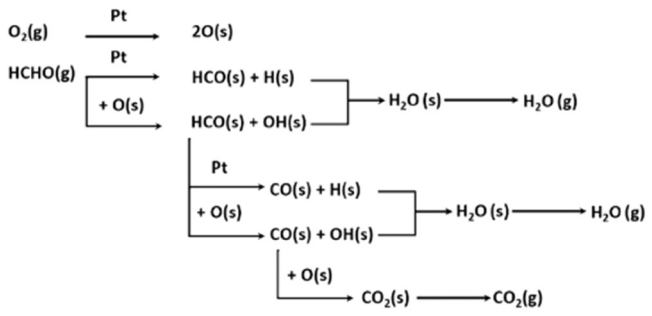

Fig. 17. Reaction scheme of formaldehyde conversion over platinum. Reprinted with permission from ref. [379]. Copyright 2018 Springer Nature.

particle size and oxidation state, which directly affects the catalyst performance. Moreover, a strong interaction with the support is expected to prevent strong sintering during exposure to high temperatures. For a rather inert support like γ-Al_2O_3, over 90% conversion of formaldehyde was found by Sodhi et al. [361] for a 5 wt.-%Pt/γ-Al_2O_3 catalyst at an oxygen-to-formaldehyde ratio over 2 in a dry gas mixture. Recently, the influence of a γ-Al_2O_3 support was directly compared with that of TiO_2-SiO_2 (9:1 wt. ratio) for a 0.5 wt.-% Pt catalyst [246]. In a model gas mixture containing 80 ppm HCHO, 10 vol.-% O_2, 12 vol.-% H_2O, and 6 vol.-% CO_2 balanced in N_2, after an initial activation by a slight reduction of Pt species, 75% formaldehyde conversion could be reached at 160 °C for the alumina-supported catalysts, whereas the same conversion was obtained at 180 °C for the TiO_2-SiO_2-supported sample. The difference in activity was explained by the lower dispersion of Pt particles on the TiO_2-SiO_2 support in comparison to that attained on the high surface area alumina. By doping a Pt/nanosized Al_2O_3 catalyst with sodium (Na), the concentration of the noble metal could be further reduced to only 0.05 wt.-% while maintaining a very high formaldehyde conversion at room temperature via a mechanism involving surface OH groups [381].

Although the corresponding Pd-catalyst shows an inferior low-temperature activity and full conversion is achieved only above 300 °C, the use of a typical Pd-Pt bimetallic methane oxidation system supported on alumina (3 wt.-% total noble metal loading, Pd:Pt = 5:1) results in a good formaldehyde conversion above 175 °C when choosing a model gas mixture containing 12 vol.-% O_2, 12 vol.-% H_2O, 6 vol.-% CO_2, 3000 ppm CH_4, 1000 ppm NO, and 100 ppm HCHO in balance N_2 (Fig. 18) [49]. Hence, using bimetallic Pd-Pt oxidation catalysts may be the technically and economically most attractive approach to simultaneously cope with CH_4 and HCHO emissions in lean natural gas engine exhausts.

The influence of the gas mixture on the activity of monometallic Pt-catalysts was systematically investigated by Schedlbauer et al. [246]. Irrespective of the catalyst support (Al_2O_3 or TiO_2-SiO_2), the addition of 700 ppm CO to the model gas mixture containing 80 ppm HCHO, 12 vol.-% H_2O, 10 vol.-% O_2 in balance N_2 shows two effects: an activity decrease at temperatures lower than the CO oxidation ignition temperature and an improvement of the formaldehyde conversion at higher temperatures. At low temperatures when no CO conversion takes place, platinum catalysts suffer from strong inhibition by carbon monoxide, presumably due to a stronger adsorption tendency compared to formaldehyde [49,246,382]. In line with the HCHO conversion mechanism over platinum involving CO surface species [350,376–379], this ultimately causes a negative reaction order with respect to formaldehyde conversion [49]. However, with an increasing temperature the presence of CO promotes the reduction of platinum particles to metallic platinum sites [383], which are considered the most active for HCHO oxidation [351].

In contrast to the monometallic Pt/Al_2O_3 catalyst, a Pd/Al_2O_3 sample does not seem to be affected by CO presence, whereas a slight inhibition is shown over a bimetallic Pd-Pt/Al_2O_3 catalyst (Fig. 18). If NO_x (350 ppm NO and 200 ppm NO_2) is added to the gas mixture, a significant decrease of the low-temperature activity is observed. Analogous to previous findings on CO and propylene (C_3H_6) oxidation over Pt/Al_2O_3 diesel oxidation catalysts [384], NO_x strongly competes with HCHO for surface sites and particularly NO_2 could oxidize platinum sites, which explains the observed inhibition [246]. The inevitable exhaust gas component water, on the other hand, which poses a major challenge for methane oxidation over palladium, does not show a negative impact on formaldehyde conversion over platinum catalysts [49].

4.3. Realistic conditions and related challenges

Considered as a compound posing the greatest concern to human health, formaldehyde concentration has been monitored for decades in the exhaust of different lean or stoichiometric combustion engines

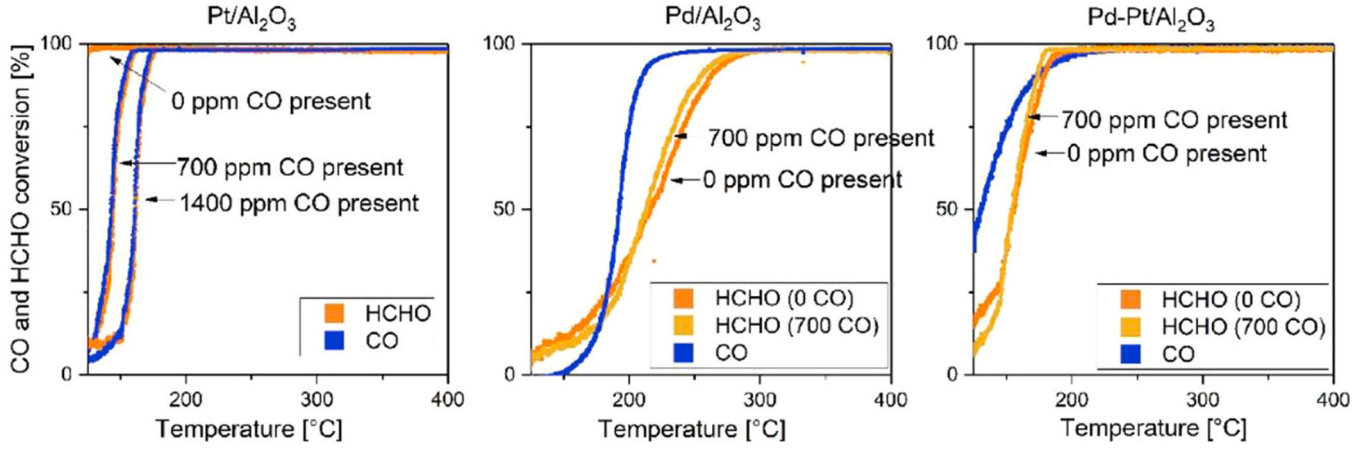

Fig. 18. Formaldehyde conversion over alumina-supported Pt, Pd, and Pd-Pt catalysts and the influence of CO addition to the reaction gas mixture. The CO oxidation light-off profile is given in blue. Reprinted with permission from ref. [49]. Copyright 2020 Elsevier.

fueled with gasoline, diesel or alternative fuels including natural gas. For both stationary and mobile sources, a clear positive effect of commercially applied technologies ranging from oxidation catalysts and three-way catalysts to EURO IV or SULEV vehicles has been observed, as summarized by Zhu et al. [385] for the time frame until 2003. In general, the extent of formaldehyde removal increased over time with up to 95% conversion when increasing the complexity of the catalytic aftertreatment system. For fulfilling newer and more stringent emission regulations the possibility of using stoichiometric CNG engines for heavy-duty applications has been explored by several manufactures [386,387]. The work of Hesterberg et al. [44] directly compares the emissions from vehicles fueled with diesel or CNG (lean and stoichiometric engines) relative to the catalyst technology used. Up to 98% of the formaldehyde emissions were reduced over an oxidation catalyst under lean conditions and complete conversion was achieved with a TWC. Analogous, by using a more advanced TWC technology, the formaldehyde concentration is decreased to levels found in background air [388], which is in line with another similar study by Lemel et al. [336]. Furthermore, Badrinarayanan et al. [389] evaluated five different commercial oxidation catalysts for their ability to reduce emissions of partial combustion products (CO, HCHO, and VOCs (volatile organic compounds)) of a lean-burn natural gas engine used for power generation. Different activity profiles were revealed with a maximum formaldehyde conversion of 90–96% but limited activity at low temperatures for most tested catalyst technologies, which is also in agreement with similar investigations [390]. Most of these catalysts are based on different loadings of one or two noble metals among Pt, Pd, and Rh [385]. Even more advanced or structured catalysts contain at least one noble metal-based component [364]. For all these catalyst formulations catalyst deactivation may occur due to catalyst poisoning and thermal aging under the exhaust conditions of a natural gas engine. Especially sulfur poisoning is known to severely affect Pd- or Pd-Pt-based catalysts, as described in detail in the previous sections. For state-of-the-art Pt-only oxidation catalysts, long-term lean operation, i.e. 100 h, at 500 °C under sulfur-free synthetic exhaust gas conditions does not considerably affect their formaldehyde conversion ability, which was maintained at around 95% above 200 °C [391].

However, although sulfur affects platinum significantly less than palladium [228], sulfur poisoning has been observed also in the context of platinum-based oxidation catalysts operated in lean atmosphere [230, 392–394]. As already comprehensively discussed in the section on bimetallic methane oxidation catalysts, platinum efficiently oxidizes sulfur species to SO_2 and finally SO_3, which is then transferred to the support material. Schedlbauer et al. [391] investigated the effect of low and high SO_2 concentrations (1.75 ppm versus 7 ppm) in the gas mixture under steady-state and transient reaction conditions for a series of commercial platinum catalysts. It was found that only the low-temperature activity for formaldehyde oxidation is affected if the catalyst is poisoned at 500 °C for 100 h; herein, the deactivation extent increased with the SO_2 concentration in the gas stream. A more pronounced deactivation was observed upon SO_2 poisoning under transient conditions, i.e. a light-off shift towards higher temperatures and a decrease of the maximum conversion at 500 °C by 5–10%, which suggests sintering of the noble particles and morphological changes that commonly occur during long-term operation of noble metal catalysts as described by Hansen et al. [395]. Notably, the transient lab-scale aging cycles resulted in a similar conversion profile to that obtained after approximately 200 days of field aging at a block heat and power plant operated with biogas (approximately 3.5 ppm S) [391]. The same trends were observed during field aging of a commercial Pt-Al_2O_3 catalyst in the exhaust of a stationary two-stroke lean-burn natural gas engine supplied with fuel directly from the city pipeline [396]. In addition to uniform sulfur deposition over approximately two months of continuous operation, phosphorous (P) and zinc (Zn) originating from lubrication oil were found to accumulate first at the front and then in the middle and rear of the periodically analyzed catalyst core. As illustrated in Fig. 19, the light-off temperature for formaldehyde conversion increased by about 50 °C, accompanied by a drop in the maximum reduction efficiency to approximately 80%, which for a pre-catalyst concentration of

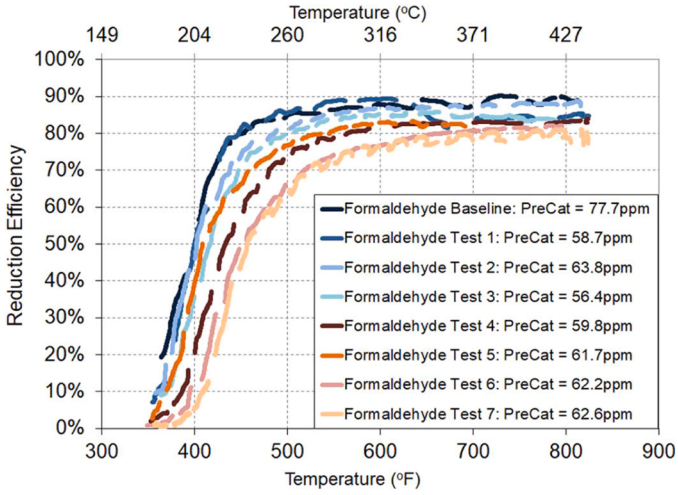

Fig. 19. Temperature-dependent HCHO reduction efficiency of a Pt/Al_2O_3-based catalyst (containing dopants) at different aging stages. Reprinted with permission from ref. [396]. Copyright 2018 ASME.

60 ppm HCHO is already close to the lowest acceptable limit to fulfill the applied emission standards.

For stoichiometric natural gas engines, aging of a three-way catalyst under realistic application conditions leads as well to thermal and chemical deactivation. Upon simulating the real-world aging conditions at a natural gas burner rig facility for a commercial Pt-Pd-Rh TWC supported on $CeZrO_x$, thermal aging was identified as the main material degradation mechanism leading to a pronounced decrease of the catalyst surface area [397,398]. Additionally, the contamination with S and P was detected at the inlet positions. While the sulfur amount can be reduced significantly by applying a dithering procedure at 700 °C or by thermal programmed decomposition up to 950 °C, phosphorous cannot be removed from field-aged catalysts by thermal treatment. Some of these effects have been already implemented in TWC aging models to predict emission profiles during driving cycles for CO, THC (total hydrocarbons), and NO_x [399]. However, to the best of our knowledge, no experimental or modeling results have been reported with respect to HCHO emissions for state-of-the-art TWC catalysts upon deactivation.

In addition to the catalytic reaction and deactivation aspects, heat and mass transfer in the catalytic converter are decisive factors to be taken into account when designing efficient exhaust gas after-treatment systems. Kinetic testing of both model-like powder catalysts and commercial monolithic samples as well as spatially resolved concentration profiles within a monolithic catalyst substrate consistently point to a pronounced external mass transfer limitation of HCHO oxidation, which impedes full formaldehyde conversion [246,379,391]. Notably, these observations regarding mass transport phenomena are in line with earlier findings by Wang et al. [400] on HCHO conversion at room temperature over a $Pd/\gamma\text{-}Al_2O_3$ catalyst for controlling indoor pollutants. In the end, the high intrinsic reaction rate of noble metal-catalyzed formaldehyde oxidation results in transport limitation, because mass transport is slow at very low HCHO levels due to a small concentration gradient between the gas phase and the boundary layer. Under consideration of the upcoming ultra-low emission limits for combustion engines, achieving near-to-zero HCHO emissions appears critical. Although longer monoliths with a higher cell density could mitigate the mass transfer limitation, the generated backpressure restricts the use of smaller channel diameters. Related, higher temperature or platinum loading increase the intrinsic reaction rate, but also the diffusive mass transfer, which becomes dominant and process limiting at about 300 °C [401]. Therefore, in the context of engine operation and process control, only reduced mass flow rates that result in higher residence times in the catalytic converter could offer the prospect to at least partly mitigate the transport limitation. As demonstrated by the simulated three-dimensional HCHO concentration distribution in Fig. 20, a non-uniform washcoat distribution additionally hampers the diffusion-limited HCHO conversion. In contrast, a uniform and thin catalyst layer along with sophisticated channel shapes that prevent ineffective thick washcoat deposits in the channel corners of the substrate have been identified as key factors governing high formaldehyde conversion rates [53].

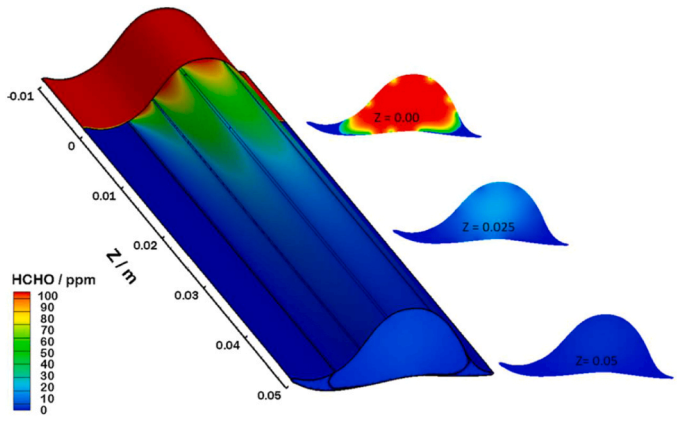

Fig. 20. Simulated 3D concentration distribution of HCHO along a sinusoidal-shaped monolith channel assuming a non-uniform coating with porous washcoat.
Reprinted with permission from ref. [53]. Copyright 2018 Elsevier.

Last but not least, the ongoing progress in additive manufacturing and 3D-printing allows to design more and more advanced geometries for modern catalytic converters [402–405]. Creating non-linear flows and inducing turbulences by advanced substrate design are feasible approaches to enhance the interactions between the washcoat and the pollutants [406], which may also be exploited for catalytic formaldehyde decomposition.

5. NO_x control by selective catalytic reduction (SCR)

Since the relatively low combustion temperatures during lean engine operation cause only comparably low NO_x emission levels [42,46] and allowed meeting past emission standards solely by tuning engine operation parameters [407–411], commonly low-temperature methane oxidation and the removal of very low HCHO levels with an oxidation catalyst are considered the most relevant hurdles within an exhaust gas after-treatment system for lean-burn gas engines. However, the current and upcoming stricter NO_x emission limits make the use of a more complex exhaust gas after-treatment system that includes a NO_x removal catalyst mandatory. In addition to a short summary on the origin of NO_x formation, the following sections point out which issues need to be addressed for efficient NO_x removal from natural gas engine exhausts.

5.1. NO_x formation

While the emission of HCs, HCHO, or CO is a predominant consequence of non-ideal combustion, i.e. due to non-homogeneous fuel-air mixtures in the combustion chamber, the origin of NO_x is commonly considered threefold [412].

1. At combustion temperatures well above 1000–1300 °C, nitrogen and oxygen can react to form thermal NO_x according to the so-called Zeldovich mechanism [47,413,414].
2. Fast reactions between fuel-born hydrocarbon radicals and molecular N_2 from air form so-called prompt NO_x [415,416].
3. Nitrogen species in the fuel itself are oxidized during the combustion process, resulting in the formation of fuel NO_x [417–419].

Although the formation pathways vary depending on the combustion conditions such as fuel composition, design of combustor and combustion chamber, flame propagation, and degree of fuel-air mixing [412, 420–423], thermal and prompt NO_x are commonly considered most relevant [424]. Nevertheless, the relevance of fuel-bound nitrogen will further increase with a more widespread biofuel usage in the future. For instance, biogas contains up to 0.05 vol.-% NH_3, which can increase the engine-out NO_x emissions [425]. That the N-content in the fuel determines the NO_x (and N_2O) levels in the engine-out raw emissions is known already since the late 1980 s [426]. Several later publications further emphasized the relevance of the nitrogen content in solid biomass and liquid bio-based energy carriers for the emission of NO_x [427–429]. Analogously, generally higher NO_x emissions were reported when operating combined heat and power plants with biogas instead of natural gas [430]. Therefore, along with sulfur and other impurities, the removal of N-containing species prior to biogas combustion has experienced growing attention [431,432]. Moreover, a more widespread usage of biofuels requires a careful optimization of both the combustion process and the exhaust gas after-treatment system [330,433]. For instance, although its presence decreases the calorific power, the CO_2 content in the biogas has been reported to suppress NO_x formation during the combustion itself [434,435]. In addition to an efficient

catalytic exhaust gas after-treatment system, exploiting such effects is an integral part during the design of near-zero emission combustion engines.

5.2. Catalytic NO_x removal

NO_x emissions of a stoichiometric natural gas engine are efficiently controlled by means of a TWC, which is able to convert CO, CH_4, and NMHC simultaneously. As mentioned in the previous sections, the catalysts tested so far contain Pd, Rh, and/or Pt typically supported on doped $CeZrO_x$ or Al_2O_3 [24]. Often in a combination with an EGR system, near-zero NO_x emissions have been achieved for various mobile and stationary applications such as refuse trucks [436,437], city buses [331], and passenger cars [438], some in line with EURO VI regulations. However, a careful control of the air-to-fuel ratio is necessary to maintain both NO_x and CH_4 conversion high. As recently shown by Gong et al. [439] for a Pd-based commercial TWC, NO is converted over a broader temperature range under slightly fuel-rich conditions, whereas at higher lambda values the high-temperature NO_x conversion drops significantly. The same impact of lambda variation was reported by several research groups and was correlated with the formation of more active metallic Pd species under fuel-rich conditions [104,440,441]. With respect to methane oxidation under the same conditions, an effect of the Pd oxidation state was identified as well, most probably combined with a water deactivation process at higher lambda values [439]. Lambda dithering/modulation conditions as present during real operation show also the potential to further improve NO_x conversion when carefully selecting the dithering amplitude to minimize the effect on other emissions [439,442,443].

For lean-operated gas engines, commonly the selective catalytic reduction of NO_x with NH_3 has been considered a feasible and well-established technology to efficiently reduce NO_x emissions in gas atmospheres that contain excess oxygen [444,445]. In diesel engine after-treatment systems, the exhaust stream typically passes the oxidation catalyst first before flowing through a $deNO_x$ catalyst that converts NO_x into nitrogen and water by using ammonia as reducing agent [446]. Similarly, for the emission control of lean-burn natural gas engines, the NH_3-SCR catalyst is usually located downstream the methane oxidation catalyst. The most applied SCR catalysts for NO_x removal are the vanadia-tungsten-titania (V_2O_5-WO_3-TiO_2) and copper/iron-zeolite systems, which are preferentially selected for different applications based on their specific characteristics.

V_2O_5-WO_3-TiO_2 enjoys great popularity especially for stationary applications where commonly a high sulfur-tolerance is required [446–449]. Due to the early industrial implementation, this less costly catalyst has been thoroughly investigated. As drawbacks, vanadia-based SCR catalysts exhibit limited low-temperature activity and moderate thermal stability, and the toxicity of the potentially volatile vanadium species triggered the development of more environmentally friendly alternatives. In contrast, iron- and copper-containing zeolites such as Fe/BEA or Cu/SSZ-13 show a better thermal stability and are preferred for applications involving a broader temperature window such as road transport [446,449–451]. Herein, Fe-zeolites that are mostly active at higher temperatures and Cu-zeolites that show high SCR activity already below 250 °C [452] can also be combined, e.g. by dual-layer or dual-brick concepts [453]. Over these catalysts, the SCR reaction strongly depends on the NO/NO_2-ratio and proceeds via the following reaction equations (Eqs. 29–31).

$$\text{Standard-SCR: } 4\ NO + 4\ NH_3 + O_2 \rightarrow 4\ N_2 + 6\ H_2O \quad (29)$$

$$\text{Fast-SCR: } NO + NO_2 + 2\ NH_3 \rightarrow 2\ N_2 + 3\ H_2O \quad (30)$$

$$NO_2\text{-SCR: } 6\ NO_2 + 8\ NH_3 \rightarrow 7\ N_2 + 12\ H_2O \quad (31)$$

As shown in a study by Olsen et al. [454], the NO_2/NO_x ratio is significantly higher (possibly >0.5) for lean-burn natural gas engines in comparison to other internal combustion engines, and can be further amplified by an oxidation catalyst. Hence, the fast-SCR and even the NO_2-SCR reaction become highly important when evaluating the NH_3-SCR performance. While we refer to the wide variety of literature with regard to mechanistic and general aspects of NH_3-SCR as suitable $deNO_x$ process in lean exhausts, we particularly discuss the specific challenges of NH_3-SCR that arise when implementing SCR catalysts into the exhaust tailpipe of lean-burn gas engines, typically after an oxidation catalyst.

5.3. Impact of other exhaust gas species on the $deNO_x$ efficiency

As summarized in a recent review article by Gramigni et al. [455], it is well-known that hydrocarbons can poison and deactivate Cu-zeolite, Fe-zeolite, and V_2O_5-based SCR catalysts due to competitive adsorption between HCs and NH_3, the formation of surface intermediates and concomitant blockage of active sites, physical blockage of pores particularly by large HCs or coke formation, or parasitic reactions between HCs and NH_3. Overall, vanadia-based SCR catalysts exhibit a slightly higher HC tolerance. Considering the composition of natural gas or biogas as well as the typical exhaust gas composition of natural gas engines (c.f. Table 1), heavy HCs are essentially irrelevant and only light NMHCs as well as CH_4 are expected to interact with the SCR catalyst if their full conversion is not achieved in the upstream oxidation catalyst.

In a recent study by Lehtoranta et al. [456], the efficiency of a V_2O_5-WO_3-TiO_2 NH_3-SCR catalyst was evaluated in combination with an upstream Pt-Pd methane oxidation catalyst or by integrating the V_2O_5-catalyst into the noble metal-based oxidation catalyst. While between 350 °C and 400 °C both systems showed over 90% conversion, at higher temperatures a lower NO_x conversion was measured in a gas mixture mimicking the emission levels of a power plant due to the competing oxidation/reduction reactions occurring in the integrated system.

Investigations on commercial Fe-BEA and Cu-SAPO SCR catalysts by Villamaina et al. [457] suggest a negligible influence of methane conversion on the selective catalytic reduction of NO_x. By combining the two catalytic systems in a serial arrangement but maintaining the total volume, about 90% NO_x reduction was obtained under standard-SCR conditions (Eq. 29) over a broad temperature range (200–550 °C). Only above 400 °C and under NO_2-SCR conditions (Eq. 31) the authors observed competing reactions with oxidation of methane to CO and CO_2.

Comparably good NO_x removal activities were reported for similar industrial SCR catalysts for heavy-duty vehicles running on compressed natural gas [458], sanitation trucks [459], or marine applications [460]. However, a series of challenges still needs to be considered in addition to the efforts necessary to further improve the SCR catalyst performance. Several studies reported recently the effect of small amounts of unreacted exhaust gas components or oxidation by-products on the $deNO_x$ efficiency. For instance, formaldehyde presence severely affects the NO_x conversion of both vanadia- and zeolite-based catalysts by inducing undesired side reactions [344,372,461,462]. This is illustrated in Fig. 21 for a Cu-SSZ-13 NH_3-SCR catalyst, which shows a dramatic drop in the low-temperature NO_x conversion combined with the formation of toxic by-products.

The mass transport-limited formaldehyde oxidation over noble metal catalysts as reported above frequently impedes complete HCHO conversion over the oxidation catalyst and makes an interaction between the gas mixture, formaldehyde, and the SCR catalyst inevitable. Under SCR conditions, formaldehyde readily reacts with ammonia to form hydrogen cyanide (HCN) [372,461,463], which is a side-reaction that detrimentally counteracts the purpose of a complex exhaust gas after-treatment system in two ways. First, the formation of HCN competes with the NH_3-SCR since it consumes the reducing agent and hereby retards the SCR activity by up to 20% as reported by Elsener et al. [461]. Second, hydrogen cyanide is an extremely poisonous substance for humans and environment [464]; short-time exposure to 300 ppm of

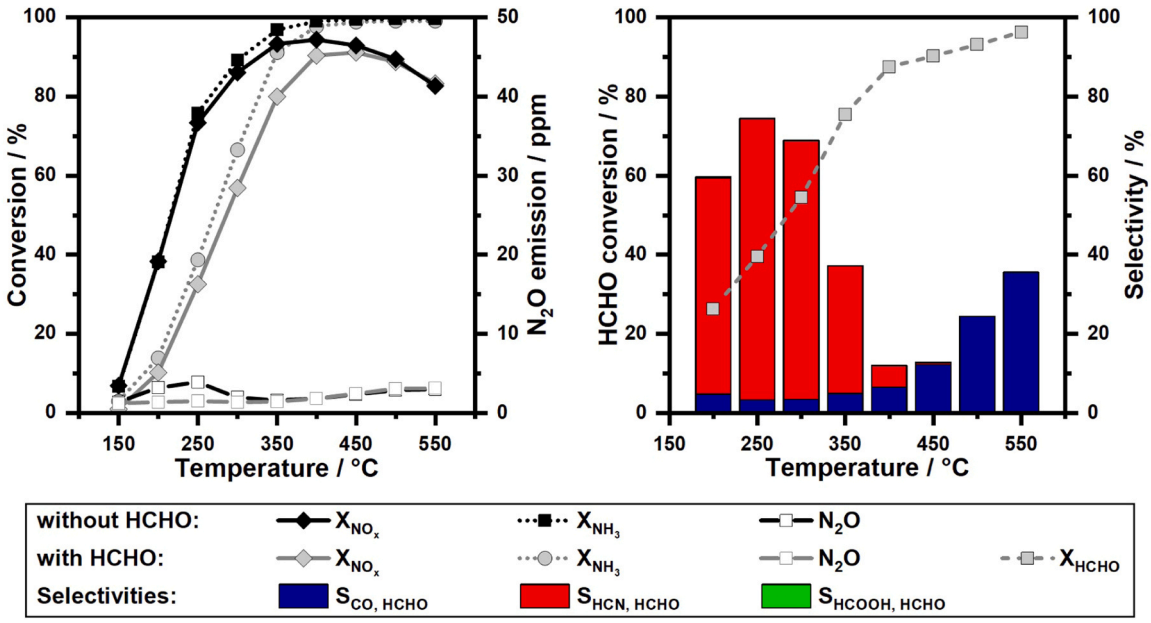

Fig. 21. NO_x and NH_3 conversion over Cu-SSZ-13 during standard-SCR with and without 80 ppm HCHO (left) and HCHO conversion and product selectivity towards CO, HCN, and HCOOH (right); HCOOH formation not observed. Reprinted with permission from ref. [372] under the terms and conditions of the Creative Commons Attribution (CC BY 4.0) license (http://creativecommons.org/licenses/by/4.0/). Copyright 2020 The Authors. Published by Wiley-VCH Verlag GmbH & Co. KGaA, Weinheim.

gaseous HCN, for instance, is considered lethal [465]. While there is consensus on the need for abatement of HCN emissions, it is not yet clear which of the formation pathways and chemical routes toward HCN that are summarized in Fig. 22 is the dominating one.

According to the DRIFTS investigations conducted by Zengel et al. [372] on Fe-ZSM-5, at low temperatures the oxidation of formaldehyde to formate species is followed by the reaction with ammonia to form formamide ($HCONH_2$), which finally converts to HCN after dehydration. A similar mechanism was suggested by Ngo et al. [463] for a V_2O_5-based SCR catalyst. In contrast, the study of Elsener et al. [461] on the HCN formation mechanism for a vanadia-based catalyst suggests that particularly at higher temperatures the decomposition of formic acid into CO and H_2O is favored. Therefore, the authors suggest an alternative formation path derived from well-known chemical reactions. According to Elsener et al. [461] and Nuguid et al. [466], the first step is rather a direct reaction between gas phase HCHO and pre-adsorbed NH_3 to form methanolamine ($HO\text{-}CH_2\text{-}NH_2$) and subsequently the dehydration of methanolamine yields HCN, either via formamide ($HCONH_2$) or via highly unstable methylene imine (H_2CNH).

In this context it should be noted that investigations on the mechanism of propene poisoning on Fe-ZSM-5 SCR catalysts uncovered the formation of formate (HCOO-) species as a consequence of C_3H_6 oxidation [467]. Under consideration of the HCN formation pathways presented in Fig. 22 that involve formic acid, future research should clarify in detail to what extent and under which reaction conditions the presence of light hydrocarbons promotes HCN formation over the SCR catalyst due to a higher surface concentration of formates. A recent study by Zengel et al. [346] on the effect of various HCs on SCR catalysis uncovered that the conversion of 200 ppm C_3H_6 over a $V_2O_5\text{-}WO_3/TiO_2$ SCR catalyst operated under standard-SCR conditions resulted in a maximum emission of 18 ppm HCN and 9 ppm HCHO at 550 °C and 1 bar.

Depending on the reaction conditions, namely temperature, catalyst composition, and HCHO inlet concentration, HCN concentrations of up to 90 ppm were found in model gas mixtures mimicking engine exhausts of lean-operated natural gas engines [463]. Considering that the

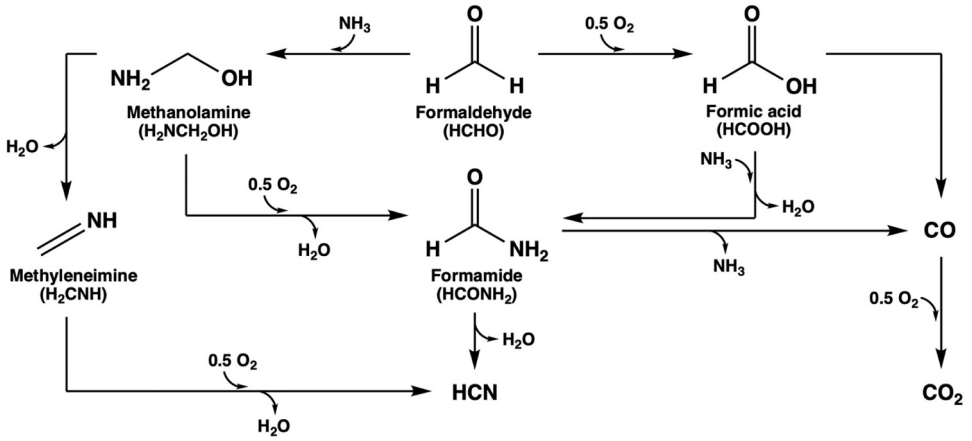

Fig. 22. Reaction pathways of HCHO conversion under SCR conditions with potential HCN formation; based on data from Zengel et al. [372], Ngo et al. [463], Elsener et al. [461], and Nuguid et al. [466].

NO_2/NO_x-ratio in natural gas engine exhausts can exceed 0.5 [454] and that a recent study by Schönberger Alvarez et al. [462] reported a significantly lower HCN formation tendency at high NO_2 levels, optimized engine operation along with a careful adjustment of the NO_2/NO_x ratio via the oxidation catalyst may mitigate HCN formation to some extent. Nevertheless, the high toxicity of HCN necessitates additional measures for HCN removal already for very low levels.

One possible solution to remove the toxic HCN emissions could be the use of ammonia slip catalysts (ASCs), which are commonly placed downstream of the SCR catalyst. ASCs are supposed to oxidize NH_3 that remains unreacted after the SCR catalyst to selectively form N_2 and they frequently contain both, a noble metal-based oxidation functionality and a SCR functionality with a composition similar to conventional SCR catalysts [468–471]. Although noble metal-based catalysts containing platinum or palladium [472,473] as well as non-noble metal-modified zeolites [474] have been evaluated for HCN abatement and showed promising conversion rates, these catalyst formulations exhibit only poor selectivity toward nitrogen. Instead, large amounts of N_2O or NO_x were formed, hereby counteracting the efforts of NO_x abatement by complex and expensive exhaust gas after-treatment systems.

5.4. Further SCR catalyst poisons

Since poisoning-related phenomena of SCR catalysts were reviewed recently in the context of diesel applications or coal- and biomass-fired power plants [475–479] and the challenges are similar for natural gas engine exhausts, this section only summarizes the main aspects in SCR catalyst poisoning and gives reference to recent research and review articles for more details. In addition to deactivation and side-reactions due to the presence of hydrocarbons [455] as discussed in the previous section, previous research considered especially poisoning of SCR catalysts by sulfur, phosphorous, and alkali and alkaline earth metals as particularly critical [476,477,480]. Although natural gas is a comparably clean fuel and the exposure to catalyst poisons is commonly higher for the oxidation catalyst because it is placed upstream of the SCR catalyst, poisonous species can pass the oxidation catalyst or evolve during its regeneration, e.g. COS, SO_2, or H_2S [222], eventually resulting in an accumulation in the downstream SCR catalyst.

A severe decrease in activity at temperatures below 300 °C was reported by Hammershøi et al. [481] for a Cu-CHA catalyst during exposure to SO_2- and especially to SO_3-containing gas mixtures, as generated over an upstream oxidation catalyst. When studying the effect of ammonium sulfate versus other S-containing species, a different response of Cu sites towards poisoning but also to catalyst desulfation was found by Jangjou et al. [482] for a series of Cu-SAPO-34 catalysts with different Si-Al ratios. The authors concluded that SO_2 directly interacts with ZCuOH species ($[CuOH]^{1+}$ charge-balanced by one zeolite framework Al atom with Z indicating an anionic site on the zeolite) leading to the formation of highly thermally stable copper bisulfites/bisulfates, whereas poisoning of Z_2Cu sites (Cu^{2+} charge-balanced by two anionic sites from the zeolite structure with Z indicating an anionic site on the zeolite) requires the presence of NH_3 and ammonium sulfate formation. Furthermore, Zhang et al. [483] found that sulfur species compete with NO_x for adsorption sites during SCR over a Cu-SAPO-34 catalyst, hereby inhibiting the SCR reaction predominantly in the low-temperature regime. By combining DRIFTS analyses of S-poisoned SCR samples with TPD experiments, the authors uncovered the formation of ammonium sulfate species. As underscored by a recent review by Guo et al. [484], ammonium bisulfate (NH_4HSO_4) formation can occur especially in the low-temperature regime below 300 °C as a consequence of SO_x-NH_3 reactions on the catalyst, which in addition to chemical poisoning results in physical deactivation, i.e. by coverage of the catalyst surface, blockage of active sites, and reduction of the specific surface area.

Due to the lower affinity of Fe for SO_x, Fe-zeolite SCR catalysts have been shown to be more resistant to sulfur poisoning and also to require lower temperatures for catalyst desulfation compared to Cu-zeolites [485]. Analogous, vanadia-based SCR catalysts are generally known to be more sulfur tolerant than zeolite-based formulations [486]. In fact, the presence of low SO_2 concentrations was reported to slightly increase the NO_x conversion of state-of-the-art V-based SCR catalysts between 200 °C and 300 °C, however, significant deactivation was observed at low temperatures due to the formation of ammonium sulfate species [487]. In this respect, $(NH_4)_2SO_4$ formation was observed also by Zengel et al. [346] during SO_2 poisoning of a V-based catalyst at temperatures below 250 °C and high-pressure conditions (5 bar), as present if the catalyst is located at pre-turbine position.

Regeneration of sulfur-poisoned SCR catalysts is possible and essentially relies on a high temperature treatment that ensures a decomposition of ammonium sulfates [346,483]. For instance, Hammershøi et al. [488] were able to restore the activity of a Cu-CHA catalyst to 80% of its fresh activity level after 120 h of rapid aging with SO_2. Based on their results, the authors suggested frequent regeneration as a feasible method for overcoming SO_2-poisoning, similar to the procedures discussed in the previous sections of this review article on regenerating methane oxidation catalysts. Note however, that the required temperature for SCR catalyst regeneration strongly depends on the catalyst formulation as well as the extent of poisoning. Kumar et al. [489] proposed an alternative strategy for sulfur removal from Cu-zeolites and suggested to induce a locally reducing reaction environment under net oxidizing conditions by dosing reductants such as NH_3, C_3H_6 or $C_{12}H_{26}$, which supposedly changes the oxidation state of Cu sites, weakens the Cu-SO_x interaction, and hereby promotes the release of sulfur.

Although the upstream oxidation catalyst can protect the downstream SCR catalyst from poisoning to some extent, e.g. by capturing phosphorus as reported by Dahlin et al. [490], in addition to sulfur deactivation, phosphorous poisoning can occur not only in oxidation catalysts, but also in SCR catalysts. While the contamination of Cu-zeolite catalysts with P traces was shown to result in mild effects, a pronounced decrease in activity and hydrothermal stability was observed after accumulation of high P concentrations on the surface of Cu-SSZ-13 catalysts [491,492]. In particular, Guo et al. [493] reported a P-induced inhibition of the NH_3-SCR activity of a Cu-SSZ-13 catalyst, which they explained by a loss of active sites along with a restricted dynamic motion of Cu species especially in the low-temperature regime that caused an inhibition of the Cu^{1+}/Cu^{2+} redox cycle. The formation of various species was reported to occur during P-poisoning on the catalyst surface or due to the interaction with the zeolite framework of Cu species, including phosphorous oxide, metaphosphate/phosphates, $AlPO_4$, as well as the formation of P-O-Cu bonds [494]. Furthermore, P was observed to physically block the pores and poison the acidic sites, and also suppresses the NH_3 and NO oxidation activity.

Similar as observed for Cu-zeolites, the formation of deposits and direct interaction with Fe-species upon P-poisoning results in catalyst deactivation for Fe-zeolite SCR catalysts as well, especially at low temperature [495]. Phosphorus was found to accumulate also over V-SCR catalysts, leading to a decrease of the ammonia storage capacity and a blockage of catalyst pores [496,497].

In order to remove phosphorous from spent catalysts, Chen et al. [498] washed a phosphated Cu-SSZ-13 catalyst with hot water for 1–5 days and hereby achieved a recovery of the acid sites and active Cu^{2+} ions, particularly when combining the washing treatment with hydrothermal treatment. Similarly, Guo et al. [499] recently reported a regeneration of P-poisoned Cu-LTA after hydrothermal aging. In contrast, the same study also found that P-poisoning of a Cu-CHA catalyst decreases the hydrothermal stability, which confirms earlier results by Xie et al. [494] who observed faster degradation during hydrothermal aging for P-poisoned Cu-SSZ-13 catalysts than for non-poisoned catalysts.

Last but not least, alkali and alkaline earth metals have been recognized as strong poisons for all classes of SCR catalysts [476,500].

While Cu-SSZ-13 was found resistant to the addition of low amounts of alkali metals that even showed a beneficial effect on the SCR activity [501,502], higher loadings deactivate the catalyst due to the conversion of isolated Cu^{2+} into CuO clusters [503–505]. Moreover, higher loadings of Na^+ and K^+ have been suggested to diminish the hydrothermal stability of Cu-SSZ-13 catalysts, especially K^+ due to the small hydration diameter and strong binding ability [505].

The contamination of a Fe-BEA catalyst with K leads to an activity decrease especially between 200 °C and 300 °C due to the replacement of Fe by K, the formation of larger iron clusters, and a decrease of the NH_3 storage capacity [495,506]. In addition to Na and K, Kern et al. [507] found a negative impact of Ca and Mg on both activity and NH_3-storage of Fe-MFI catalysts. For V-based SCR catalysts, poisoning with alkali and alkaline earth metals was suggested to be due to the bonding of the alkali metal to V-OH sites, which are the Brønsted acidic sites responsible for NH_3 adsorption during the SCR process but also the redox active species [508,509]. Herein, the polymeric metavanadates seem to be more tolerant to the alkali poisons compared with the isolated vanadyl groups [510].

Although the poisoning resistance can be increased by doping with metals like Ce and Zr [511,512] or by optimizing the catalyst structure by introducing core-shell functionalities [513], regeneration frequently remains mandatory for catalysts used in real-world applications. Similar as applied for oxidation catalysts, washing with solutions of weak acids, e.g. acetic acid, or diluted solutions of strong acids like sulfuric acid has been applied for the regeneration of V-based SCR catalysts [500, 514–516]. However, also alternative approaches such as the regeneration by means of electrophoresis were suggested, which allowed Peng et al. [517] to remove approximately 95% of K or Na ions from an alkali-poisoned V_2O_5-WO_3/TiO_2 catalyst.

6. Pre-turbine applications

The application of a turbocharger offers the potential to increase the engine efficiency, especially for heavy-duty and large-bore gas engines, and can be combined with a catalytic converter that is placed upstream of the turbocharger. Utilization of such a pre-turbo system is a comprehensive measure that impacts engine performance, emissions, fuel economy, and the catalytic converter and therefore requires an overall concept for the entire process [518]. With respect to emission control, pre-turbine positioning of the catalyst allows to utilize the comparably high upstream temperatures and the increased pressure in front of the turbocharger. Under the assumption of a constant mass flow, a higher pressure level results in a higher density and consequently in a lower space velocity that increases the residence time of pollutants. In addition, the rate of pressure-dependent reactions can increase upon an increasing pressure in the exhaust tailpipe. In the context of removing pollutants from lean exhausts, not only methane oxidation catalysts can benefit from higher exhaust gas temperatures and residence times in case of pre-turbine positioning [51], but also NO_x reduction by SCR [519]. Ultimately, the increase of the efficiency of the emission control system by pre-turbine positioning offers the possibility of reducing the size of the catalyst system or its (noble) metal loading, which is of both technical and economic interest.

However, catalyst placement upstream the turbocharger also results in a higher partial pressure of water, which enhances the inhibitory effect of steam over Pd-based catalysts [52]. By using multiscale models based on first-principle surface kinetics, Florén et al. [520–522] refined the mechanistic understanding of methane oxidation over Pd/Al_2O_3 at different pressure. The model predicts that an increasing pressure causes a declining reaction rate especially at temperatures below 420 °C, as active sites are covered by adsorbed surface species, e.g. hydroxyls or bicarbonates. As derived from the multiscale model, Fig. 23 underscores that the fraction of available surface sites decreases with increasing pressure, hereby reducing the probability of CH_4 dissociation that occurs most easily on free Pd-O site pairs. Once the temperature exceeds 450 °C, the thermal energy efficiently promotes the desorption of hindering surface species and thus enhances methane conversion. Experimental investigations confirmed the trends predicted by multiscale modeling, but also pointed to a high relevance of external mass transfer effects and residence times [522]. Since the bulk gas diffusion is inversely proportional to the total pressure, the external mass transfer resistance increases with increasing pressure. At the same time, the higher residence time usually increases the conversion at the same rate. In line with an earlier study by Rammelt et al. [523] on NH_3-SCR in front of the turbocharger for NO_x reduction of heavy-duty diesel off-gas, Florén et al. [522] conclude that "increasing the total pressure creates a trade-off between the positive effect of a longer residence time and the negative effect of a decreased bulk diffusion", resulting in pressure-dependent conversion profiles as shown in Fig. 23. Earlier research by Gremminger et al. [221] underscores that this conclusion is also highly relevant in the context of catalyst poisoning, since the authors observed a higher sulfur uptake if Pd-Pt bimetallic methane oxidation catalysts were operated at a moderate temperature of 450 °C in the presence of SO_2 and under pressure up to 5 bar compared to operation at ambient pressure.

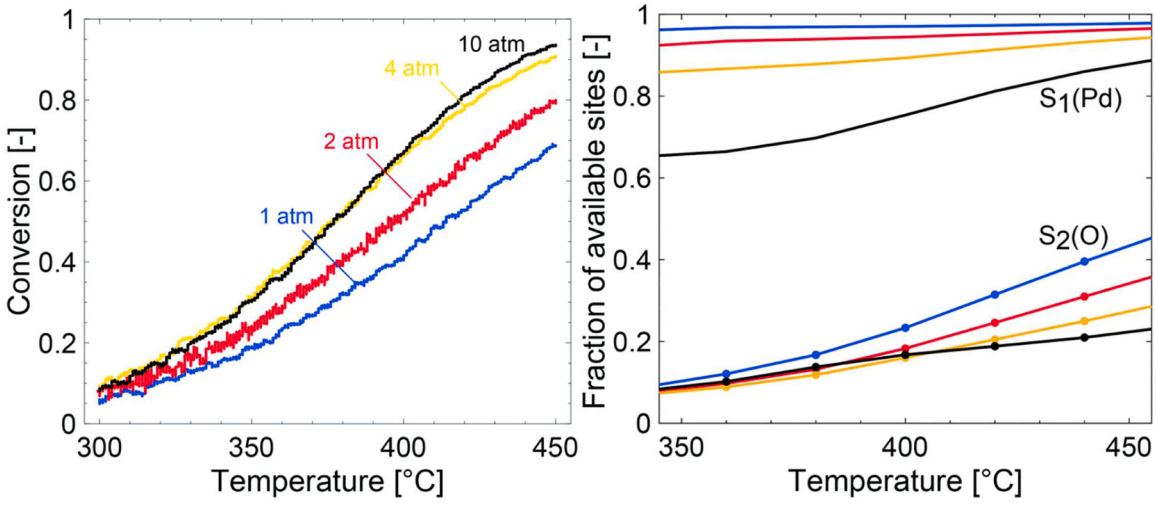

Fig. 23. Experimentally measured pressure-dependent CH_4 light-off over Pd/Al_2O_3 (left) and corresponding fraction of palladium (S_1(Pd)) and oxygen (S_2(O)) sites available for methane adsorption and conversion according to multiscale modeling (right). Reprinted with permission from ref. [522] under a Creative Commons Attribution-NonCommercial 3.0 Unported Licence (CC BY-NC 3.0; https://creativecommons.org/licenses/by-nc/3.0/). The Royal Society of Chemistry 2020.

In addition to heterogeneously catalyzed reactions over methane oxidation and SCR catalysts, temperature and pressure conditions in pre-turbo applications allow for gas phase chemistry, which is particularly relevant for the conversion of unburnt hydrocarbons with NO_x. As elucidated by numerous fundamental studies, NO_x can promote the homogeneous oxidation of light alkanes [524–531], presumably due to an increased formation rate of OH radicals that induce the abstraction of H-atoms from CH_4 [527,528]. Exploiting this intricate gas phase chemistry as demonstrated by a number of recent studies [532–535] may offer an elegant strategy for overcoming obstacles of heterogeneous catalysis such as sulfur poisoning or water inhibition, since typical strong catalyst poisons such as SO_2 do not negatively impact homogeneous gas phase oxidation of methane under pre-turbine conditions representative for lean-burn gas engines [536]. Although homogeneous gas phase oxidation can supplement heterogeneous catalysts, its overall conversion rates are insufficient for a catalyst-free exhaust gas after-treatment system. Consequently, an optimized process considering temperature, pressure, space velocity, gas composition, and the impact on homogeneous and heterogeneous catalysts is imperative, in particular for suppressing the formation of undesired side-products such as HCHO or N_2O [534,536] or for suppressing the consumption of critical components needed for heterogeneous reactions [534,537].

For instance, SCR catalysts at pre-turbine position can only efficiently remove NO_x if gas phase reactions do not consume the major share of ammonia or NO_x, since this would influence the NH_3/NO_x ratio. In this respect, homogeneous gas phase reactions in lean gas mixtures promote the oxidation of NO to NO_2 and cause a pronounced over-consumption of NH_3 [346,347]. Furthermore, hydrocarbons that are not converted over the oxidation catalyst and that end up in the SCR catalyst can cause undesired side-reactions. Over representative zeolite-based catalyst formulations, i.e. Fe-ZSM-5 and Cu-SSZ-13, Zengel et al. [346, 348] observed an incomplete conversion of hydrocarbons that leads to the formation of undesired by-products, among which HCHO and HCN were found. Although the higher pressure increased both NO_x conversion and hydrocarbon oxidation and consequently decreased the formation of toxic HCN compared to experiments at ambient pressure, sufficiently low by-product levels were only found at high temperatures [348].

7. Conclusions and perspectives

Using natural gas with its main component methane as a fuel for modern internal combustion engines is a concept that has already been used for decades and which still enjoys growing popularity. The existing natural gas infrastructure allows a fast and wide-ranging transition from established gasoline and diesel engines towards a progressive gas-based technology and offers great potential for reducing anthropogenic carbon dioxide emissions from combustion engines, particularly in the stationary and heavy-duty sector. In addition, the continuous replacement of fossil feedstock by renewable methane originating from biogas or power-to-gas processes will further increase the sustainability of gas engines. In the light of upcoming ultra-low emission limits, we outlined the main challenges that arise in the context of lean-operated natural gas engines, namely complete oxidation of the greenhouse gas methane, conversion of potentially carcinogenic formaldehyde, efficient NO_x control, and abatement of secondary emissions. This review shines light on the fundamentals of all these aspects and underscores how the tuning of the catalyst composition, the optimization of the operation procedure, and the combination of different well-harmonized technologies can create advantageous synergies.

As illustrated in Fig. 24, comprehensive knowledge allows the design of complex emission control systems that exhibit very high pollutant conversion rates, which were far beyond imagination back in 1956, when the patent for the very first exhaust gas catalyst was granted to pioneer Eugene J. Houdry and his *Oxy-Catalyst Company* [538]. Based on the previously presented literature review, the first element in an exhaust gas after-treatment system for lean-burn gas engines will be an oxidation catalyst that is capable of sustaining high hydrocarbon conversion over a broad range of operating conditions and during long-term use. Possibly, this catalytic converter will exhibit different zones, for instance a first zone that is coated with a three-way catalyst and a second zone that consists of an oxidation catalyst for methane and formaldehyde oxidation, as exemplary described in previous studies that aimed at improving sulfur tolerance and regeneration properties of the oxidation catalyst [316,318]. As a matter of course, secondary emissions such as SO_x, N_2O, or NH_3 must be considered adequately when planning long-term operation procedures including different operational points for regeneration purposes [317], as these will impact the consecutive catalytic systems in the exhaust tailpipe. Analogous to diesel engines, a system for selective catalytic reduction (SCR) removes NO_x by using NH_3 as reducing agent, e.g. provided by thermo-catalytic decomposition of a urea-water solution, and finally the entire system is complemented by an ammonia slip catalyst (ASC). Although so far only a limited number of studies specifically investigated the coupling of a noble metal-based oxidation catalyst with an SCR system for lean-burn gas engines, the outcome of these investigations is encouraging. On a synthetic gas test bench scale, Adouane et al. [458] combined a palladium-platinum oxidation catalyst with a SCR catalyst originally developed for diesel exhaust gas after-treatment and achieved almost full CO conversion, 40% CH_4 conversion, and approximately 70% NO_x conversion at 415 °C.

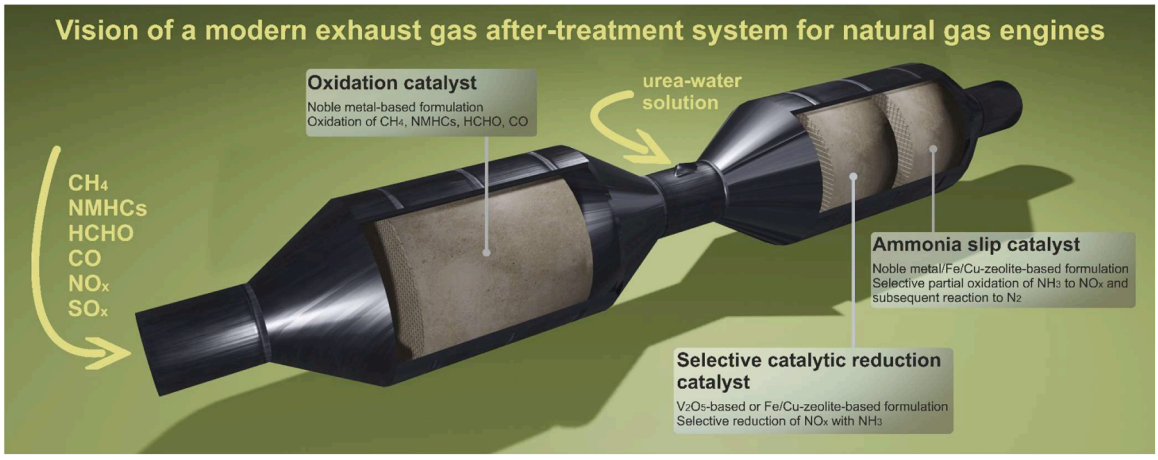

Fig. 24. Vision of a modern emission control system for lean-operated natural gas engines that combines an oxidation catalyst, a catalyst for selective catalytic reduction, and an ammonia slip catalyst.

Similarly, Keenan et al. [318] describe the outcome of the EU-funded HDGAS project (Heavy Duty Gas Engines integrated into vehicles), recommending the combination of a Pd-Rh three-way catalyst with a Pd-Pt methane oxidation catalyst, an urea injector, and a sequence of Fe- and Cu-zeolite-based SCR catalysts for medium and high temperature NO_x control, finally supplemented with an ammonia slip catalyst. Simulations of the world harmonized transient cycle (WHTC) suggest that such a complex and expensive system can remove pollutants very efficiently, hereby complying with current emission regulations [318].

Overall, the system proposed in Fig. 24 strongly resembles the concept used for emission reduction of diesel engines and its adaption for lean-burn gas engines poses only moderate technological hurdles for widespread use. Despite this rather high degree of market-readiness, meeting upcoming emission limits for combustion engines aiming at near-zero emissions will be challenging. Particularly an efficient conversion of methane at low temperatures in the presence of steam and sulfur species and the removal of very low formaldehyde levels over the oxidation catalyst requires additional research efforts, whereas a careful operation of state-of-the-art deNO_x systems allows current and future regulations to be met. Moreover, the importance of thermal management in such increasingly complex future exhaust gas after-treatment systems will grow, especially for large-bore engines as frequently used in stationary applications. For instance, low exhaust temperatures and disadvantageous placement of heat exchangers for exhaust cooling can lead to exhaust gas condensation [539,540]. In the context of gas engines, the reaction between SO_3 and water vapor can result in H_2SO_4 formation, which is particularly problematic since its condensation promotes corrosion and reduces the longevity of the catalytic converters and materials. After all, not only technological but also economic considerations will be of paramount importance when designing efficient exhaust tailpipe configurations.

The gain in fundamental knowledge and its efficient transfer into real-world applications is a prerequisite for designing the next generation of catalytic converters and operation procedures. Since monitoring catalysts at work and the detailed description of the complex multiphase-processes is vital for understanding the heterogeneous catalytic processes on the nano-, meso-, and macro-scale as well as their implications for technical full-scale converters, the steady advancement in the field of *operando* techniques as well as in the field of multiscale modeling will reveal novel and invaluable facets in the future [69,541]. Especially transient engine operation can change the reaction environment rapidly, e.g. during lean-rich cycling as discussed above for (re-) activating methane oxidation catalysts. Only profound knowledge on the most active (surface) sites and catalyst structures under realistic working conditions allows the derivation of structure-activity relations of highly dynamic catalyst systems that are not only the basis for a rational catalyst synthesis, but also mandatory for establishing operation procedures ensuring high activity and durability.

Comprehensive spatiotemporal investigations of the temperature and structure of an oxidation catalyst could pave the way for generating individual zones within a single catalyst bed, in which each zone exhibits maximum activity for one specific pollutant [313]. Recent advances in the field of *operando* X-ray spectrotomography allowed gradients in oxidation state and coordination environment in copper SCR catalysts to be uncovered, which are a consequence of chemical species interactions with the catalyst as well as mass transport phenomena, hereby providing direct three-dimensional information during catalyst operation under realistic conditions [542]. Such non-invasive approaches provide three-dimensional structure-activity relationships that are not accessible by conventional characterization techniques [543].

Moreover, since the reliable prediction of the behavior of the catalyst over a wide range of conditions by means of mathematical models is the basis for a cost-efficient design of technical devices and processes, the development and refinement of detailed reaction mechanisms becomes more and more important. Performing numerous expensive density functional theory calculations will surely remain a powerful approach for developing first-principle kinetic models that can be exploited for describing adsorbate thermochemistry and kinetics within an uncertainty range, e.g. as successfully used to describe CH_4 oxidation over PdO(101) surfaces [100]. However, the ongoing progress in the field of automated mechanism generation and optimization can substantially accelerate mechanism development even for complex reaction networks, for instance as recently demonstrated for methane oxidation over PdO [544] or for the conversion of vehicle pollutants over Pt(111) surfaces [545,546]. In this respect, digitalization and unified (research) data infrastructures [547–550] as well as the continuous advancement in developing dynamic kinetic and multiscale models [69,551–553] can build the foundation for more powerful theoretical tools that facilitate the design and development of novel materials, catalytic converters, and application strategies, hereby covering all time and length scales relevant in exhaust gas after-treatment.

Last but not least, high-throughput synthesis and screening approaches can efficiently sustain the material development, as lately resulted in the development of a palladium-containing denary multi-element oxide catalyst exhibiting high and stable methane conversion for 100 h [77]. Such high-throughput preparation techniques facilitate a time- and cost-efficient development of increasingly complex catalyst formulations whose design is guided by the continuous experimental and theoretical progress that allows a better understanding of catalysts at work. In summary, all these advances that were only possible due to concerted efforts in synthesis, testing, advanced *operando* characterization methods, and modeling are encouraging with regard to modern emission control for lean-burn natural gas engines and their widespread application.

CRediT authorship contribution statement

Patrick Lott: Conceptualization, Data curation, Formal analysis, Methodology, Project administration, Visualization, Writing – original draft, Writing – review & editing. **Maria Casapu:** Conceptualization, Funding acquisition, Methodology, Project administration, Resources, Writing – original draft, Writing – review & editing. **Jan-Dierk Grunwaldt:** Conceptualization, Funding acquisition, Project administration, Resources, Supervision, Writing – review & editing. **Olaf Deutschmann:** Conceptualization, Funding acquisition, Project administration, Resources, Supervision, Writing – review & editing.

Declaration of Competing Interest

The authors declare that they have no known competing financial interests or personal relationships that could have appeared to influence the work reported in this paper.

Data availability

No data was used for the research described in the article.

Acknowledgements

We gratefully acknowledge all our former and present colleagues at KIT who significantly contributed to the research in the field of emission control of gas engines and hereby advanced this topic. Equally important, we express our sincere gratitude to the many national and international partners from academia and industry who supported our work with financial and infrastructural resources and invaluable expertise during vibrant collaborations and many fruitful scientific discussions. In particular, financial support by the Deutsche Forschungsgemeinschaft (DFG, German Research Foundation) via SFB 1441, Project-ID 426888090 is acknowledged. C. Janzer (ITCP, KIT) is acknowledged for proof-reading this manuscript.

References

[1] Regulation (EU) 2019/631 of the European Parliament and of the Council of 17 April 2019 setting CO2 emission performance standards for new passenger cars and for new light commercial vehicles, and repealing Regulations (EC) No 443/2009 and (EU) No 510/2011 (Text with EEA relevance.), in: Official Journal of the European Union, 2019.

[2] Erstes Gesetz zur Änderung des Bundesklimaschutzgesetzes, in: Bundesgesetzblatt Jahrgang 2021 Teil I Nr. 59, 2021.

[3] O.M. Horgen, Rolls-Royce Marine – the"Environship Concept". System Solutions & Wave Piercing Technology, SNAME GL&GR Meeting Cleveland, 2012.

[4] N. Scarlat, J.F. Dallemand, F. Fahl, Biogas: developments and perspectives in Europe, Renew. Energy 129 (2018) 457–472, https://doi.org/10.1016/j.renene.2018.03.006.

[5] M. Prussi, M. Padella, M. Conton, E.D. Postma, L. Lonza, Review of technologies for biomethane production and assessment of Eu transport share in 2030, J. Clean. Prod. 222 (2019) 565–572, https://doi.org/10.1016/j.jclepro.2019.02.271.

[6] S. Achinas, V. Achinas, G.J.W. Euverink, A technological overview of biogas production from biowaste, Engineering 3 (2017) 299–307, https://doi.org/10.1016/J.Eng.2017.03.002.

[7] I.U. Khan, M.H.D. Othman, H. Hashim, T. Matsuura, A.F. Ismail, M. Rezaei-DashtArzhandi, I.W. Azelee, Biogas as a renewable energy fuel - A review of biogas upgrading, utilisation and storage, Energy Convers. Manage. 150 (2017) 277–294, https://doi.org/10.1016/j.enconman.2017.08.035.

[8] M. Götz, J. Lefebvre, F. Mörs, A.M. Koch, F. Graf, S. Bajohr, R. Reimert, T. Kolb, Renewable power-to-gas: a technological and economic review, Renew. Energy 85 (2016) 1371–1390, https://doi.org/10.1016/j.renene.2015.07.066.

[9] H. Blanco, A. Faaij, A review at the role of storage in energy systems with a focus on power to gas and long-term storage, Renew. Sustain. Energy Rev. 81 (2018) 1049–1086, https://doi.org/10.1016/j.rser.2017.07.062.

[10] K. Ghaib, F.Z. Ben-Fares, Power-to-methane: a state-of-the-art review, Renew. Sustain. Energy Rev. 81 (2018) 433–446, https://doi.org/10.1016/j.rser.2017.08.004.

[11] A. Varone, M. Ferrari, Power to liquid and power to gas: an option for the German Energiewende, Renew. Sustain. Energy Rev. 45 (2015) 207–218, https://doi.org/10.1016/j.rser.2015.01.049.

[12] R. Schlögl, Chemical energy storage enables the transformation of fossil energy systems to sustainability, Green. Chem. 23 (2021) 1584–1593, https://doi.org/10.1039/d0gc03171b.

[13] M. Jentsch, T. Trost, M. Sterner, Optimal use of power-to-gas energy storage systems in an 85% renewable energy scenario, Energy Procedia 46 (2014) 254–261, https://doi.org/10.1016/j.egypro.2014.01.180.

[14] P. Lott, O. Deutschmann, Lean-burn natural gas engines: challenges and concepts for an efficient exhaust gas aftertreatment system, Emiss. Control Sci. Technol. 7 (2021) 1–6, https://doi.org/10.1007/s40825-020-00176-w.

[15] G. Myhre, D. Shindell, F.-M. Bréon, W. Collins, J. Fuglestvedt, J. Huang, D. Koch, J.-F. Lamarque, D. Lee, B. Mendoza, T. Nakajima, A. Robock, G. Stephens, T. Takemura, H. Zhan, Anthropogenic and Natural Radiative Forcing, in: T. F. Stocker, D. Qin, G.-K. Plattner, M. Tignor, S.K. Allen, J. Boschung, A. Nauels, Y. Xia, V. Bex, P.M. Midgley (Eds.), Climate Change 2013: The Physical Science Basis. Contribution of Working Group I to the Fifth Assessment Report of the Intergovernmental Panel on Climate Change, Cambridge University Press, Cambridge, United Kingdom and New York, NY, USA, 2013, https://doi.org/10.1017/CBO9781107415324.018.

[16] R.J. Farrauto, Low-temperature oxidation of methane, Science 337 (2012) 659–660, https://doi.org/10.1126/science.1226310.

[17] O. Deutschmann, J.-D. Grunwaldt, Exhaust gas aftertreatment in mobile systems: status, challenges, and perspectives, Chem. Ing. Tech. 85 (2013) 595–617, https://doi.org/10.1002/cite.201200188.

[18] H.M. Cho, B.Q. He, Spark ignition natural gas engines - a review, Energy Convers. Manage. 48 (2007) 608–618, https://doi.org/10.1016/j.enconman.2006.05.023.

[19] A. Wahbi, A. Tsolakis, J. Herreros, Emissions Control Technologies for Natural Gas Engines, in: K.K. Srinivasan, A.K. Agarwal, S.R. Krishnan, V. Mulone (Eds.), Natural Gas Engines For Transportation and Power Generation, Springer, Singapore, 2019, pp. 359–379.

[20] A. Winkler, P. Dimopoulos, R. Hauert, C. Bach, M. Aguirre, Catalytic activity and aging phenomena of three-way catalysts in a compressed natural gas/gasoline powered passenger car, Appl. Catal. B 84 (2008) 162–169, https://doi.org/10.1016/j.apcatb.2008.03.013.

[21] C.K. Lambert, Current state of the art and future needs for automotive exhaust catalysis, Nat. Catal. 2 (2019) 554–557, https://doi.org/10.1038/s41929-019-0303-x.

[22] P. Einewall, P. Tunestal, B. Johansson, Lean Burn Natural Gas Operation vs. Stoichiometric Operation with EGR and a Three Way Catalyst, SAE Technical Paper 2005–01-0250, (2005). https://doi.org/10.4271/2005–01-0250.

[23] A. Raj, Methane Emission Control - A review of mobile and stationary source emissions abatement technologies for natural gas engines, Johnson Matthey Technol. Rev. 60 (2016) 228–235, https://doi.org/10.1595/205651316X692554.

[24] C.Y. Huang, W.P. Shan, Z.H. Lian, Y. Zhang, H. He, Recent advances in three-way catalysts of natural gas vehicles, Catal. Sci. Technol. 10 (2020) 6407–6419, https://doi.org/10.1039/d0cy01320j.

[25] B. Ruscic, M. Litorja, R.L. Asher, Ionization energy of methylene revisited: Improved values for the enthalpy of formation of CH_2 and the bond dissociation energy of CH_3 via simultaneous solution of the local thermochemical network, J. Phys. Chem. A 103 (1999) 8625–8633, https://doi.org/10.1021/jp992403v.

[26] S.J. Blanksby, G.B. Ellison, Bond dissociation energies of organic molecules, Acc. Chem. Res. 36 (2003) 255–263, https://doi.org/10.1021/ar020230d.

[27] B. Ruscic, Active thermochemical tables: sequential bond dissociation enthalpies of methane, ethane, and methanol and the related thermochemistry, J. Phys. Chem. A 119 (2015) 7810–7837, https://doi.org/10.1021/acs.jpca.5b01346.

[28] Q. Zhang, M.H. Li, G.X. Li, S.D. Shao, P.X. Li, Transient emission characteristics of a heavy-duty natural gas engine at stoichiometric operation with EGR and TWC, Energy 132 (2017) 225–237, https://doi.org/10.1016/j.energy.2017.05.039.

[29] P. Gélin, M. Primet, Complete oxidation of methane at low temperature over noble metal based catalysts: a review, Appl. Catal. B 39 (2002) 1–37, https://doi.org/10.1016/S0926-3373(02)00076-0.

[30] A. Gremminger, J.-D. Grunwaldt, O. Deutschmann, Methan katalytisch - Untersuchung der Wirkmechanismen bei katalytischer Methanreduktion, Forschungsvereinigung Verbrennungskraftmaschinen e.V. (FVV), Frankfurt am Main, 2013.

[31] A. Boubnov, M. Casapu, A. Gremminger, B. Torkashvand, M. Merts, J.-D. Grunwaldt, O. Deutschmann, B. Veenhuizen, Methane catalytic II - Methane oxidation catalysts: influence of catalyst composition, pressure and gas composition on activity, aging and reactivation, Forschungsvereinigung Verbrennungskraftmaschinen e.V. (FVV), Frankfurt am Main, 2017.

[32] C.E. Mitchell, D.B. Olsen, Formaldehyde formation in large bore natural gas engines Part 1: formation mechanisms, J. Eng. Gas. Turbines Power 122 (2000) 603–610, https://doi.org/10.1115/1.1290585.

[33] M. Bauer, G. Wachtmeister, Formation of formaldehyde in lean-burn gas engines, MTZ Worldw. 70 (2009) 50–57, https://doi.org/10.1007/BF03226970.

[34] K.H. Kim, S.A. Jahan, J.T. Lee, Exposure to formaldehyde and its potential human health hazards, J. Environ. Sci. Health, Part C: Environ. Carcinog. Ecotoxicol. Rev. 29 (2011) 277–299, https://doi.org/10.1080/10590501.2011.629972.

[35] Regulation (EC) No 1272/2008 of the European Parliament and of the Council of 16 December 2008 on classification, labelling and packaging of substances and mixtures, amending and repealing Directives 67/548/EEC and 1999/45/EC, and amending Regulation (EC) No 1907/2006 (Text with EEA relevance), in: Official Journal of the European Union, 2008.

[36] A. Schröder, T. Schedlbauer, G. Wachtmeister, M. Prager, M. Casapu, O. Deutschmann, J.-D. Grunwaldt, Formaldehyde - Final Report, Forschungsvereinigung Verbrennungskraftmaschinen e.V., Frankfurt am Main, 2019.

[37] D.B. Olsen, C.E. Mitchell, Formaldehyde formation in large bore engines Part 2: Factors affecting measured CH_2O, J. Eng. Gas. Turbines Power 122 (2000) 611–616, https://doi.org/10.1115/1.1290586.

[38] D.B. Olsen, B.D. Willson, The Effect of Parametric Variations on Formaldehyde Emissions From a Large Bore Natural Gas Engine, Proceedings of the ASME 2002 Internal Combustion Engine Division Spring Technical Conference. Design, Operation, and Application of Modern Internal Combustion Engines and Associated Systems, ASME, Rockford, Illinois, USA, 2002, pp. 19–26.

[39] W.A. Givens, W.H. Buck, A. Jackson, A. Kaldor, A. Hertzberg, W. Moehrmann, S. Mueller-Lunz, N. Pelz, G. Wenninger, Lube Formulation Effects on Transfer of Elements to Exhaust After-Treatment System Components, SAE Technical Paper 2003–01-3109, (2003). https://doi.org/10.4271/2003-01-3109.

[40] E.A. Bardasz, S. Cowling, A. Panesar, J. Durham, T.N. Tadrous, Effects of Lubricant Derived Chemistries on Performance of the Catalyzed Diesel Particulate Filters, SAE Technical Paper 2005–01-2168, (2005). https://doi.org/10.4271/2005-01-2168.

[41] M. Manni, A. Pedicillo, F. Bazzano, A Study of Lubricating Oil Impact on Diesel Particulate Filters by Means of Accelerated Engine Tests, SAE Technical Paper 2006–01-3416, (2006). https://doi.org/10.4271/2006-01-3416.

[42] A. Ayala, N.Y. Kado, R.A. Okamoto, B.A. Holmen, P.A. Kuzmicky, R. Kobayashi, K.E. Stiglitz, Diesel and CNG Heavy-duty Transit Bus Emissions over Multiple Driving Schedules: Regulated Pollutants and Project Overview, SAE Technical Paper 2002–01-1722, (2002). https://doi.org/10.4271/2002–01-1722.

[43] D. Schreiber, A.-M. Forss, M. Mohr, P. Dimopoulos, Particle Characterisation of Modern CNG, Gasoline and Diesel Passenger Cars, SAE Technical Paper 2007–24-0123, (2007). https://doi.org/10.4271/2007–24-0123.

[44] T.W. Hesterberg, C.A. Lapin, W.B. Bunn, A comparison of emissions from vehicles fueled with diesel or compressed natural gas, Environ. Sci. Technol. 42 (2008) 6437–6445, https://doi.org/10.1021/es071718i.

[45] N.O. Nylund, V. Karvonen, H. Kuutti, J. Laurikko, Comparison of Diesel and Natural Gas Bus Performance, SAE Technical Paper 2014–01-2432, (2014). https://doi.org/10.4271/2014–01-2432.

[46] H.M. Cho, B.Q. He, Combustion and emission characteristics of a lean burn natural gas engine, Int. J. Automot. Technol. 9 (2008) 415–422, https://doi.org/10.1007/s12239-008-0050-5.

[47] Y.B. Zeldovich, The oxidation of nitrogen in combustion and explosions, Acta Physicochim. USSR 21 (1946) 577–628, https://doi.org/10.1515/9781400862979.404.

[48] D. Ciuparu, M.R. Lyubovsky, E. Altman, L.D. Pfefferle, A. Datye, Catalytic combustion of methane over palladium-based catalysts, Catal. Rev.: Sci. Eng. 44 (2002) 593–649, https://doi.org/10.1081/CR-120015482.

[49] A. Gremminger, J. Pihl, M. Casapu, J.-D. Grunwaldt, T.J. Toops, O. Deutschmann, PGM based catalysts for exhaust-gas after-treatment under typical diesel, gasoline and gas engine conditions with focus on methane and formaldehyde oxidation, Appl. Catal. B 265 (2020), https://doi.org/10.1016/j.apcatb.2019.118571.

[50] M. Reinke, J. Mantzaras, R. Schaeren, R. Bombach, A. Inauen, S. Schenker, High-pressure catalytic combustion of methane over platinum: In situ experiments and detailed numerical predictions, Combust. Flame 136 (2004) 217–240, https://doi.org/10.1016/j.combustflame.2003.10.003.

[51] R. Bank, U. Etzien, B. Buchholz, H. Harndorf, Methane catalysts at an upstream turbine position, MTZ Ind. 5 (2015) 14–21, https://doi.org/10.1007/s40353-015-0503-z.

[52] B. Torkashvand, A. Gremminger, S. Valchera, M. Casapu, J.-D. Grunwaldt, O. Deutschmann, The Impact of Pre-Turbine Catalyst Placement on Methane Oxidation in Lean-Burn Gas Engines: An Experimental and Numerical Study, SAE Technical Paper 2017–01-1019, (2017). https://doi.org/10.4271/2017–01-1019.

[53] B. Torkashvand, L. Maier, M. Hettel, T. Schedlbauer, J.-D. Grunwaldt, O. Deutschmann, On the challenges and constrains of ultra-low emission limits: Formaldehyde oxidation in catalytic sinusoidal-shaped channels, Chem. Eng. Sci. 195 (2019) 841–850, https://doi.org/10.1016/j.ces.2018.10.031.

[54] F. Birkhold, U. Meingast, P. Wassermann, O. Deutschmann, Modeling and simulation of the injection of urea-water-solution for automotive SCR DeNO$_x$-systems, Appl. Catal. B 70 (2007) 119–127, https://doi.org/10.1016/j.apcatb.2005.12.035.

[55] V.O. Strots, S. Santhanam, B.J. Adelman, G.A. Griffin, E.M. Derybowski, Deposit Formation in Urea-SCR Systems, SAE Int. J. Fuels Lubr. 2 (2010) 283–289, https://doi.org/10.4271/2009-01-2780.

[56] A. Roppertz, S. Fuger, S. Kureti, Investigation of Urea-SCR at Low Temperatures, Top. Catal. 60 (2017) 199–203, https://doi.org/10.1007/s11244-016-0597-8.

[57] S. Tischer, M. Börnhorst, J. Amsler, G. Schoch, O. Deutschmann, Thermodynamics and reaction mechanism of urea decomposition, Phys. Chem. Chem. Phys. 21 (2019) 16785–16797, https://doi.org/10.1039/c9cp01529a.

[58] J. Dörnhöfer, M. Börnhorst, C. Ates, N. Samkhaniani, J. Pfeil, M. Wörner, R. Koch, H.-J. Bauer, O. Deutschmann, B. Frohnapfel, T. Koch, A Holistic View on Urea Injection for NO$_x$ Emission Control: Impingement, Re-atomization, and Deposit Formation, Emiss. Control Sci. Technol. 6 (2020) 228–243, https://doi.org/10.1007/s40825-019-00151-0.

[59] M. Börnhorst, O. Deutschmann, Advances and challenges of ammonia delivery by urea-water sprays in SCR systems, Prog. Energy Combust. Sci. 87 (2021), https://doi.org/10.1016/j.pecs.2021.100949.

[60] C. Kuntz, C. Kuhn, H. Weickenmeier, S. Tischer, M. Börnhorst, O. Deutschmann, Kinetic modeling and simulation of high-temperature by-product formation from urea decomposition, Chem. Eng. Sci. 246 (2021), https://doi.org/10.1016/j.ces.2021.116876.

[61] I. Czekaj, O. Kröcher, Decomposition of Urea in the SCR Process: Combination of DFT Calculations and Experimental Results on the Catalytic Hydrolysis of Isocyanic Acid on TiO_2 and Al_2O_3, Top. Catal. 52 (2009) 1740–1745, https://doi.org/10.1007/s11244-009-9344-8.

[62] A. Lundström, T. Snelling, P. Morsing, P. Gabrielsson, E. Senar, L. Olsson, Urea decomposition and HNCO hydrolysis studied over titanium dioxide, Fe-Beta γ-Alumina, Appl. Catal. B 106 (2011) 273–279, https://doi.org/10.1016/j.apcatb.2011.05.010.

[63] M. Goldbach, A. Roppertz, P. Langenfeld, M. Wackerhagen, S. Fuger, S. Kureti, Urea decomposition in selective catalytic reduction on $V_2O_5/WO_3/TiO_2$ catalyst in diesel exhaust, Chem. Eng. Technol. 40 (2017) 2035–2043, https://doi.org/10.1002/ceat.201700261.

[64] Y.J. Wu, F.S. Wang, W.Y. Tang, R. Kakwani, Y.L. Hou, G. Feng, Urea decomposition and implication for NO$_x$ reduction with Cu-zeolite and vanadia-selective catalytic reduction, Chem. Eng. Technol. 43 (2020) 1758–1764, https://doi.org/10.1002/ceat.202000036.

[65] M. Eck, P. Lott, D. Schweigert, M. Börnhorst, O. Deutschmann, Spatially resolved measurements of HNCO hydrolysis over SCR catalysts, Chem. Ing. Tech. 94 (2022) 738–746, https://doi.org/10.1002/cite.202100192.

[66] C. Kuntz, H. Weickenmeier, M. Börnhorst, O. Deutschmann, Deposition and decomposition of urea and its by-products on TiO_2 and VWT-SCR catalysts, Int. J. Heat. Fluid Flow. 95 (2022), https://doi.org/10.1016/j.ijheatfluidflow.2022.108969.

[67] S. Gierth, S. Hartl, M. Pollack, C. Hasse, U. Hofmann, G. Zikoridse, H. Rautenberg, F. Will, C. Hahn, S. Kureti, Urea conversion for low-temperature selective catalytic reduction in a swirled diesel exhaust gas configuration, Chem. Eng. Technol. 45 (2022) 610–619, https://doi.org/10.1002/ceat.202100571.

[68] M. Masoudi, N. Poliakov, S. Noorfeshan, J. Hensel, E. Tegeler, A Heated AdBlue/DEF Mixer for High Efficiency NOx Reduction in Low Temperature Drive Cycles, RDE and City Driving, Top. Catal. 66 (2023) 771–776, https://doi.org/10.1007/s11244-022-01714-2.

[69] P. Lott, O. Deutschmann, Heterogeneous chemical reactions—A cornerstone in emission reduction of local pollutants and greenhouse gases, Proc. Combust. Inst. 39 (2023) 3183–3215, https://doi.org/10.1016/j.proci.2022.06.001.

[70] R. Burch, M.J. Hayes, C-H bond activation in hydrocarbon oxidation on solid catalysts, J. Mol. Catal. A: Chem. 100 (1995) 13–33, https://doi.org/10.1016/1381-1169(95)00133-6.

[71] R. Burch, D.J. Crittle, M.J. Hayes, C-H bond activation in hydrocarbon oxidation on heterogeneous catalysts, Catal. Today 47 (1999) 229–234, https://doi.org/10.1016/S0920-5861(98)00303-4.

[72] A.J. Zarur, J.Y. Ying, Reverse microemulsion synthesis of nanostructured complex oxides for catalytic combustion, Nature 403 (2000) 65–67, https://doi.org/10.1038/47450.

[73] F.F. Tao, J.J. Shan, L. Nguyen, Z.Y. Wang, S.R. Zhang, L. Zhang, Z.L. Wu, W. X. Huang, S.B. Zeng, P. Hu, Understanding complete oxidation of methane on spinel oxides at a molecular level, Nat. Commun. 6 (2015), https://doi.org/10.1038/Ncomms8798.

[74] J.H. Chen, H. Arandiyan, X. Gao, J.H. Li, Recent advances in catalysts for methane combustion, Catal. Surv. Asia 19 (2015) 140–171, https://doi.org/10.1007/s10563-015-9191-5.

[75] Y. Nishihata, J. Mizuki, T. Akao, H. Tanaka, M. Uenishi, M. Kimura, T. Okamoto, N. Hamada, Self-regeneration of a Pd-perovskite catalyst for automotive emissions control, Nature 418 (2002) 164–167, https://doi.org/10.1038/nature00893.

[76] J. Shen, R.E. Hayes, X.X. Wu, N. Semagina, 100° Temperature Reduction of Wet Methane Combustion: Highly Active Pd-Ni/Al_2O_3 Catalyst versus Pd/$NiAl_2O_4$, ACS Catal. 5 (2015) 2916–2920, https://doi.org/10.1021/acscatal.5b00060.

[77] T.Y. Li, Y.G. Yao, Z.N. Huang, P.F. Xie, Z.Y. Liu, M.H. Yang, J.L. Gao, K.Z. Zeng, A. H. Brozena, G. Pastel, M.L. Jiao, Q. Dong, J.Q. Dai, S.K. Li, H. Zong, M.F. Chi, J. Luo, Y.F. Mo, G.F. Wang, C. Wang, R. Shahbazian-Yassar, L.B. Hu, Denary oxide nanoparticles as highly stable catalysts for methane combustion, Nat. Catal. 4 (2021) 62–70, https://doi.org/10.1038/s41929-020-00554-1.

[78] T.V. Choudhary, S. Banerjee, V.R. Choudhary, Catalysts for combustion of methane and lower alkanes, Appl. Catal. A 234 (2002) 1–23, https://doi.org/10.1016/S0926-860x(02)00231-4.

[79] M. Monai, T. Montini, R.J. Gorte, P. Fornasiero, Catalytic Oxidation of Methane: Pd and Beyond, Eur. J. Inorg. Chem. (2018) 2884–2893, https://doi.org/10.1002/ejic.201800326.

[80] D. Jiang, K. Khivantsev, Y. Wang, Low-temperature methane oxidation for efficient emission control in natural gas vehicles: Pd and beyond, ACS Catal. 10 (2020) 14304–14314, https://doi.org/10.1021/acscatal.0c03338.

[81] G.J. Bang, G.H. Gu, J. Noh, Y. Jung, Activity trends of methane oxidation catalysts under emission conditions, ACS Catal. 12 (2022) 10255–10263, https://doi.org/10.1021/acscatal.2c00842.

[82] F. Nkinahamira, R.J. Yang, R.S. Zhu, J.W. Zhang, Z.Y. Ren, S.L. Sun, H.F. Xiong, Z.Y. Zeng, Current progress on methods and technologies for catalytic methane activation at low temperatures, Adv. Sci. 10 (2023) 2204566, https://doi.org/10.1002/advs.202204566.

[83] Z.Y. Tang, T. Zhang, D.C. Luo, Y.J. Wang, Z. Hu, R.T. Yang, Catalytic combustion of methane: from mechanism and materials properties to catalytic performance, ACS Catal. 12 (2022) 13457–13474, https://doi.org/10.1021/acscatal.2c0332113457.

[84] G.S. Bugosh, V.G. Easterling, I.A. Rusakova, M.P. Harold, Anomalous steady-state and spatio-temporal features of methane oxidation on Pt/Pd/Al_2O_3 monolith spanning lean and rich conditions, Appl. Catal. B 165 (2015) 68–78, https://doi.org/10.1016/j.apcatb.2014.09.058.

[85] F.J. Huang, J.J. Chen, W. Hu, G.X. Li, Y. Wu, S.D. Yuan, L. Zhong, Y.Q. Chen, Pd or PdO: Catalytic active site of methane oxidation operated close to stoichiometric air-to-fuel for natural gas vehicles, Appl. Catal. B 219 (2017) 73–81, https://doi.org/10.1016/j.apcatb.2017.07.037.

[86] O. Mihai, G. Smedler, U. Nylen, M. Olofsson, L. Olsson, The effect of water on methane oxidation over Pd/Al_2O_3 under lean, stoichiometric and rich conditions, Catal. Sci. Technol. 7 (2017) 3084–3096, https://doi.org/10.1039/c6cy02329k.

[87] S. Seimanides, M. Stoukides, Catalytic oxidation of methane on polycrystalline palladium supported on stabilized zirconia, J. Catal. 98 (1986) 540–549, https://doi.org/10.1016/0021-9517(86)90342-8.

[88] A. Giannikos, A.D. Frantzis, C. Pliangos, S. Bebelis, C.G. Vayenas, Electrochemical promotion of CH_4 oxidation on Pd, Ionics 4 (1998) 53–60, https://doi.org/10.1007/Bf02375780.

[89] S. Specchia, F. Conti, V. Specchia, Kinetic studies on Pd/$Ce_xZr_{1-x}O_2$ catalyst for methane combustion, Ind. Eng. Chem. Res. 49 (2010) 11101–11111, https://doi.org/10.1021/ie100532x.

[90] C. Jiménez-Borja, B. Delgado, F. Dorado, J.L. Valverde, Experimental data and kinetic modeling of the catalytic and electrochemically promoted CH_4 oxidation over Pd catalyst-electrodes, Chem. Eng. J. 225 (2013) 315–322, https://doi.org/10.1016/j.cej.2013.03.095.

[91] P. Hurtado, S. Ordónez, H. Sastre, F.V. Díez, Development of a kinetic model for the oxidation of methane over Pd/Al_2O_3 at dry and wet conditions, Appl. Catal. B 51 (2004) 229–238, https://doi.org/10.1016/j.apcatb.2004.03.006.

[92] R. Mezaki, C.C. Watson, Catalytic oxidation of methane, Ind. Eng. Chem. Process Des. Dev. 5 (1966) 62–65, https://doi.org/10.1021/i260017a013.

[93] P. Velin, F. Hemmingsson, A. Schaefer, M. Skoglundh, K.A. Lomachenko, A. Raj, D. Thompsett, G. Smedler, P.A. Carlsson, Hampered PdO redox dynamics by water suppresses lean methane oxidation over realistic palladium catalysts, ChemCatChem 13 (2021) 3765–3771, https://doi.org/10.1002/cctc.202100829.

[94] P. Mars, D.W. van Krevelen, Oxidations carried out by means of vanadium oxide catalysts, Chem. Eng. Sci. 3 (1954) 41–59, https://doi.org/10.1016/S0009-2509(54)80005-4.

[95] C.A. Müller, M. Maciejewski, R.A. Koeppel, R. Tschan, A. Baiker, Role of lattice oxygen in the combustion of methane over PdO/ZrO_2: Combined pulse TG/DTA and MS study with ^{18}O-labeled catalyst, J. Phys. Chem. 100 (1996) 20006–20014, https://doi.org/10.1021/jp961903a.

[96] C.A. Müller, M. Maciejewski, R.A. Koeppel, A. Baiker, Combustion of methane over palladium/zirconia: effect of Pd-particle size and role of lattice oxygen, Catal. Today 47 (1999) 245–252, https://doi.org/10.1016/S0920-5861(98)00305-8.

[97] D. Ciuparu, E. Altman, L. Pfefferle, Contributions of lattice oxygen in methane combustion over PdO-based catalysts, J. Catal. 203 (2001) 64–74, https://doi.org/10.1006/jcat.2001.3331.

[98] S. Todorova, A. Naydenov, H. Kolev, G. Ivanov, A. Ganguly, S. Mondal, S. Saha, A. K. Ganguli, Reaction kinetics and mechanism of complete methane oxidation on Pd/Mn_2O_3 catalyst, React. Kinet., Mech. Catal. 123 (2018) 585–605, https://doi.org/10.1007/s11144-018-1343-y.

[99] H. Stotz, L. Maier, A. Boubnov, A.T. Gremminger, J.-D. Grunwaldt, O. Deutschmann, Surface reaction kinetics of methane oxidation over PdO, J. Catal. 370 (2019) 152–175, https://doi.org/10.1016/j.jcat.2018.12.007.

[100] M. Van den Bossche, H. Grönbeck, Methane Oxidation over PdO(101) Revealed by First-Principles Kinetic Modeling, J. Am. Chem. Soc. 137 (2015) 12035–12044, https://doi.org/10.1021/jacs.5b06069.
[101] S.K. Matam, M.H. Aguirre, A. Weidenkaff, D. Ferri, Revisiting the problem of active sites for methane combustion on Pd/Al_2O_3 by operando XANES in a lab-scale fixed-bed reactor, J. Phys. Chem. C 114 (2010) 9439–9443, https://doi.org/10.1021/jp1019697.
[102] J.-D. Grunwaldt, N. van Vegten, A. Baiker, Insight into the structure of supported palladium catalysts during the total oxidation of methane, Chem. Commun. (2007) 4635–4637, https://doi.org/10.1039/b710222d.
[103] P. Lott, P. Dolcet, M. Casapu, J.-D. Grunwaldt, O. Deutschmann, The Effect of Prereduction on the Performance of Pd/Al_2O_3 and Pd/CeO_2 Catalysts during Methane Oxidation, Ind. Eng. Chem. Res. 58 (2019) 12561–12570, https://doi.org/10.1021/acs.iecr.9b01267.
[104] D. Wang, J. Gong, J.Y. Luo, J.H. Li, K. Kamasamudram, N. Currier, A. Yezerets, Distinct reaction pathways of methane oxidation on different oxidation states over Pd-based three-way catalyst (TWC), Appl. Catal. A 572 (2019) 44–50, https://doi.org/10.1016/j.apcata.2018.12.022.
[105] G. Groppi, W. Ibashi, E. Tronconi, P. Forzatti, Structured reactors for kinetic measurements under severe conditions in catalytic combustion over palladium supported systems, Catal. Today 69 (2001) 399–408, https://doi.org/10.1016/S0920-5861(01)00398-4.
[106] G. Groppi, W. Ibashi, M. Valentini, P. Forzatti, High-temperature combustion of CH_4 over PdO/Al_2O_3: kinetic measurements in a structured annular reactor, Chem. Eng. Sci. 56 (2001) 831–839, https://doi.org/10.1016/S0009-2509(00)00295-5.
[107] G. Groppi, Combustion of CH_4 over a PdO/ZrO_2 catalyst: an example of kinetic study under severe conditions, Catal. Today 77 (2003) 335–346, https://doi.org/10.1016/S0920-5861(02)00378-4.
[108] R.J. Farrauto, M.C. Hobson, T. Kennelly, E.M. Waterman, Catalytic chemistry of supported palladium for combustion of methane, Appl. Catal. A 81 (1992) 227–237, https://doi.org/10.1016/0926-860x(92)80095-T.
[109] J.G. McCarty, Kinetics of PdO combustion catalysis, Catal. Today 26 (1995) 283–293, https://doi.org/10.1016/0920-5861(95)00150-7.
[110] J.N. Carstens, S.C. Su, A.T. Bell, Factors affecting the catalytic activity of Pd/ZrO_2 for the combustion of methane, J. Catal. 176 (1998) 136–142, https://doi.org/10.1006/jcat.1998.2029.
[111] T.R. Baldwin, R. Burch, Catalytic combustion of methane over supported palladium catalysts: II. support and possible morphological effects, Appl. Catal. 66 (1990) 359–381, https://doi.org/10.1016/S0166-9834(00)81649-8.
[112] A.K. Datye, J. Bravo, T.R. Nelson, P. Atanasova, M. Lyubovsky, L. Pfefferle, Catalyst microstructure and methane oxidation reactivity during the Pd <-> PdO transformation on alumina supports, Appl. Catal. A 198 (2000) 179–196, https://doi.org/10.1016/S0926-860x(99)00512-8.
[113] P. Legare, L. Hilaire, G. Maire, G. Krill, A. Amamou, Interaction of oxygen and hydrogen with palladium, Surf. Sci. 107 (1981) 533–546, https://doi.org/10.1016/0039-6028(81)90543-4.
[114] Y.S. Ho, C.B. Wang, C.T. Yeh, Calorimetric study on interaction of dioxygen with alumina supported palladium, J. Mol. Catal. A: Chem. 112 (1996) 287–294, https://doi.org/10.1016/1381-1169(96)00129-X.
[115] J.J. Chen, E. Ruckenstein, Role of interfacial phenomena in the behavior of alumina-supported palladium crystallites in oxygen, J. Phys. Chem. 85 (1981) 1606–1612, https://doi.org/10.1021/j150611a029.
[116] E. Ruckenstein, J.J. Chen, Spreading and surface tension driven phenomena during heating of alumina-supported palladium crystallites in oxygen, J. Catal. 70 (1981) 233–236, https://doi.org/10.1016/0021-9517(81)90334-1.
[117] E. Ruckenstein, J.J. Chen, Wetting Phenomena during Alternating Heating in O_2 and H_2 of Supported Metal Crystallites, J. Colloid Interface Sci. 86 (1982) 1–11, https://doi.org/10.1016/0021-9797(82)90034-0.
[118] R. Burch, F.J. Urbano, Investigation of the active state of supported palladium catalysts in the combustion of methane, Appl. Catal. A 124 (1995) 121–138, https://doi.org/10.1016/0926-860x(94)00252-5.
[119] Z.P. Liu, P. Hu, General rules for predicting where a catalytic reaction should occur on metal surfaces: a density functional theory study of C-H and C-O bond breaking/making on flat, stepped, and kinked metal surfaces, J. Am. Chem. Soc. 125 (2003) 1958–1967, https://doi.org/10.1021/ja0207551.
[120] J.-D. Grunwaldt, N. van Vegten, A. Baiker, W. van Beek, Insight into the structure of Pd/ZrO_2 during the total oxidation of methane using combined in situ XRD, X-ray absorption and Raman spectroscopy, J. Phys.: Conf. Ser. 190 (2009), 012160, https://doi.org/10.1088/1742-6596/190/1/012160.
[121] A.Y. Stakheev, A.M. Batkin, N.S. Teleguina, G.O. Bragina, V.I. Zaikovsky, I. P. Prosvirin, A.K. Khudorozhkov, V.I. Bukhtiyarov, Particle Size Effect on CH_4 Oxidation Over Noble Metals: Comparison of Pt and Pd Catalysts, Top. Catal. 56 (2013) 306–310, https://doi.org/10.1007/s11244-013-9971-y.
[122] J. Au-Yeung, K.D. Chen, A.T. Bell, E. Iglesia, Isotopic studies of methane oxidation pathways on PdO catalysts, J. Catal. 188 (1999) 132–139, https://doi.org/10.1006/jcat.1999.2643.
[123] D. Ciuparu, L. Pfefferle, Contributions of lattice oxygen to the overall oxygen balance during methane combustion over PdO-based catalysts, Catal. Today 77 (2002) 167–179, https://doi.org/10.1016/S0920-5861(02)00243-2.
[124] Y.H. Chin, C. Buda, M. Neurock, E. Iglesia, Consequences of Metal-Oxide Interconversion for C-H Bond Activation during CH_4 Reactions on Pd Catalysts, J. Am. Chem. Soc. 135 (2013) 15425–15442, https://doi.org/10.1021/ja405004m.
[125] P. Castellazzi, G. Groppi, P. Forzatti, A. Baylet, P. Marecot, D. Duprez, Role of Pd loading and dispersion on redox behaviour and CH_4 combustion activity of Al_2O_3 supported catalysts, Catal. Today 155 (2010) 18–26, https://doi.org/10.1016/j.cattod.2009.02.029.
[126] M. Lyubovsky, L. Pfefferle, A. Datye, J. Bravo, T. Nelson, TEM study of the microstructural modifications of an alumina-supported palladium combustion catalyst, J. Catal. 187 (1999) 275–284, https://doi.org/10.1006/jcat.1999.2545.
[127] J. Xu, L.K. Ouyang, W. Mao, X.J. Yang, X.C. Xu, J.J. Su, T.Z. Zhuang, H. Li, Y. F. Han, Operando and Kinetic Study of Low-Temperature, Lean-Burn Methane Combustion over a Pd/γ-Al_2O_3 Catalyst, ACS Catal. 2 (2012) 261–269, https://doi.org/10.1021/cs200694k.
[128] H.F. Xiong, M.H. Wiebenga, C. Carrillo, J.R. Gaudet, H.N. Pham, D. Kunwar, S. H. Oh, G.S. Qi, C.H. Kim, A.K. Datye, Design considerations for low-temperature hydrocarbon oxidation reactions on Pd based catalysts, Appl. Catal. B 236 (2018) 436–444, https://doi.org/10.1016/j.apcatb.2018.05.049.
[129] R.F. Hicks, H.H. Qi, M.L. Young, R.G. Lee, Effect of catalyst structure on methane oxidation over palladium on alumina, J. Catal. 122 (1990) 295–306, https://doi.org/10.1016/0021-9517(90)90283-P.
[130] W.S. Epling, G.B. Hoflund, Catalytic oxidation of methane over ZrO_2-supported Pd catalysts, J. Catal. 182 (1999) 5–12, https://doi.org/10.1006/jcat.1998.2341.
[131] G.W. Graham, D. Konig, B.D. Poindexter, J.T. Remillard, W.H. Weber, Ellipsometric study of a palladium catalyst during the oxidation of carbon monoxide and methane, Top. Catal. 8 (1999) 35–43, https://doi.org/10.1023/A:1019128203919.
[132] N.M. Kinnunen, J.T. Hirvi, M. Suvanto, T.A. Pakkanen, Role of the Interface between Pd and PdO in Methane Dissociation, J. Phys. Chem. C 115 (2011) 19197–19202, https://doi.org/10.1021/jp204360c.
[133] A. Hellman, A. Resta, N.M. Martin, J. Gustafson, A. Trinchero, P.A. Carlsson, O. Balmes, R. Felici, R. van Rijn, J.W.M. Frenken, J.N. Andersen, E. Lundgren, H. Grönbeck, The active phase of palladium during methane oxidation, J. Phys. Chem. Lett. 3 (2012) 678–682, https://doi.org/10.1021/jz300069s.
[134] N.M. Martin, M. Van den Bossche, A. Hellman, H. Grönbeck, C. Hakanoglu, J. Gustafson, S. Blomberg, N. Johansson, Z. Liu, S. Axnanda, J.F. Weaver, E. Lundgren, Intrinsic Ligand Effect Governing the Catalytic Activity of Pd Oxide Thin Films, ACS Catal. 4 (2014) 3330–3334, https://doi.org/10.1021/cs5010163.
[135] J. Nilsson, P.A. Carlsson, S. Fouladvand, N.M. Martin, J. Gustafson, M.A. Newton, E. Lundgren, H. Grönbeck, M. Skoglundh, Chemistry of Supported Palladium Nanoparticles during Methane Oxidation, ACS Catal. 5 (2015) 2481–2489, https://doi.org/10.1021/cs502036d.
[136] E.J. Jang, J. Lee, D.G. Oh, J.H. Kwak, CH_4 Oxidation Activity in Pd and Pt-Pd Bimetallic Catalysts: Correlation with Surface PdO_x Quantified from the DRIFTS Study, ACS Catal. 11 (2021) 5894–5905, https://doi.org/10.1021/acscatal.1c00156.
[137] S.C. Su, J.N. Carstens, A.T. Bell, A study of the dynamics of Pd oxidation and PdO reduction by H_2 and CH_4, J. Catal. 176 (1998) 125–135, https://doi.org/10.1006/jcat.1998.2028.
[138] D. Ciuparu, L. Pfefferle, Methane combustion activity of supported palladium catalysts after partial reduction, Appl. Catal. A 218 (2001) 197–209, https://doi.org/10.1016/S0926-860x(01)00643-3.
[139] W.R. Schwartz, D. Ciuparu, L.D. Pfefferle, Combustion of methane over palladium-based catalysts: catalytic deactivation and role of the support, J. Phys. Chem. C 116 (2012) 8587–8593, https://doi.org/10.1021/jp212236e.
[140] Y. Mahara, K. Murata, K. Ueda, J. Ohyama, K. Kato, A. Satsuma, Time Resolved in situ DXAFS Revealing Highly Active Species of PdO Nanoparticle Catalyst for CH_4 Oxidation, ChemCatChem 10 (2018) 3384–3387, https://doi.org/10.1002/cctc.201800573.
[141] G.B. Hoflund, H.A.E. Hagelin, J.F. Weaver, G.N. Salaita, ELS and XPS study of Pd/PdO methane oxidation catalysts, Appl. Surf. Sci. 205 (2003) 102–112, https://doi.org/10.1016/S0169-4332(02)01084-X.
[142] E. Broclawik, J. Haber, A. Endou, A. Stirling, R. Yamauchi, M. Kubo, A. Miyamoto, Electronic structure and adsorption properties of precious metals and their oxides: Density functional calculations, J. Mol. Catal. A: Chem. 119 (1997) 35–44, https://doi.org/10.1016/S1381-1169(97)80042-8.
[143] J. Wang, G.-C. Wang, Dynamic evolution of methane oxidation on Pd-based catalysts: a reactive force field molecular dynamics study, J. Phys. Chem. C 126 (2022) 14201–14210, https://doi.org/10.1021/acs.jpcc.2c04841.
[144] Y.L. Chen, J. Lin, X.H. Chen, S.Q. Fan, Y. Zheng, Engineering multicomponent metal-oxide units for efficient methane combustion over palladium-based catalysts, Catal. Sci. Technol. 11 (2021) 152–161, https://doi.org/10.1039/d0cy01742f.
[145] R.L. Mortensen, H.D. Noack, K. Pedersen, S. Mossin, J. Mielby, Recent advances in complete methane oxidation using zeolite-supported metal nanoparticle catalysts, ChemCatChem 14 (2022), e202101924, https://doi.org/10.1002/cctc.202101924.
[146] H.Y. Chen, J. Lu, J.M. Fedeyko, A. Raj, Zeolite supported Pd catalysts for the complete oxidation of methane: a critical review, Appl. Catal. A 633 (2022) 118534, https://doi.org/10.1016/j.apcata.2022.118534.
[147] K. Okumura, S. Matsumoto, N. Nishiaki, M. Niwa, Support effect of zeolite on the methane combustion activity of palladium, Appl. Catal. B 40 (2003) 151–159, https://doi.org/10.1016/S0926-3373(02)00149-2.
[148] I. Friberg, A.H. Clark, P.H. Ho, N. Sadokhina, G.J. Smales, J. Woo, X. Auvray, D. Ferri, M. Nachtegaal, O. Kröcher, L. Olsson, Structure and performance of zeolite supported Pd for complete methane oxidation, Catal. Today 382 (2021) 3–12, https://doi.org/10.1016/j.cattod.2020.11.026.
[149] P. Losch, W.X. Huang, O. Vozniuk, E.D. Goodman, W. Schmidt, M. Cargnello, Modular Pd/Zeolite Composites Demonstrating the Key Role of Support

Hydrophobic/Hydrophilic Character in Methane Catalytic Combustion, ACS Catal. 9 (2019) 4742–4753, https://doi.org/10.1021/acscatal.9b00596.
[150] A.W. Petrov, D. Ferri, F. Krumeich, M. Nachtegaal, J.A. van Bokhoven, O. Kröcher, Stable complete methane oxidation over palladium based zeolite catalysts, Nat. Commun. 9 (2018) 2545, https://doi.org/10.1038/S41467-018-04748-X.
[151] A.W. Petrov, D. Ferri, O. Kröcher, J.A. van Bokhoven, Design of Stable Palladium-Based Zeolite Catalysts for Complete Methane Oxidation by Postsynthesis Zeolite Modification, ACS Catal. 9 (2019) 2303–2312, https://doi.org/10.1021/acscatal.8b04486.
[152] A. Trovarelli, Catalytic properties of ceria and CeO_2-containing materials, Catal. Rev.: Sci. Eng. 38 (1996) 439–520, https://doi.org/10.1080/01614949608006464.
[153] S. Colussi, A. Gayen, M.F. Camellone, M. Boaro, J. Llorca, S. Fabris, A. Trovarelli, Nanofaceted Pd-O sites in Pd-Ce surface superstructures: enhanced activity in catalytic combustion of methane, Angew. Chem., Int. Ed. 48 (2009) 8481–8484, https://doi.org/10.1002/anie.200903581.
[154] M. Cargnello, J.J.D. Jaen, J.C.H. Garrido, K. Bakhmutsky, T. Montini, J.J. C. Gamez, R.J. Gorte, P. Fornasiero, Exceptional activity for methane combustion over modular Pd@CeO_2 subunits on functionalized Al_2O_3, Science 337 (2012) 713–717, https://doi.org/10.1126/science.1222887.
[155] V. Muravev, G. Spezzati, Y.Q. Su, A. Parastaev, F.K. Chiang, A. Longo, C. Escudero, N. Kosinov, E.J.M. Hensen, Interface dynamics of Pd-CeO_2 single-atom catalysts during CO oxidation, Nat. Catal. 4 (2021) 469–478, https://doi.org/10.1038/s41929-021-00621-1.
[156] V. Muravev, J.F.M. Simons, A. Parastaev, M.A. Verheijen, J.J.C. Struijs, N. Kosinov, E.J.M. Hensen, Operando spectroscopy unveils the catalytic role of different palladium oxidation states in CO oxidation on Pd/CeO_2 catalysts, Angew. Chem., Int. Ed. 61 (2022), e202200434, https://doi.org/10.1002/anie.202200434.
[157] T.P. Senftle, A.C.T. van Duin, M.J. Janik, Methane Activation at the Pd/CeO_2 Interface, ACS Catal. 7 (2017) 327–332, https://doi.org/10.1021/acscatal.6b02447.
[158] J. Lee, T.H. Lim, E. Lee, D.H. Kim, Promoting the Methane Oxidation on Pd/CeO_2 Catalyst by Increasing the Surface Oxygen Mobility via Defect Engineering, ChemCatChem 13 (2021) 3706–3712, https://doi.org/10.1002/cctc.202100653.
[159] S.Y. Chen, S.D. Li, R.Y. You, Z.Y. Guo, F. Wang, G.X. Li, W.T. Yuan, B.E. Zhu, Y. Gao, Z. Zhang, H.S. Yang, Y. Wang, Elucidation of Active Sites for CH_4 Catalytic Oxidation over Pd/CeO_2 Via Tailoring Metal-Support Interactions, ACS Catal. 11 (2021) 5666–5677, https://doi.org/10.1021/acscatal.1c00839.
[160] H. Yoshida, T. Nakajima, Y. Yazawa, T. Hattori, Support effect on methane combustion over palladium catalysts, Appl. Catal. B 71 (2007) 70–79, https://doi.org/10.1016/j.apcatb.2006.08.010.
[161] J.J. Willis, A. Gallo, D. Sokaras, H. Aljama, S.H. Nowak, E.D. Goodman, L.H. Wu, C.J. Tassone, T.F. Jaramillo, F. Abild-Pedersen, M. Cargnello, Systematic structure-property relationship studies in palladium-catalyzed methane complete combustion, ACS Catal. 7 (2017) 7810–7821, https://doi.org/10.1021/acscatal.7b02414.
[162] K. Murata, D. Kosuge, J. Ohyama, Y. Mahara, Y. Yamamoto, S. Arai, A. Satsuma, Exploiting metal-support interactions to tune the redox properties of supported Pd catalysts for methane combustion, ACS Catal. 10 (2020) 1381–1387, https://doi.org/10.1021/acscatal.9b04524.
[163] K. Fujimoto, F.H. Ribeiro, M. Avalos-Borja, E. Iglesia, Structure and reactivity of PdO_x/ZrO_2, catalysts for methane oxidation at low temperatures, J. Catal. 179 (1998) 431–442, https://doi.org/10.1006/jcat.1998.2178.
[164] W.X. Huang, E.D. Goodman, P. Losch, M. Cargnello, Deconvoluting transient water effects on the activity of Pd methane combustion catalysts, Ind. Eng. Chem. Res. 57 (2018) 10261–10268, https://doi.org/10.1021/acs.iecr.8b01915.
[165] R. Burch, F.J. Urbano, P.K. Loader, Methane combustion over palladium catalysts: The effect of carbon dioxide and water on activity, Appl. Catal. A 123 (1995) 173–184, https://doi.org/10.1016/0926-860x(94)00251-7.
[166] A.T. Gremminger, H.W.P. de Carvalho, R. Popescu, J.-D. Grunwaldt, O. Deutschmann, Influence of gas composition on activity and durability of bimetallic Pd-Pt/Al_2O_3 catalysts for total oxidation of methane, Catal. Today 258 (2015) 470–480, https://doi.org/10.1016/j.cattod.2015.01.034.
[167] D. Ciuparu, L. Pfefferle, Support and water effects on palladium based methane combustion catalysts, Appl. Catal. A 209 (2001) 415–428, https://doi.org/10.1016/S0926-860x(00)00783-3.
[168] R. Kikuchi, S. Maeda, K. Sasaki, S. Wennerstrom, K. Eguchi, Low-temperature methane oxidation over oxide-supported Pd catalysts: inhibitory effect of water vapor, Appl. Catal. A 232 (2002) 23–28, https://doi.org/10.1016/S0926-860x(02)00096-0.
[169] D. Ciuparu, E. Perkins, L. Pfefferle, In situ DR-FTIR investigation of surface hydroxyls on γ-Al_2O_3 supported PdO catalysts during methane combustion, Appl. Catal. A 263 (2004) 145–153, https://doi.org/10.1016/j.apcata.2003.12.006.
[170] K. Keller, P. Lott, H. Stotz, L. Maier, O. Deutschmann, Microkinetic modeling of the oxidation of methane over PdO catalysts - towards a better understanding of the water inhibition effect, Catalysts 10 (2020) 922, https://doi.org/10.3390/Catal10080922.
[171] F.H. Ribeiro, M. Chow, R.A. Dallabetta, Kinetics of the complete oxidation of methane over supported palladium catalysts, J. Catal. 146 (1994) 537–544, https://doi.org/10.1006/jcat.1994.1092.
[172] J.C. van Giezen, F.R. van den Berg, J.L. Kleinen, A.J. van Dillen, J.W. Geus, The effect of water on the activity of supported palladium catalysts in the catalytic combustion of methane, Catal. Today 47 (1999) 287–293, https://doi.org/10.1016/S0920-5861(98)00309-5.
[173] D. Ciuparu, F. Bozon-Verduraz, L. Pfefferle, Oxygen exchange between palladium and oxide supports in combustion catalysts, J. Phys. Chem. B 106 (2002) 3434–3442, https://doi.org/10.1021/jp013577r.
[174] C.F. Cullis, T.G. Nevell, D.L. Trimm, Role of the catalyst support in the oxidation of methane over palladium, J. Chem. Soc., Faraday Trans. 1 68 (1971) 1406–1412, https://doi.org/10.1039/F19726801406.
[175] D. Roth, P. Gélin, M. Primet, E. Tena, Catalytic behaviour of Cl-free and Cl-containing Pd/Al_2O_3 catalysts in the total oxidation of methane at low temperature, Appl. Catal. A 203 (2000) 37–45, https://doi.org/10.1016/S0926-860x(00)00465-8.
[176] S. Eriksson, M. Boutonnet, S. Jaras, Catalytic combustion of methane in steam and carbon dioxide-diluted reaction mixtures, Appl. Catal. A 312 (2006) 95–101, https://doi.org/10.1016/j.apcata.2006.06.032.
[177] C. Coney, C. Stere, P. Millington, A. Raj, S. Wilkinson, M. Caracotsios, G. McCullough, C. Hardacre, K. Morgan, D. Thompsett, A. Goguet, Spatially-resolved investigation of the water inhibition of methane oxidation over palladium, Catal. Sci. Technol. 10 (2020) 1858–1874, https://doi.org/10.1039/D0CY00154F.
[178] W. Barrett, J. Shen, Y.F. Hu, R.E. Hayes, R.W.J. Scott, N. Semagina, Understanding the Role of SnO_2 Support in Water-Wolerant Methane Combustion: *In situ* Observation of $Pd(OH)_2$ and Comparison with Pd/Al_2O_3, ChemCatChem 12 (2020) 944–952, https://doi.org/10.1002/cctc.201901744.
[179] A. Boubnov, A. Gremminger, M. Casapu, O. Deutschmann, J.-D. Grunwaldt, Dynamics of the reversible inhibition during methane oxidation on bimetallic Pd-Pt catalysts studied by modulation-excitation XAS and DRIFTS, ChemCatChem 14 (2022), e202200573, https://doi.org/10.1002/cctc.202200573.
[180] X.S. Li, X. Wang, K. Roy, J.A. van Bokhoven, L. Artiglia, Role of water on the structure of palladium for complete oxidation of methane, ACS Catal. 10 (2020) 5783–5792, https://doi.org/10.1021/acscatal.0c01069.
[181] K. Keller, P. Lott, S. Tischer, M. Casapu, J.-D. Grunwaldt, O. Deutschmann, Methane oxidation over PdO: towards a better understanding of the influence of the support material, ChemCatChem 15 (2023), e202300366, https://doi.org/10.1002/cctc.202300366.
[182] K. Murata, J. Ohyama, Y. Yamamoto, S. Arai, A. Satsuma, Methane Combustion over Pd/Al_2O_3 Catalysts in the Presence of Water: Effects of Pd Particle Size and Alumina Crystalline Phase, ACS Catal. 10 (2020) 8149–8156, https://doi.org/10.1021/acscatal.0c02050.
[183] D.J. Fullerton, A.V.K. Westwood, R. Brydson, M.V. Twigg, J.M. Jones, Deactivation and regeneration of Pt/γ-alumina and Pt/ceria-alumina catalysts for methane combustion in the presence of H_2S, Catal. Today 81 (2003) 659–671, https://doi.org/10.1016/S0920-5861(03)00164-0.
[184] G. Azimi, R. Dhiman, H.M. Kwon, A.T. Paxson, K.K. Varanasi, Hydrophobicity of rare-earth oxide ceramics, Nat. Mater. 12 (2013) 315–320, https://doi.org/10.1038/Nmat3545.
[185] M. Monai, T. Montini, C. Chen, E. Fonda, R.J. Gorte, P. Fornasiero, Methane catalytic combustion over hierarchical Pd@CeO_2/Si-Al_2O_3: effect of the presence of water, ChemCatChem 7 (2015) 2038–2046, https://doi.org/10.1002/cctc.201402717.
[186] L.S. Escandón, D. Nino, E. Díaz, S. Ordónez, F.V. Díez, Effect of hydrothermal ageing on the performance of Ce-promoted PdO/ZrO_2 for methane combustion, Catal. Commun. 9 (2008) 2291–2296, https://doi.org/10.1016/j.catcom.2008.05.026.
[187] F. Arosio, S. Colussi, A. Trovarelli, G. Groppi, Effect of alternate CH_4-reducing/lean combustion treatments on the reactivity of fresh and S-poisoned Pd/CeO_2/Al_2O_3 catalysts, Appl. Catal. B 80 (2008) 335–342, https://doi.org/10.1016/j.apcatb.2007.11.030.
[188] K.A. Karinshak, P. Lott, M.P. Harold, O. Deutschmann, *In situ* activation of bimetallic Pd-Pt methane oxidation catalysts, ChemCatChem 12 (2020) 3712–3720, https://doi.org/10.1002/cctc.202000603.
[189] T. Franken, M. Roger, A.W. Petrov, A.H. Clark, M. Agote-Arán, F. Krumeich, O. Kröcher, D. Ferri, Effect of Short Reducing Pulses on the Dynamic Structure, Activity, and Stability of Pd/Al_2O_3 for Wet Lean Methane Oxidation, ACS Catal. 11 (2021) 4870–4879, https://doi.org/10.1021/acscatal.1c00328.
[190] C. Nyberg, P. Uvdal, The Oxygen-Water Reaction on Pd(100) - Observation of a Precursor Complex, J. Chem. Phys. 84 (1986) 4631–4635, https://doi.org/10.1063/1.449988.
[191] K. Nomura, K. Noro, Y. Nakamura, Y. Yazawa, H. Yoshida, A. Satsuma, T. Hattori, Pd-Pt bimetallic catalyst supported on SAPO-5 for catalytic combustion of diluted methane in the presence of water vapor, Catal. Lett. 53 (1998) 167–169, https://doi.org/10.1023/A:1019082611978.
[192] H. Yamamoto, H. Uchida, Oxidation of methane over Pt and Pd supported on alumina in lean-burn natural-gas engine exhaust, Catal. Today 45 (1998) 147–151, https://doi.org/10.1016/S0920-5861(98)00265-X.
[193] K. Narui, H. Yata, K. Furuta, A. Nishida, Y. Kohtoku, T. Matsuzaki, Effects of addition of Pt to PdO/Al_2O_3 catalyst on catalytic activity for methane combustion and TEM observations of supported particles, Appl. Catal. A 179 (1999) 165–173, https://doi.org/10.1016/S0926-860x(98)00306-8.
[194] C.L. Pieck, C.R. Vera, E.M. Peirotti, J.C. Yori, Effect of water vapor on the activity of Pt-Pd/Al_2O_3 catalysts for methane combustion, Appl. Catal. A 226 (2002) 281–291, https://doi.org/10.1016/S0926-860x(01)00914-0.
[195] G. Lapisardi, L. Urfels, P. Gélin, M. Primet, A. Kaddouri, E. Garbowski, S. Toppi, E. Tena, Superior catalytic behaviour of Pt-doped Pd catalysts in the complete oxidation of methane at low temperature, Catal. Today 117 (2006) 564–568, https://doi.org/10.1016/j.cattod.2006.06.004.

[196] P. Castellazzi, G. Groppi, P. Forzatti, Effect of Pt/Pd ratio on catalytic activity and redox behavior of bimetallic Pt-Pd/Al_2O_3 catalysts for CH_4 combustion, Appl. Catal. B 95 (2010) 303–311, https://doi.org/10.1016/j.apcatb.2010.01.008.

[197] N. Sadokhina, G. Smedler, U. Nylen, M. Olofsson, L. Olsson, Deceleration of SO_2 poisoning on PtPd/Al_2O_3 catalyst during complete methane oxidation, Appl. Catal. B 236 (2018) 384–395, https://doi.org/10.1016/j.apcatb.2018.05.018.

[198] J. Park, D. Kim, S.W. Byun, H. Shin, Y. Ju, H. Min, Y.J. Kim, I. Heo, M.J. Hazlett, M. Kim, S.B. Kang, Impact of Pd:Pt ratio of Pd/Pt bimetallic catalyst on CH_4 oxidation, Appl. Catal. B 316 (2022), 121623, https://doi.org/10.1016/j.apcatb.2022.121623.

[199] K. Persson, A. Ersson, K. Jansson, J.L.G. Fierro, S.G. Jaras, Influence of molar ratio on Pd-Pt catalysts for methane combustion, J. Catal. 243 (2006) 14–24, https://doi.org/10.1016/j.jcat.2006.06.019.

[200] R. Strobel, J.-D. Grunwaldt, A. Camenzind, S.E. Pratsinis, A. Baiker, Flame-made alumina supported Pd-Pt nanoparticles: structural properties and catalytic behavior in methane combustion, Catal. Lett. 104 (2005) 9–16, https://doi.org/10.1007/s10562-005-7429-y.

[201] K. Persson, L.D. Pfefferle, W. Schwartz, A. Ersson, S.G. Jaras, Stability of palladium-based catalysts during catalytic combustion of methane: The influence of water, Appl. Catal. B 74 (2007) 242–250, https://doi.org/10.1016/j.apcatb.2007.02.015.

[202] M.L. Hou, X. Zhang, C. Fu, W.L. Cen, J.X. Chen, Effects of a Pd/Pt bimetal supported by a γ-Al_2O_3 surface on methane activation, Phys. Chem. Chem. Phys. 22 (2020) 4692–4698, https://doi.org/10.1039/c9cp05920b.

[203] A. Large, J. Seymour, W.Q. Garzon, K. Roy, F. Venturini, D.C. Grinter, L. Artiglia, E. Brooke, M.B. de Gutierrez, A. Raj, K.R.J. Lovelock, R.A. Bennett, T. Eralp-Erden, G. Held, Operando characterisation of alumina-supported bimetallic Pd-Pt catalysts during methane oxidation in dry and wet conditions, J. Phys. D: Appl. Phys. 54 (2021) 174006, https://doi.org/10.1088/1361-6463/abde67.

[204] A.I. Large, R.A. Bennett, T. Eralp-Erden, G. Held, *In situ* surface analysis of palladium-platinum alloys in methane oxidation conditions, Faraday Discuss. 236 (2022) 157–177, https://doi.org/10.1039/d1fd00113b.

[205] A. Morlang, U. Neuhausen, K.V. Klementiev, F.-W. Schütze, G. Miehe, H. Fuess, E. S. Lox, Bimetallic Pt/Pd diesel oxidation catalysts - Structural characterisation and catalytic behaviour, Appl. Catal. B 60 (2005) 191–199, https://doi.org/10.1016/j.apcatb.2005.03.007.

[206] E.D. Goodman, S. Dai, A.C. Yang, C.J. Wrasman, A. Gallo, S.R. Bare, A. S. Hoffman, T.F. Jaramillo, G.W. Graham, X.Q. Pan, M. Cargnello, Uniform Pt/Pd bimetallic nanocrystals demonstrate platinum effect on palladium methane combustion activity and stability, ACS Catal. 7 (2017) 4372–4380, https://doi.org/10.1021/acscatal.7b00393.

[207] H. Nassiri, R.E. Hayes, N. Semagina, Stability of Pd-Pt catalysts in low-temperature wet methane combustion: metal ratio and particle reconstruction, Chem. Eng. Sci. 186 (2018) 44–51, https://doi.org/10.1016/j.ces.2018.04.028.

[208] J. Schütz, H. Störmer, P. Lott, O. Deutschmann, Effects of hydrothermal aging on CO and NO oxidation activity over monometallic and bimetallic Pt-Pd catalysts, Catalysts 11 (2021) 300, https://doi.org/10.3390/Catal11030300.

[209] Y. Yang, J. Lee, R. Dorakhan, H. Nie, G. Fu, A. Quarantotto, J.Y. Howe, Y.-H. Chin, Active site structure and methane oxidation reactivity of bimetallic Pd and Pt nanoparticles, Appl. Catal. A 629 (2022), 118290, https://doi.org/10.1016/j.apcata.2021.118290.

[210] N.J. Divins, A. Braga, X. Vendrell, I. Serrano, X. Garcia, L. Soler, I. Lucentini, M. Danielis, A. Mussio, S. Colussi, I.J. Villar-Garcia, C. Escudero, A. Trovarelli, J. Llorca, Investigation of the evolution of Pd-Pt supported on ceria for dry and wet methane oxidation, Nat. Commun. 13 (2022) 5080, https://doi.org/10.1038/s41467-022-32765-4.

[211] P. Hurtado, S. Ordónez, H. Sastre, F.V. Díez, Combustion of methane over palladium catalyst in the presence of inorganic compounds: inhibition and deactivation phenomena, Appl. Catal. B 47 (2004) 85–93, https://doi.org/10.1016/S0926-3373(03)00328-X.

[212] L.S. Escandón, S. Ordónez, F.V. Díez, H. Sastre, Ammonia oxidation over conventional combustion catalysts, React. Kinet. Catal. Lett. 76 (2002) 61–68, https://doi.org/10.1023/A:1015661227325.

[213] N. Sadokhina, G. Smedler, U. Nylen, M. Olofsson, L. Olsson, The influence of gas composition on Pd-based catalyst activity in methane oxidation - inhibition and promotion by NO, Appl. Catal. B 200 (2017) 351–360, https://doi.org/10.1016/j.apcatb.2016.07.012.

[214] M.D. Argyle, C.H. Bartholomew, Heterogeneous catalyst deactivation and regeneration: a review, Catalysts 5 (2015) 145–269, https://doi.org/10.3390/catal5010145.

[215] H. Cui, S.Q. Turn, M.A. Reese, Removal of sulfur compounds from utility pipelined synthetic natural gas using modified activated carbons, Catal. Today 139 (2009) 274–279, https://doi.org/10.1016/j.cattod.2008.03.024.

[216] A.V. Milkov, Methanogenic biodegradation of petroleum in the West Siberian Basin (Russia): Significance for formation of giant Cenomanian gas pools, AAPG Bull. 94 (2010) 1485–1541, https://doi.org/10.1306/01051009122.

[217] V. Smil, Natural Gas: Fuel for the 21st Century, John Wiley & Sons, Ltd,, Chicester, West Sussex, United Kingdom, 2015.

[218] J.K. Lampert, M.S. Kazi, R.J. Farrauto, Methane Emissions Abatement from Lean Burn Natural Gas Vehicle Exhaust: Sulfur's Impact on Catalyst Performance, SAE Technical Paper 961971, (1996). https://doi.org/10.4271/961971.

[219] J.K. Lampert, M.S. Kazi, R.J. Farrauto, Palladium catalyst performance for methane emissions abatement from lean burn natural gas vehicles, Appl. Catal. B 14 (1997) 211–223, https://doi.org/10.1016/S0926-3373(97)00024-6.

[220] P. Gélin, L. Urfels, M. Primet, E. Tena, Complete oxidation of methane at low temperature over Pt and Pd catalysts for the abatement of lean-burn natural gas fuelled vehicles emissions: influence of water and sulphur containing compounds, Catal. Today 83 (2003) 45–57, https://doi.org/10.1016/S0920-5861(03)00215-3.

[221] A. Gremminger, P. Lott, M. Merts, M. Casapu, J.-D. Grunwaldt, O. Deutschmann, Sulfur poisoning and regeneration of bimetallic Pd-Pt methane oxidation catalysts, Appl. Catal. B 218 (2017) 833–843, https://doi.org/10.1016/j.apcatb.2017.06.048.

[222] P. Lott, M. Eck, D.E. Doronkin, A. Zimina, S. Tischer, R. Popescu, S. Belin, V. Briois, M. Casapu, J.-D. Grunwaldt, O. Deutschmann, Understanding sulfur poisoning of bimetallic Pd-Pt methane oxidation catalysts and their regeneration, Appl. Catal. B 278 (2020), 119244, https://doi.org/10.1016/j.apcatb.2020.119244.

[223] D.L. Mowery, M.S. Graboski, T.R. Ohno, R.L. McCormick, Deactivation of PdO-Al_2O_3 oxidation catalyst in lean-burn natural gas engine exhaust: aged catalyst characterization and studies of poisoning by H_2O and SO_2, Appl. Catal. B 21 (1999) 157–169, https://doi.org/10.1016/S0926-3373(99)00017-X.

[224] D.L. Mowery, R.L. McCormick, Deactivation of alumina supported and unsupported PdO methane oxidation catalyst: the effect of water on sulfate poisoning, Appl. Catal. B 34 (2001) 287–297, https://doi.org/10.1016/S0926-3373(01)00222-3.

[225] M. Monai, T. Montini, M. Melchionna, T. Duchon, P. Kus, C. Chen, N. Tsud, L. Nasi, K.C. Prince, K. Veltruska, V. Matolin, M.M. Khader, R.J. Gorte, P. Fornasiero, The effect of sulfur dioxide on the activity of hierarchical Pd-based catalysts in methane combustion, Appl. Catal. B 202 (2017) 72–83, https://doi.org/10.1016/j.apcatb.2016.09.016.

[226] P. Auvinen, J.T. Hirvi, N.M. Kinnunen, M. Suvanto, $PdSO_4$ surfaces in methane oxidation catalysts: DFT studies on stability, reactivity, and water inhibition, ACS Catal. 10 (2020) 12943–12953, https://doi.org/10.1021/acscatal.0c03686.

[227] M.S. Wilburn, W.S. Epling, SO_2 adsorption and desorption characteristics of Pd and Pt catalysts: Precious metal crystallite size dependence, Appl. Catal. A 534 (2017) 85–93, https://doi.org/10.1016/j.apcata.2017.01.015.

[228] H.N. Sharma, V. Sharma, A.B. Mhadeshwar, R. Ramprasad, Why Pt Survives but Pd Suffers From SO_x Poisoning? J. Phys. Chem. Lett. 6 (2015) 1140–1148, https://doi.org/10.1021/jz5027147.

[229] T. Hamzehlouyan, C.S. Sampara, J.H. Li, A. Kumar, W.S. Epling, Kinetic study of adsorption and desorption of SO_2 over γ-Al_2O_3 and Pt/γ-Al_2O_3, Appl. Catal. B 181 (2016) 587–598, https://doi.org/10.1016/j.apcatb.2015.08.003.

[230] T. Hamzehlouyan, C. Sampara, J.N. Li, A. Kumar, W. Epling, Sulfur Poisoning of a Pt/Al_2O_3 Oxidation Catalyst: Understanding of SO_2, SO_3 and H_2SO_4 Impacts, Top. Catal. 59 (2016) 1028–1032, https://doi.org/10.1007/s11244-016-0592-0.

[231] R. Streber, C. Papp, M.P.A. Lorenz, O. Höfert, E. Darlatt, A. Bayer, R. Denecke, H. P. Steinrück, SO_2 adsorption and thermal evolution on clean and oxygen precovered Pt(111), Chem. Phys. Lett. 494 (2010) 188–192, https://doi.org/10.1016/j.cplett.2010.06.007.

[232] M.S. Wilburn, W.S. Epling, Sulfur deactivation and regeneration of mono- and bimetallic Pd-Pt methane oxidation catalysts, Appl. Catal. B 206 (2017) 589–598, https://doi.org/10.1016/j.apcatb.2017.01.050.

[233] M.S. Wilburn, W.S. Epling, SO_2 adsorption and desorption characteristics of bimetallic Pd-Pt catalysts: Pd:Pt ratio dependency, Catal. Today 320 (2019) 11–19, https://doi.org/10.1016/j.cattod.2017.08.054.

[234] M.S. Wilburn, W.S. Epling, Formation and Decomposition of Sulfite and Sulfate Species on Pt/Pd Catalysts: An SO_2 Oxidation and Sulfur Exposure Study, ACS Catal. 9 (2019) 640–648, https://doi.org/10.1021/acscatal.8b03529.

[235] D.E. Doronkin, T.S. Khan, T. Bligaard, S. Fogel, P. Gabrielsson, S. Dahl, Sulfur poisoning and regeneration of the Ag/γ-Al_2O_3 catalyst for H_2-assisted SCR of NO_x by ammonia, Appl. Catal. B 117 (2012) 49–58, https://doi.org/10.1016/j.apcatb.2012.01.002.

[236] L. Hu, S. Williams, Sulfur Poisoning and Regeneration of Pd Catalyst under Simulated Emission Conditions of Natural Gas Engine, SAE Technical Paper 2007–01-4037, (2007). https://doi.org/10.4271/2007–01-4037.

[237] M. Waqif, A. Pieplu, O. Saur, J.C. Lavalley, G. Blanchard, Use of CeO_2-Al_2O_3 as a SO_2 sorbent, Solid State Ion. 95 (1997) 163–167, https://doi.org/10.1016/S0167-2738(96)00577-2.

[238] M. Waqif, P. Bazin, O. Saur, J.C. Lavalley, G. Blanchard, O. Touret, Study of ceria sulfation, Appl. Catal. B 11 (1997) 193–205, https://doi.org/10.1016/S0926-3373(96)00040-9.

[239] T. Luo, J.M. Vohs, R.J. Gorte, An Examination of Sulfur Poisoning on Pd/Ceria Catalysts, J. Catal. 210 (2002) 397–404, https://doi.org/10.1006/jcat.2002.3689.

[240] T. Luo, R.J. Gorte, Characterization of SO_2-poisoned ceria-zirconia mixed oxides, Appl. Catal. B 53 (2004) 77–85, https://doi.org/10.1016/j.apcatb.2004.04.020.

[241] M.Y. Smirnov, A.V. Kalinkin, A.V. Pashis, I.P. Prosvirin, V.I. Bukhtiyarov, Interaction of SO_2 with Pt model supported catalysts studied by XPS, J. Phys. Chem. C 118 (2014) 22120–22135, https://doi.org/10.1021/jp5069126.

[242] C.C. Chang, Infrared studies of SO_2 on γ-alumina, J. Catal. 53 (1978) 374–385, https://doi.org/10.1016/0021-9517(78)90109-4.

[243] M.Y. Smirnov, A.V. Kalinkin, A.V. Pashis, A.M. Sorokin, A.S. Noskov, K.C. Kharas, V.I. Bukhtiyarov, Interaction of Al_2O_3 and CeO_2 surfaces with SO_2 and SO_2+O_2 studied by X-ray photoelectron spectroscopy, J. Phys. Chem. B 109 (2005) 11712–11719, https://doi.org/10.1021/jp0508249.

[244] S. Matsumoto, Y. Ikeda, H. Suzuki, M. Ogai, N. Miyoshi, NO_x storage-reduction catalyst for automotive exhaust with improved tolerance against sulfur poisoning, Appl. Catal. B 25 (2000) 115–124, https://doi.org/10.1016/S0926-3373(99)00124-1.

[245] H. Hirata, I. Hachisuka, Y. Ikeda, S. Tsuji, S. Matsumoto, NO_x storage-reduction three-way catalyst with improved sulfur tolerance, Top. Catal. 16 (2001) 145–149, https://doi.org/10.1023/A:1016603502952.
[246] T. Schedlbauer, P. Lott, M. Casapu, H. Störmer, O. Deutschmann, J.-D. Grunwaldt, Impact of the Support on the Catalytic Performance, Inhibition Effects and SO_2 Poisoning Resistance of Pt-Based Formaldehyde Oxidation Catalysts, Top. Catal. 62 (2019) 198–205, https://doi.org/10.1007/s11244-018-1122-z.
[247] A.M. Venezia, R. Murania, G. Pantaleo, G. Deganello, Pd and PdAu on mesoporous silica for methane oxidation: Effect of SO_2, J. Catal. 251 (2007) 94–102, https://doi.org/10.1016/j.jcat.2007.07.013.
[248] D.E. Doronkin, S. Fogel, P. Gabrielsson, J.-D. Grunwaldt, S. Dahl, Ti and Si doping as a way to increase low temperature activity of sulfated Ag/Al_2O_3 in H_2-assisted NH_3-SCR of NO_x, Appl. Catal. B 148–149 (2014) 62–69, https://doi.org/10.1016/j.apcatb.2013.10.040.
[249] A.M. Venezia, G. Di Carlo, G. Pantaleo, L.F. Liotta, G. Melaet, N. Kruse, Oxidation of CH_4 over Pd supported on TiO_2-doped SiO_2: Effect of Ti(IV) loading and influence of SO_2, Appl. Catal. B 88 (2009) 430–437, https://doi.org/10.1016/j.apcatb.2008.10.023.
[250] J. Lin, X.H. Chen, Y. Zheng, Y.H. Xiao, Y. Zheng, L.L. Jiang, Sulfur-resistant methane combustion invoked by surface property regulation on palladium-based catalysts, Appl. Surf. Sci. 587 (2022) 152835, https://doi.org/10.1016/j.apsusc.2022.152835.
[251] N. Ottinger, R. Veele, Y. Xi, Z.G. Liu, Desulfation of Pd-based oxidation catalysts for lean-burn natural gas and dual-fuel applications, SAE Int. J. Engines 8 (2015) 1472–1477, https://doi.org/10.4271/2015-01-0991.
[252] T.C. Yu, H. Shaw, The effect of sulfur poisoning on methane oxidation over palladium supported on γ-alumina catalysts, Appl. Catal. B 18 (1998) 105–114, https://doi.org/10.1016/S0926-3373(98)00031-9.
[253] J.M. Jones, V.A. Dupont, R. Brydson, D.J. Fullerton, N.S. Nasri, A.B. Ross, A.V. K. Westwood, Sulphur poisoning and regeneration of precious metal catalysed methane combustion, Catal. Today 81 (2003) 589–601, https://doi.org/10.1016/S0920-5861(03)00157-3.
[254] S. Ordónez, P. Hurtado, F.V. Díez, Methane catalytic combustion over Pd/Al_2O_3 in presence of sulphur dioxide: development of a regeneration procedure, Catal. Lett. 100 (2005) 27–34, https://doi.org/10.1007/s10562-004-3081-1.
[255] F. Arosio, S. Colussi, G. Groppi, A. Trovarelli, Regeneration of S-poisoned Pd/Al_2O_3 catalysts for the combustion of methane, Catal. Today 117 (2006) 569–576, https://doi.org/10.1016/j.cattod.2006.06.006.
[256] N.M. Kinnunen, J.T. Hirvi, K. Kallinen, T. Maunula, M. Keenan, M. Suvanto, Case study of a modern lean-burn methane combustion catalyst for automotive applications: what are the deactivation and regeneration mechanisms? Appl. Catal. B 207 (2017) 114–119, https://doi.org/10.1016/j.apcatb.2017.02.018.
[257] M. Honkanen, J. Wang, M. Kärkkäinen, M. Huuhtanen, H. Jiang, K. Kallinen, R. L. Keiski, J. Akola, M. Vippola, Regeneration of sulfur-poisoned Pd-based catalyst for natural gas oxidation, J. Catal. 358 (2018) 253–256, https://doi.org/10.1016/j.jcat.2017.12.021.
[258] P. Lott, M. Eck, D.E. Doronkin, R. Popescu, M. Casapu, J.-D. Grunwaldt, O. Deutschmann, Regeneration of sulfur poisoned $Pd-Pt/CeO_2-ZrO_2-Y_2O_3-La_2O_3$ and $Pd-Pt/Al_2O_3$ methane oxidation catalysts, Top. Catal. 62 (2019) 164–171, https://doi.org/10.1007/s11244-018-1121-0.
[259] V.H. Nissinen, N.M. Kinnunen, M. Suvanto, Regeneration of a sulfur-poisoned methane combustion catalyst: Structural evidence of Pd_4S formation, Appl. Catal. B 237 (2018) 110–115, https://doi.org/10.1016/j.apcatb.2018.05.057.
[260] J.B. Miller, D.R. Alfonso, B.H. Howard, C.P. O'Brien, B.D. Morreale, Hydrogen dissociation on Pd_4S surfaces, J. Phys. Chem. C 113 (2009) 18800–18806, https://doi.org/10.1021/jp906694k.
[261] C.H. Bartholomew, Mechanisms of catalyst deactivation, Appl. Catal. A 212 (2001) 17–60, https://doi.org/10.1016/S0926-860x(00)00843-7.
[262] M.J. Rokosz, A.E. Chen, C.K. Lowe-Ma, A.V. Kucherov, D. Benson, M.C.P. Peck, R. W. McCabe, Characterization of phosphorus-poisoned automotive exhaust catalysts, Appl. Catal. B 33 (2001) 205–215, https://doi.org/10.1016/S0926-3373(01)00165-5.
[263] A.K. Neyestanaki, F. Klingstedt, T. Salmi, D.Y. Murzin, Deactivation of postcombustion catalysts, a review, Fuel 83 (2004) 395–408, https://doi.org/10.1016/j.fuel.2003.09.002.
[264] A. Winkler, D. Ferri, R. Hauert, Influence of aging effects on the conversion efficiency of automotive exhaust gas catalysts, Catal. Today 155 (2010) 140–146, https://doi.org/10.1016/j.cattod.2008.11.021.
[265] C. Larese, F. Cabello Galisteo, M. López Granados, R. Mariscal, J.L.G. Fierro, M. Furió, R. Fernández Ruiz, Deactivation of real three way catalysts by $CePO_4$ formation, Appl. Catal. B 40 (2003) 305–317, https://doi.org/10.1016/S0926-3373(02)00161-3.
[266] M. López Granados, C. Larese, F. Cabello Galisteo, R. Mariscal, J.L.G. Fierro, R. Fernández-Ruíz, R. Sanguino, M. Luna, Effect of mileage on the deactivation of vehicle-aged three-way catalysts, Catal. Today, 107- 108 (2005) 77–85, https://doi.org/10.1016/j.cattod.2005.07.064.
[267] M. Honkanen, M. Kärkkäinen, O. Heikkinen, K. Kallinen, T. Kolli, M. Huuhtanen, J. Lahtinen, R.L. Keiski, T. Lepistö, M. Vippola, The Effect of Phosphorus Exposure on Diesel Oxidation Catalysts–Part II: Characterization of Structural Changes by Transmission Electron Microscopy, Top. Catal. 58 (2015) 971–976, https://doi.org/10.1007/s11244-015-0465-y.
[268] W.B. Williamson, J. Perry, H.S. Gandhi, J.L. Bomback, Effects of oil phosphorus on deactivation of monolithic three-way catalysts, Appl. Catal. 15 (1985) 277–292, https://doi.org/10.1016/S0166-9834(00)81842-4.
[269] S.Y. Christou, S. García-Rodríguez, J.L.G. Fierro, A.M. Efstathiou, Deactivation of $Pd/Ce_{0.5}Zr_{0.5}O_2$ model three-way catalyst by P, Ca and Zn deposition, Appl. Catal. B 111 (2012) 233–245, https://doi.org/10.1016/j.apcatb.2011.10.004.
[270] A. Williams, J. Burton, R.L. McCormick, T.J. Toops, A.A. Wereszczak, E.E. Fox, M. J. Lance, G. Cavataio, D. Dobson, J. Warner, R. Brezny, K. Nguyen, D.W. Brookshear, Impact of Fuel Metal Impurities on the Durability of a Light-Duty Diesel Aftertreatment System, SAE Technical Paper 2013–01-0513, (2013). https://doi.org/10.4271/2013–01-0513.
[271] S.L. Bergman, J. Granestrand, S. Xi, Y. Du, Y. Tang, C. Tang, L. Kienkas, L. J. Pettersson, S.L. Bernasek, Probing the Oxidation/Reduction Dynamics of Fresh and P-, Na-, and K-Contaminated $Pt/Pd/Al_2O_3$ Diesel Oxidation Catalysts by STEM, TPR, and in Situ XANES, J. Phys. Chem. C 124 (2020) 2945–2952, https://doi.org/10.1021/acs.jpcc.9b07655.
[272] B.G. Bunting, K. More, S. Lewis, T. Toops, Phosphorous Poisoning and Phosphorous Exhaust Chemistry with Diesel Oxidation Catalysts, SAE Technical Paper 2005–01-1758, (2005). https://doi.org/10.4271/2005–01-1758.
[273] J. Franz, J. Schmidt, C. Schoen, M. Harperscheid, S. Eckhoff, M. Roesch, J. Leyrer, Deactivation of TWC as a Function of Oil Ash Accumulation - A Parameter Study, SAE Technical Paper 2005–01-1097, (2005). https://doi.org/10.4271/2005–01-1097.
[274] P. Lanzerath, A. Guethenke, A. Massner, U. Gaertner, Analytical investigations on ageing phenomena of catalytic exhaust gas aftertreatment components, Catal. Today 147 (2009) S265–S270, https://doi.org/10.1016/j.cattod.2009.07.028.
[275] M.H. Wiebenga, C.H. Kim, S.J. Schmieg, S.H. Oh, D.B. Brown, D.H. Kim, J.-H. Lee, C.H.F. Peden, Deactivation mechanisms of Pt/Pd-based diesel oxidation catalysts, Catal. Today 184 (2012) 197–204, https://doi.org/10.1016/j.cattod.2011.11.014.
[276] M. Agote-Arán, M. Elsener, F.W. Schütze, C.M. Schilling, M. Sridhar, E. Katsaounis, O. Kröcher, D. Ferri, Understanding the impact of poison distribution on the performance of Diesel oxidation catalysts, Appl. Catal. B 299 (2021), 120684, https://doi.org/10.1016/j.apcatb.2021.120684.
[277] L. Xu, G. Guo, D. Uy, A.E. O'Neill, W.H. Weber, M.J. Rokosz, R.W. McCabe, Cerium phosphate in automotive exhaust catalyst poisoning, Appl. Catal. B 50 (2004) 113–125, https://doi.org/10.1016/j.apcatb.2004.01.017.
[278] M. Kärkkäinen, T. Kolli, M. Honkanen, O. Heikkinen, M. Huuhtanen, K. Kallinen, T. Lepistö, J. Lahtinen, M. Vippola, R.L. Keiski, The Effect of Phosphorus Exposure on Diesel Oxidation Catalysts–Part I: Activity Measurements, Elementary and Surface Analyses, Top. Catal. 58 (2015) 961–970, https://doi.org/10.1007/s11244-015-0464-z.
[279] P. Anguita, J.M. García-Vargas, F. Gaillard, E. Iojoiu, S. Gil, A. Giroir-Fendler, Effect of Na, K, Ca and P-impurities on diesel oxidation catalysts (DOCs), Chem. Eng. J. 352 (2018) 333–342, https://doi.org/10.1016/j.cej.2018.07.040.
[280] M. Agote-Arán, M. Elsener, F.W. Schütze, C.M. Schilling, M. Sridhar, E. Katsaounis, O. Kröcher, D. Ferri, On the relevance of P poisoning in real-world DOC aging, Appl. Catal. B 291 (2021), 120062, https://doi.org/10.1016/j.apcatb.2021.120062.
[281] R. Dewil, L. Appels, J. Baeyens, Energy use of biogas hampered by the presence of siloxanes, Energy Convers. Manage. 47 (2006) 1711–1722, https://doi.org/10.1016/j.enconman.2005.10.016.
[282] S. Rasi, A. Veijanen, J. Rintala, Trace compounds of biogas from different biogas production plants, Energy 32 (2007) 1375–1380, https://doi.org/10.1016/j.energy.2006.10.018.
[283] N. de Arespacochaga, C. Valderrama, J. Raich-Montiu, M. Crest, S. Mehta, J. L. Cortina, Understanding the effects of the origin, occurrence, monitoring, control, fate and removal of siloxanes on the energetic valorization of sewage biogas–A review, Renew. Sustain. Energy Rev. 52 (2015) 366–381, https://doi.org/10.1016/j.rser.2015.07.106.
[284] S. Rasi, J. Läntelä, J. Rintala, Trace compounds affecting biogas energy utilisation – A review, Energy Convers. Manage. 52 (2011) 3369–3375, https://doi.org/10.1016/j.enconman.2011.07.005.
[285] J. Álvarez-Flórez, E. Egusquiza, Analysis of damage caused by siloxanes in stationary reciprocating internal combustion engines operating with landfill gas, Eng. Fail. Anal. 50 (2015) 29–38, https://doi.org/10.1016/j.engfailanal.2015.01.010.
[286] N.H. Elsayed, A. Elwell, B. Joseph, J.N. Kuhn, Effect of silicon poisoning on catalytic dry reforming of simulated biogas, Appl. Catal. A 538 (2017) 157–164, https://doi.org/10.1016/j.apcata.2017.03.024.
[287] V. Chiodo, S. Maisano, G. Zafarana, F. Urbani, Effect of pollutants on biogas steam reforming, Int. J. Hydrog. Energy 42 (2017) 1622–1628, https://doi.org/10.1016/j.ijhydene.2016.07.251.
[288] T.N. Angelidis, V.G. Papadakis, Partial regeneration of an aged commercial automotive catalyst, Appl. Catal. B 12 (1997) 193–206, https://doi.org/10.1016/S0926-3373(96)00067-7.
[289] D.D. Beck, J.W. Sommers, C.L. DiMaggio, D.R. Monroe, D.A. Frank, Impact of Oil-Derived Catalyst Poisons on FTP Performance of LEV Catalyst Systems, SAE Technical Paper 972842 (1997). https://doi.org/10.4271/972842.
[290] D.D. Beck, J.W. Sommers, C.L. DiMaggio, Axial characterization of catalytic activity in close-coupled lightoff and underfloor catalytic converters, Appl. Catal. B 11 (1997) 257–272, https://doi.org/10.1016/S0926-3373(96)00050-1.
[291] F. Cabello Galisteo, R. Mariscal, M. López Granados, J.L.G. Fierro, P. Brettes, O. Salas, Reactivation of a commercial diesel oxidation catalyst by acid washing, Environ. Sci. Technol. 39 (2005) 3844–3848, https://doi.org/10.1021/es040062f.
[292] S.Y. Christou, H. Birgersson, J.L.G. Fierro, A.M. Efstathiou, Reactivation of an aged commercial three-way catalyst by oxalic and citric acid washing, Environ. Sci. Technol. 40 (2006) 2030–2036, https://doi.org/10.1021/es052310t.

[293] S.T. Darr, R.A. Choksi, C.P. Hubbard, M.D. Johnson, R.W. McCabe, Effects of Oil-Derived Contaminants on Emissions from TWC-Equipped Vehicles, SAE Technical Paper 2000–01-1881, (2000). https://doi.org/10.4271/2000–01-1881.
[294] S.Y. Christou, J. Gåsste, H.L. Karlsson, J.L.G. Fierro, A.M. Efstathiou, Regeneration of aged commercial three-way catalytic converters, Top. Catal. 52 (2009) 2029–2034, https://doi.org/10.1007/s11244-009-9398-7.
[295] A.N. Shigapov, G.W. Graham, R.W. McCabe, M. Paputa Peck, H. Kiel Plummer, The preparation of high-surface-area cordierite monolith by acid treatment, Appl. Catal. A 182 (1999) 137–146, https://doi.org/10.1016/S0926-860X(99)00003-4.
[296] M. Ajhar, M. Travesset, S. Yüce, T. Melin, Siloxane removal from landfill and digester gas – A technology overview, Bioresour. Technol. 101 (2010) 2913–2923, https://doi.org/10.1016/j.biortech.2009.12.018.
[297] K. Oshita, Y. Ishihara, M. Takaoka, N. Takeda, T. Matsumoto, S. Morisawa, A. Kitayama, Behaviour and adsorptive removal of siloxanes in sewage sludge biogas, Water Sci. Technol. 61 (2010) 2003–2012, https://doi.org/10.2166/wst.2010.101.
[298] E. Ryckebosch, M. Drouillon, H. Vervaeren, Techniques for transformation of biogas to biomethane, Biomass Bioenergy 35 (2011) 1633–1645, https://doi.org/10.1016/j.biombioe.2011.02.033.
[299] P. Gislon, S. Galli, G. Monteleone, Siloxanes removal from biogas by high surface area adsorbents, Waste Manage. 33 (2013) 2687–2693, https://doi.org/10.1016/j.wasman.2013.08.023.
[300] Y.Y. Zhang, Y. Kawasaki, K. Oshita, M. Takaoka, D. Minami, G. Inoue, T. Tanaka, Economic assessment of biogas purification systems for removal of both H_2S and siloxane from biogas, Renew. Energy 168 (2021) 119–130, https://doi.org/10.1016/j.renene.2020.12.058.
[301] R.A. Maynal, V. Maske, D. Saini, S. Rao, A. Ristori, Phosphorous Poisoning Study for Diesel Oxidation Catalyst, SAE Technical Paper 2021–26-0204, (2021). https://doi.org/10.4271/2021–26-0204.
[302] G. Zhang, J. Chen, Y. Wu, X. Liu, P. Qu, P. Shen, L. Zhong, Y. Chen, Pd supported on alumina modified by phosphate: Highly phosphorus-resistant three-way catalyst for natural gas vehicles, J. Taiwan Inst. Chem. Eng. 115 (2020) 108–116, https://doi.org/10.1016/j.jtice.2020.09.032.
[303] J. Chen, W. Hu, F. Huang, Y. Wu, S. Yuan, L. Zhong, Y. Chen, P promotion on the performance of Pd-based catalyst for emission control of natural gas driven vehicles, J. Taiwan Inst. Chem. Eng. 91 (2018) 323–331, https://doi.org/10.1016/j.jtice.2018.05.037.
[304] A.M. Gänzler, M. Casapu, P. Vernoux, S. Loridant, F.J.C.S. Aires, T. Epicier, B. Betz, R. Hoyer, J.-D. Grunwaldt, Tuning the Structure of Platinum Particles on Ceria In Situ for Enhancing the Catalytic Performance of Exhaust Gas Catalysts, Angew. Chem., Int. Ed. 56 (2017) 13078–13082, https://doi.org/10.1002/anie.201707842.
[305] K. Lehtoranta, P. Koponen, H. Vesala, K. Kallinen, T. Maunula, Performance and regeneration of methane oxidation catalyst for LNG ships, J. Mar. Sci. Eng. 9 (2021) 111, https://doi.org/10.3390/Jmse9020111.
[306] J.Y. Luo, D. Kisinger, A. Abedi, W.S. Epling, Sulfur release from a model Pt/Al_2O_3 diesel oxidation catalyst: temperature-programmed and step-response techniques characterization, Appl. Catal. A 383 (2010) 182–191, https://doi.org/10.1016/j.apcata.2010.05.049.
[307] O. Saur, M. Bensitel, A.B.M. Saad, J.C. Lavalley, C.P. Tripp, B.A. Morrow, The structure and stability of sulfated alumina and titania, J. Catal. 99 (1986) 104–110, https://doi.org/10.1016/0021-9517(86)90203-4.
[308] P. Auvinen, N.M. Kinnunen, J.T. Hirvi, T. Maunula, K. Kallinen, M. Keenan, M. Suvanto, Effects of NO and NO_2 on fresh and SO_2 poisoned methane oxidation catalyst – Harmful or beneficial? Chem. Eng. J. 417 (2021), 128050 https://doi.org/10.1016/j.cej.2020.128050.
[309] Y. Nagai, K. Dohmae, Y. Ikeda, N. Takagi, T. Tanabe, N. Hara, G. Guilera, S. Pascarelli, M.A. Newton, O. Kuno, H.Y. Jiang, H. Shinjoh, S. Matsumoto, In Situ Redispersion of Platinum Autoexhaust Catalysts: An On-Line Approach to Increasing Catalyst Lifetimes? Angew. Chem., Int. Ed. 47 (2008) 9303–9306, https://doi.org/10.1002/anie.200803126.
[310] A.M. Gänzler, M. Casapu, F. Maurer, H. Störmer, D. Gerthsen, G. Ferré, P. Vernaux, B. Bornmann, R. Frahm, V. Murzin, M. Nachtegaal, M. Votsmeier, J.-D. Grunwaldt, Tuning the Pt/CeO_2 Interface by in Situ Variation of the Pt Particle Size, ACS Catal. 8 (2018) 4800–4811, https://doi.org/10.1021/acscatal.8b00330.
[311] F. Maurer, J. Jelic, J.J. Wang, A. Gänzler, P. Dolcet, C. Wöll, Y.M. Wang, F. Studt, M. Casapu, J.-D. Grunwaldt, Tracking the formation, fate and consequence for catalytic activity of Pt single sites on CeO_2, Nat. Catal. 3 (2020) 824–833, https://doi.org/10.1038/s41929-020-00508-7.
[312] F.C. Meunier, L. Cardenas, H. Kaper, B. Šmíd, M. Vorokhta, R. Grosjean, D. Aubert, K. Dembélé, T. Lunkenbein, Synergy between Metallic and Oxidized Pt Sites Unravelled during Room Temperature CO Oxidation on Pt/Ceria, Angew. Chem., Int. Ed. 60 (2021) 3799–3805, https://doi.org/10.1002/anie.202013223.
[313] F. Maurer, A. Gänzler, P. Lott, B. Betz, M. Votsmeier, S. Loridant, P. Vernoux, V. Murzin, B. Bornmann, R. Frahm, O. Deutschmann, M. Casapu, J.-D. Grunwaldt, Spatiotemporal investigation of the temperature and structure of a Pt/CeO_2 oxidation catalyst for CO and hydrocarbon oxidation during pulse activation, Ind. Eng. Chem. Res. 60 (2021) 6662–6675, https://doi.org/10.1021/acs.iecr.0c05798.
[314] J. Sa, D.L.A. Fernandes, F. Aiouache, A. Goguet, C. Hardacre, D. Lundie, W. Naeem, W.P. Partridge, C. Stere, SpaciMS: spatial and temporal *operando* resolution of reactions within catalytic monoliths, Analyst 135 (2010) 2260–2272, https://doi.org/10.1039/c0an00303d.
[315] M. Hettel, C. Diehm, B. Torkashvand, O. Deutschmann, Critical evaluation of in situ probe techniques for catalytic honeycomb monoliths, Catal. Today 216 (2013) 2–10, https://doi.org/10.1016/j.cattod.2013.05.005.
[316] N.M. Kinnunen, M. Keenan, K. Kallinen, T. Maunula, M. Suvanto, Engineered Sulfur-Resistant Catalyst System with an Assisted Regeneration Strategy for Lean-Burn Methane Combustion, ChemCatChem 10 (2018) 1556–1560, https://doi.org/10.1002/cctc.201701884.
[317] P. Auvinen, P. Nevalainen, M. Suvanto, F. Oliva, X. Llamas, B. Barciela, O. Sippula, N.M. Kinnunen, A detailed study on regeneration of SO_2 poisoned exhaust gas after-treatment catalysts: In pursuance of high durability and low methane, NH_3 and N_2O emissions of heavy-duty vehicles, Fuel 291 (2021), 120223, https://doi.org/10.1016/j.fuel.2021.120223.
[318] M. Keenan, R. Pickett, E. Tronconi, I. Nova, N. Kinnunen, M. Suvanto, T. Maunula, K. Kallinen, R. Baert, The Catalytic Challenges of Implementing a Euro VI Heavy Duty Emissions Control System for a Dedicated Lean Operating Natural Gas Engine, Top. Catal. 62 (2019) 273–281, https://doi.org/10.1007/s11244-018-1127-7.
[319] Proposal for a Regulation of the European Parliament and of the Council on type-approval of motor vehicles and engines and of systems, components and separate technical units intended for such vehicles, with respect to their emissions and battery durability (Euro 7) and repealing Regulations (EC) No 715/2007 and (EC) No 595/2009 (Text with EEA relevance), 2022.
[320] ANNEXES to the Proposal for a Regulation of the European Parliament and the Council on type-approval of motor vehicles and engines and of systems, components and separate technical units intended for such vehicles, with respect to their emissions and battery durability (Euro 7) and repealing Regulations (EC) No 715/2007 and (EC) No 595/2009, 2022.
[321] P. Lott, S. Bastian, H. Többen, L. Zimmermann, O. Deutschmann, Formation of nitrous oxide over Pt-Pd oxidation catalysts: Secondary emissions by interaction of hydrocarbons and nitric oxide, Appl. Catal. A 651 (2023), 119028, https://doi.org/10.1016/j.apcata.2023.119028.
[322] H. Többen, P. Weinmann, T. Wolf, P. Lott, S. Bastian, O. Deutschmann, Formation of N2O in the exhaust line of combustion engines,SAE Technical Paper 2023-01-5045 (2023), https://doi.org/10.4271/2023-01-5045.
[323] M. Keenan, J. Nicole, D. Poojary, Ozone as an enabler for low temperature methane control over a current production Fe-BEA catalyst, Top. Catal. 62 (2019) 351–355, https://doi.org/10.1007/s11244-018-1098-8.
[324] S. Yasumura, K. Saita, T. Miyakage, K. Nagai, K. Kon, T. Toyao, Z. Maeno, T. Taketsugu, K.-i Shimizu, Designing main-group catalysts for low-temperature methane combustion by ozone, Nat. Commun. 14 (2023) 3926, https://doi.org/10.1038/s41467-023-39541-y.
[325] R.-J. Wu, S.-J. Chen, Y.-F. Lin, Ozone generator with reduced NOx and method thereof, Patent No. US6517787B2, USA, 2001.
[326] X.Y. Wang, H.X. Wang, S.L. Wang, Ambient formaldehyde and its contributing factor to ozone and OH radical in a rural area, Atmos. Environ. 44 (2010) 2074–2078, https://doi.org/10.1016/j.atmosenv.2010.03.023.
[327] IARC Monographs on the Evaluation of Carcinogenic Risks to Humans: Formaldehyde, 2-Buoxyethanol and 1-tert-Butoxypropan-2-ol, World Health Organization, International Agency for Research on Cancer, Lyon, 2006.
[328] T. Salthammer, Formaldehyde in the ambient atmosphere: from an indoor pollutant to an outdoor pollutant? Angew. Chem., Int. Ed. 52 (2013) 3320–3327, https://doi.org/10.1002/anie.201205984.
[329] J.S. Gaffney, N.A. Marley, The impacts of combustion emissions on air quality and climate - From coal to biofuels and beyond, Atmos. Environ. 43 (2009) 23–36, https://doi.org/10.1016/j.atmosenv.2008.09.016.
[330] K. Kohse-Höinghaus, P. Osswald, T.A. Cool, T. Kasper, N. Hansen, F. Qi, C. K. Westbrook, P.R. Westmoreland, Biofuel combustion chemistry: from ethanol to biodiesel, Angew. Chem., Int. Ed. 49 (2010) 3572–3597, https://doi.org/10.1002/anie.200905335.
[331] S. Lee, U.H. Yi, H. Jang, C. Park, C. Kim, Evaluation of emission characteristics of a stoichiometric natural gas engine fueled with compressed natural gas and biomethane, Energy 220 (2021), 119766, https://doi.org/10.1016/j.energy.2021.119766.
[332] R. Suarez-Bertoa, T. Selleri, R. Gioria, A.D. Melas, C. Ferrarese, J. Franzetti, B. Arlitt, N. Nagura, T. Hanada, B. Giechaskiel, Real-time measurements of formaldehyde emissions from modern vehicles, Energies 15 (2022) 7680, https://doi.org/10.3390/en15207680.
[333] D.G. Vlachos, L.D. Schmidt, R. Aris, Products in methane combustion near surfaces, AIChE J. 40 (1994) 1018–1025, https://doi.org/10.1002/aic.690400612.
[334] D.B. Olsen, R.K. Palmer, C.E. Mitchell, Modeling of Formaldehyde Formation From Crevices in a Large Bore Natural Gas Engine, ASME/IEEE 2007 Joint Rail Conference and Internal Combustion Engine Division Spring Technical Conference, 2007, pp. 537–543.
[335] M. Mehne, S. Kureti, CH_4 and CH_2O oxidation in lean gas engine exhaust using Fe_2O_3 catalysts, Top. Catal. 66 (2023) 954–963, https://doi.org/10.1007/s11244-022-01730-2.
[336] M. Lemel, A. Hultqvist, A. Vressner, H. Nordgren, H. Persson, B. Johansson, Quantification of the Formaldehyde Emissions from Different HCCI Engines Running on a Range of Fuels, SAE Technical Paper 2005–01-3724, (2005). https://doi.org/10.4271/2005–01-3724.
[337] W.H. Peng, J.C. Yang, J. Corbin, U. Trivanovic, P. Lobo, P. Kirchen, S. Rogak, S. Gagne, J.W. Miller, D. Cocker, Comprehensive analysis of the air quality impacts of switching a marine vessel from diesel fuel to natural gas, Environ. Pollut. 266 (2020) 115404, https://doi.org/10.1016/j.envpol.2020.115404.

[338] B. Zavala, C. Henry, S. Kroll, Detailed Characterization of Gaseous Emissions from Advanced Internal Combustion Engines, SAE Technical Paper 2021-01-0634, (2021). https://doi.org/10.4271/2021–01-0634.
[339] C.A. Van Roekel, D.T. Montgomery, J. Singh, D.B. Olsen, Evaluating dedicated exhaust gas recirculation on a stoichiometric industrial natural gas engine, Int. J. Eng. Res. 22 (2021) 491–502, https://doi.org/10.1177/1468087419864733.
[340] S.M. Corrêa, G. Arbilla, Formaldehyde and acetaldehyde associated with the use of natural gas as a fuel for light vehicles, Atmos. Environ. 39 (2005) 4513–4518, https://doi.org/10.1016/j.atmosenv.2005.03.042.
[341] G. Karavalakis, M. Hajbabaei, T.D. Durbin, K.C. Johnson, Z. Zheng, W.J. Miller, The effect of natural gas composition on the regulated emissions, gaseous toxic pollutants, and ultrafine particle number emissions from a refuse hauler vehicle, Energy 50 (2013) 280–291, https://doi.org/10.1016/j.energy.2012.10.044.
[342] G. Karavalakis, M. Hajbabaei, Y. Jiang, J.C. Yang, K.C. Johnson, D.R. Cocker, T. D. Durbin, Regulated, greenhouse gas, and particulate emissions from lean-burn and stoichiometric natural gas heavy-duty vehicles on different fuel compositions, Fuel 175 (2016) 146–156, https://doi.org/10.1016/j.fuel.2016.02.034.
[343] C. Bertole, Formaldehyde Oxidation over Emission Control Catalysts, SAE Technical Paper 2018–01-1274, (2018). https://doi.org/10.4271/2018–01-1274.
[344] L. Zheng, M. Casapu, M. Stehle, O. Deutschmann, J.-D. Grunwaldt, Selective Catalytic Reduction of NO_x with Ammonia and Hydrocarbon Oxidation Over V_2O_5–MoO_3/TiO_2 and V_2O_5–WO_3/TiO_2 SCR Catalysts, Top. Catal. 62 (2019) 129–139, https://doi.org/10.1007/s11244-018-1097-9.
[345] L. Zheng, A. Zimina, M. Casapu, J.-D. Grunwaldt, Hydrocarbon and soot oxidation over cerium and iron doped vanadium SCR Catalysts, ChemCatChem 12 (2020) 6272–6284, https://doi.org/10.1002/cctc.202001314.
[346] D. Zengel, M. Stehle, O. Deutschmann, M. Casapu, J.-D. Grunwaldt, Impact of gas phase reactions and catalyst poisons on the NH_3-SCR activity of a V_2O_5-WO_3/TiO_2 catalyst at pre-turbine position, Appl. Catal. B 288 (2021), 119991, https://doi.org/10.1016/j.apcatb.2021.119991.
[347] T. Günter, J. Pesek, K. Schäfer, A.B. Abai, M. Casapu, O. Deutschmann, J.-D. Grunwaldt, Cu-SSZ-13 as pre-turbine NO_x-removal-catalyst: Impact of pressure and catalyst poisons, Appl. Catal. B 198 (2016) 548–557, https://doi.org/10.1016/j.apcatb.2016.06.005.
[348] D. Zengel, S. Barth, M. Casapu, J.-D. Grunwaldt, The impact of pressure and hydrocarbons on NO_x abatement over Cu- and Fe-zeolites at pre-turbocharger position, Catalysts 11 (2021) 336, https://doi.org/10.3390/catal11030336.
[349] C.B. Zhang, H. He, K. Tanaka, Perfect catalytic oxidation of formaldehyde over a Pt/TiO_2 catalyst at room temperature, Catal. Commun. 6 (2005) 211–214, https://doi.org/10.1016/j.catcom.2004.12.012.
[350] C.B. Zhang, H. He, K. Tanaka, Catalytic performance and mechanism of a Pt/TiO_2 catalyst for the oxidation of formaldehyde at room temperature, Appl. Catal. B 65 (2006) 37–43, https://doi.org/10.1016/j.apcatb.2005.12.010.
[351] H.B. Huang, D.Y.C. Leung, Complete elimination of indoor formaldehyde over supported Pt catalysts with extremely low Pt content at ambient temperature, J. Catal. 280 (2011) 60–67, https://doi.org/10.1016/j.jcat.2011.03.003.
[352] C.B. Zhang, F.D. Liu, Y.P. Zhai, H. Ariga, N. Yi, Y.C. Liu, K. Asakura, M. Flytzani-Stephanopoulos, H. He, Alkali-Metal-Promoted Pt/TiO_2 Opens a More Efficient Pathway to Formaldehyde Oxidation at Ambient Temperatures, Angew. Chem., Int. Ed. 51 (2012) 9628–9632, https://doi.org/10.1002/anie.201202034.
[353] B.-B. Chen, X.-B. Zhu, M. Crocker, Y. Wang, C. Shi, Complete oxidation of formaldehyde at ambient temperature over γ-Al_2O_3 supported Au catalyst, Catal. Commun. 42 (2013) 93–97, https://doi.org/10.1016/j.catcom.2013.08.008.
[354] J.Q. Torres, S. Royer, J.P. Bellat, J.M. Giraudon, J.F. Lamonier, Formaldehyde: catalytic oxidation as a promising soft way of elimination, ChemSusChem 6 (2013) 578–592, https://doi.org/10.1002/cssc.201200809.
[355] S. Colussi, M. Boaro, L. de Rogatis, A. Pappacena, C. de Leitenburg, J. Llorca, A. Trovarelli, Room temperature oxidation of formaldehyde on Pt-based catalysts: A comparison between ceria and other supports (TiO_2, Al_2O_3 and ZrO_2), Catal. Today 253 (2015) 163–171, https://doi.org/10.1016/j.cattod.2015.02.028.
[356] D.D. Li, G.L. Yang, P.L. Li, J.L. Wang, P.Y. Zhang, Promotion of formaldehyde oxidation over Ag catalyst by Fe doped MnO_x support at room temperature, Catal. Today 277 (2016) 257–265, https://doi.org/10.1016/j.cattod.2016.02.040.
[357] B.Y. Bai, Q. Qiao, J.H. Li, J.M. Hao, Progress in research on catalysts for catalytic oxidation of formaldehyde, Chin. J. Catal. 37 (2016) 102–122, https://doi.org/10.1016/S1872-2067(15)61007-5.
[358] A. Yusuf, C. Snape, J. He, H.H. Xu, C.J. Liu, M. Zhao, G.Z. Chen, B.C. Tang, C. J. Wang, J.W. Wang, S.N. Behera, Advances on transition metal oxides catalysts for formaldehyde oxidation: A review, Catal. Rev.: Sci. Eng. 59 (2017) 189–233, https://doi.org/10.1080/01614940.2017.1342476.
[359] J.H. Guo, C.X. Lin, C.J. Jiang, P.Y. Zhang, Review on noble metal-based catalysts for formaldehyde oxidation at room temperature, Appl. Surf. Sci. 475 (2019) 237–255, https://doi.org/10.1016/j.apsusc.2018.12.238.
[360] M.A. Elliott, G.F. Nebel, F.G. Rounds, The composition of exhaust gases from diesel, gasoline and propane powered motor coaches, J. Air Pollut. Control Assoc. 5 (1955) 103–108, https://doi.org/10.1080/00966665.1955.10467686.
[361] D. Sodhi, M.A. Abraham, J.C. Summers, The kinetics of formaldehyde oxidation and emissions reduction in methanol fueled vehicles, J. Air Waste Manage. Assoc. 40 (1990) 352–356, https://doi.org/10.1080/10473289.1990.10466693.
[362] F. Zhang, S.J. Shuai, Z. Wang, X. Zhang, J.X. Wang, A detailed oxidation mechanism for the prediction of formaldehyde emission from methanol-gasoline SI engines, Proc. Combust. Inst., 33 (2011) 3151–3158. https://doi.org/10.1016/j.proci.2010.07.029.
[363] M.C. Rodrigues, L.L.N. Guarieiro, M.P. Cardoso, L.S. Carvalho, G.O. da Rocha, J. B. de Andrade, Acetaldehyde and formaldehyde concentrations from sites impacted by heavy-duty diesel vehicles and their correlation with the fuel composition: Diesel and diesel/biodiesel blends, Fuel 92 (2012) 258–263, https://doi.org/10.1016/j.fuel.2011.07.023.
[364] A.O. Hasan, A. Abu-Jrai, A.H. Al-Muhtaseb, A. Tsolakis, H.M. Xu, Formaldehyde, acetaldehyde and other aldehyde emissions from HCCI/SI gasoline engine equipped with prototype catalyst, Fuel 175 (2016) 249–256, https://doi.org/10.1016/j.fuel.2016.02.005.
[365] M.U. Alzueta, P. Glarborg, Formation and destruction of CH_2O in the exhaust system of a gas engine, Environ. Sci. Technol. 37 (2003) 4512–4516, https://doi.org/10.1021/es026144q.
[366] A. Ayala, M.E. Gebel, R.A. Okamoto, P.L. Rieger, N.Y. Kado, C. Cotter, N. Verma, Oxidation Catalyst Effect on CNG Transit Bus Emissions, SAE Technical Paper 2003–01-1900, (2003). https://doi.org/10.4271/2003–01-1900.
[367] X.F. Tang, Y.G. Li, X.M. Huang, Y.D. Xu, H.Q. Zhu, J.G. Wang, W.J. Shen, MnO_x-CeO_2 mixed oxide catalysts for complete oxidation of formaldehyde: Effect of preparation method and calcination temperature, Appl. Catal. B 62 (2006) 265–273, https://doi.org/10.1016/j.apcatb.2005.08.004.
[368] H.R. Wu, S.C. Ma, W.Y. Song, E.J.M. Hensen, Density Functional Theory Study of the Mechanism of Formaldehyde Oxidation on Mn-Doped Ceria, J. Phys. Chem. C 120 (2016) 13071–13077, https://doi.org/10.1021/acs.jpcc.6b03218.
[369] J. Tan, C. Solbrig, S.J. Schmieg, The Development of Advanced 2-Way SCR/DPF Systems to Meet Future Heavy-Duty Diesel Emissions, SAE Technical Paper 2011–01-1140, (2011). https://doi.org/10.4271/2011–01-1140.
[370] M. Naseri, S. Chatterjee, M. Castagnola, H.-Y. Chen, J. Fedeyko, H. Hess, J. Li, Development of SCR on Diesel Particulate Filter System for Heavy Duty Applications, SAE Int. J. Engines 4 (2011) 1798–1809, https://doi.org/10.4271/2011-01-1312.
[371] K. Johansen, A. Widd, F. Zuther, H. Viecenz, Passive NO2 Regeneration and NOx Conversion for DPF with an Integrated Vanadium SCR Catalyst, SAE Technical Paper 2016–01-0915, (2016). https://doi.org/10.4271/2016–01-0915.
[372] D. Zengel, P. Koch, B. Torkashvand, J.-D. Grunwaldt, M. Casapu, O. Deutschmann, Emission of Toxic HCN During NO_x Removal by Ammonia SCR in the Exhaust of Lean-Burn Natural Gas Engines, Angew. Chem., Int. Ed. 59 (2020) 14423–14428, https://doi.org/10.1002/anie.202003670.
[373] T. Sakai, B.-C. Choi, R. Osuga, Y. Ko, E. Kim, Unburned Fuel and Formaldehyde Purification Characteristics of Catalytic Converters for Natural Gas Fueled Automotive Engine, SAE Technical Paper 920596, (1992). https://doi.org/10.4271/920596.
[374] J.X. Peng, S.D. Wang, Performance and characterization of supported metal catalysts for complete oxidation of formaldehyde at low temperatures, Appl. Catal. B 73 (2007) 282–291, https://doi.org/10.1016/j.apcatb.2006.12.012.
[375] C. Zhang, H. He, A comparative study of TiO_2 supported noble metal catalysts for the oxidation of formaldehyde at room temperature, Catal. Today 126 (2007) 345–350, https://doi.org/10.1016/j.cattod.2007.06.010.
[376] R.W. McCabe, D.F. McCready, Formaldehyde Oxidation on Pt: Kinetic Evidence for Adsorbed Carbon-Monoxide Intermediate, Chem. Phys. Lett. 111 (1984) 89–93, https://doi.org/10.1016/0009-2614(84)80442-X.
[377] G.A. Attard, H.D. Ebert, R. Parsons, Formaldehyde Decomposition and Oxidation on Pt(110), Surf. Sci. 240 (1990) 125–135, https://doi.org/10.1016/0039-6028(90)90736-R.
[378] H. Sharma, A. Mhadeshwar, A detailed microkinetic model for diesel engine emissions oxidation on platinum based diesel oxidation catalysts (DOC), Appl. Catal. B 127 (2012) 190–204, https://doi.org/10.1016/j.apcatb.2012.08.021.
[379] B. Torkashvand, L. Maier, P. Lott, T. Schedlbauer, J.-D. Grunwaldt, O. Deutschmann, Formaldehyde Oxidation Over Platinum: On the Kinetics Relevant to Exhaust Conditions of Lean-Burn Natural Gas Engines, Top. Catal. 62 (2019) 206–213, https://doi.org/10.1007/s11244-018-1087-y.
[380] S. Li, X. Lu, W. Guo, H. Zhu, M. Li, L. Zhao, Y. Li, H. Shan, Formaldehyde oxidation on the Pt/TiO_2(101) surface: A DFT investigation, J. Organomet. Chem. 704 (2012) 38–48, https://doi.org/10.1016/j.jorganchem.2012.01.002.
[381] Z.L. Zhang, G.Z. He, Y.B. Li, C.B. Zhang, J.Z. Ma, H. He, Effect of hydroxyl groups on metal anchoring and formaldehyde oxidation performance of Pt/Al_2O_3, Environ. Sci. Technol. 56 (2022) 10916–10924, https://doi.org/10.1021/acs.est.2c01278.
[382] R.W. McCabe, P.J. Mitchell, Exhaust-catalyst development for methanol-fueled vehicles: III. Formaldehyde oxidation, Appl. Catal. 44 (1988) 73–93, https://doi.org/10.1016/S0166-9834(00)80045-7.
[383] A.M. Gänzler, M. Casapu, A. Boubnov, O. Müller, S. Conrad, H. Lichtenberg, R. Frahm, J.-D. Grunwaldt, *Operando* spatially and time-resolved X-ray absorption spectroscopy and infrared thermography during oscillatory CO oxidation, J. Catal. 328 (2015) 216–224, https://doi.org/10.1016/j.jcat.2015.01.002.
[384] M. Al-Harbi, R. Hayes, M. Votsmeier, W.S. Epling, Competitive NO, CO and hydrocarbon oxidation reactions over a diesel oxidation catalyst, Can. J. Chem. Eng. 90 (2012) 1527–1538, https://doi.org/10.1002/cjce.20659.
[385] X.B. Zhu, T.D. Durbin, J.M. Norbeck, D. Cocker, Internal Combustion Engine (ICE) Air Toxic Emissions - Final Report, Bourns College of Engineering-Center for Environmental Research and Technology, University of California, 2004.
[386] F. Posada, C.N.G. Bus Emissions Roadmap: from Euro III to EURO VI, in: D. Lowell (Ed.), The International Council on Clean Transportation, 2009.
[387] S. Yoon, J. Collins, A. Thiruvengadam, M. Gautam, J. Herner, A. Ayala, Criteria pollutant and greenhouse gas emissions from CNG transit buses equipped with three-way catalysts compared to lean-burn engines and oxidation catalyst technologies, in: J. Air Waste Manage. Assoc., 2013, pp. 926–933, https://doi.org/10.1080/10962247.2013.800170.
[388] M. Gautam, A. Thiruvengadam, D. Carder, M. Besch, B. Shade, G. Thompson, N. Clark, Testing of Volatile and Nonvolatile Emissions from Advanced Technology

Natural Gas Vehicles - Final Report, Center for Alternative Fuels, Engines & Emissions, West Virginia University, 2011.
[389] K. Badrinarayanan, Performance evaluation of multiple oxidation catalysts on a lean burn natural gas engine, Master's thesis, Department of Mechanical Engineering, Colorado State University, Fort Collins, 2012.
[390] H.K. Kappanna, Reduction of Toxic Air Contaminants (TACs) and particulate matter emissions from heavy-duty natural gas engines, Master's thesis, Department of Mechanical and Aerospace Engineering, West Virginia University, Morgantown, 2006.
[391] T. Schedlbauer, A. Gremminger, M. Casapu, O. Deutschmann, J.-D. Grunwaldt, Impact of the Gas Mixture and Aging Conditions on Formaldehyde Conversion over a Series of Commercial Pt-Based Catalysts, SAE Technical Paper 2018-01-5021, (2018). https://doi.org/10.4271/2018-01-5021.
[392] K. Bodek, V. Wong, The Effects of Sulfated Ash, Phosphorus and Sulfur on Diesel Aftertreatment Systems - A Review, SAE Technical Paper 2007–01-1922, (2007). https://doi.org/10.4271/2007–01-1922.
[393] J. Li, A. Kumar, X. Chen, N. Currier, A. Yezerets, Impact of Different Forms of Sulfur Poisoning on Diesel Oxidation Catalyst Performance, SAE Technical Paper 2013–01-0514, (2013). https://doi.org/10.4271/2013–01-0514.
[394] A. Kumar, J. Li, J. Luo, S. Joshi, A. Yezerets, K. Kamasamudram, N. Schmidt, K. Pandya, P. Kale, T. Mathuraiveeran, Catalyst Sulfur Poisoning and Recovery Behaviors: Key for Designing Advanced Emission Control Systems, SAE Technical Paper 2017–26-0133, (2017). https://doi.org/10.4271/2017–26-0133.
[395] T.W. Hansen, A.T. Delariva, S.R. Challa, A.K. Datye, Sintering of Catalytic Nanoparticles: Particle Migration or Ostwald ripening? Acc. Chem. Res. 46 (2013) 1720–1730, https://doi.org/10.1021/ar3002427.
[396] M.E. Baumgardner, D.B. Olsen, Performance Degradation and Poison Build-Up of an Oxidation Catalyst in Two-Stroke Natural Gas Engine Exhaust, J. Energy Resour. Technol. 140 (2018), 072208, https://doi.org/10.1115/1.4039547.
[397] D. Wang, H. An, J. Gong, J. Li, K. Kamasamudram, N. Currier, A. Yezerets, Diagnostics of Field-Aged Three-Way Catalyst (TWC) on Stoichiometric Natural Gas Engines, SAE Technical Paper 2019–01-0998, (2019). https://doi.org/10.4271/2019–01-0998.
[398] M.-Y. Kim, J. Gong, K. Kamasamudram, M. Cunningham, A. Yezerets, Impact of Chemical Contaminants on Stoichiometric Natural Gas Engine Three-Way Catalysts with High Mileage History, SAE Technical Paper 2022–01-0542, (2022). https://doi.org/10.4271/2022–01-0542.
[399] J. Le Louvetel-Poilly, S. Balaji, F. Lafossas, Development of Three Way Catalyst Aging Model: Application to Real Driving Emission Condition, SAE Technical Paper 2019–24-0047, (2019). https://doi.org/10.4271/2019–24-0047.
[400] Z.Q. Wang, J.J. Pei, J.S. Zhang, Catalytic oxidization of indoor formaldehyde at room temperature - Effect of operation conditions, Build. Environ. 65 (2013) 49–57, https://doi.org/10.1016/j.buildenv.2013.03.007.
[401] S. Wan, B. Torkashvand, T. Häber, R. Suntz, O. Deutschmann, Investigation of HCHO Catalytic Oxidation over Platinum using Planar Laser-Induced Fluorescence, Appl. Catal. B 264 (2020) 118473, https://doi.org/10.1016/j.apcatb.2019.118473.
[402] J.C. Ruiz-Morales, A. Tarancón, J. Canales-Vázquez, J. Méndez-Ramos, L. Hernández-Afonso, P. Acosta-Mora, J.R. Marín Rueda, R. Fernández-González, Three dimensional printing of components and functional devices for energy and environmental applications, Energy Environ. Sci. 10 (2017) 846–859, https://doi.org/10.1039/c6ee03526d.
[403] P. Anish Mathews, S. Koonisetty, S. Bhardwaj, P. Biswas, R. Johnson, G. Padmanabham, Patent Trends in Additive Manufacturing of Ceramic Materials, in: {C}{C}Y.R. Mahajan, R. Johnson{C}{C} (Eds.) Handbook of Advanced Ceramics and Composites: Defense, Security, Aerospace and Energy Applications, Springer International Publishing, Cham, 2020, pp. 319–354.
[404] O.H. Laguna, P.F. Lietor, F.J. Iglesias Godino, F.A. Corpas-Iglesias, A review on additive manufacturing and materials for catalytic applications: Milestones, key concepts, advances and perspectives, Mater. Des. 208 (2021), 109927, https://doi.org/10.1016/j.matdes.2021.109927.
[405] C.L. Cramer, E. Ionescu, M. Graczyk-Zajac, A.T. Nelson, Y. Katoh, J.J. Haslam, L. Wondraczek, T.G. Aguirre, S. LeBlanc, H. Wang, M. Masoudi, E. Tegeler, R. Riedel, P. Colombo, M. Minary-Jolandan, Additive manufacturing of ceramic materials for energy applications: Road map and opportunities, J. Eur. Ceram. Soc. 42 (2022) 3049–3088, https://doi.org/10.1016/j.jeurceramsoc.2022.01.058.
[406] M. Masoudi, Catalytic converters having non-linear flow channels, Patent No. US10815856, USA, 2020.
[407] S.R. Krishnan, K.K. Srinivasan, S. Singh, S.R. Bell, K.C. Midkiff, W. Gong, S. B. Fiveland, M. Willi, Strategies for Reduced NO_x Emissions in Pilot-Ignited Natural Gas Engines, J. Eng. Gas. Turbines Power 126 (2004) 665–671, https://doi.org/10.1115/1.1760530.
[408] W. Li, Z. Liu, Z. Wang, Y. Xu, Experimental investigation of the thermal and diluent effects of EGR components on combustion and NOx emissions of a turbocharged natural gas SI engine, Energy Convers. Manage. 88 (2014) 1041–1050, https://doi.org/10.1016/j.enconman.2014.09.051.
[409] J.P. Bhasker, E. Porpatham, Effects of compression ratio and hydrogen addition on lean combustion characteristics and emission formation in a Compressed Natural Gas fuelled spark ignition engine, Fuel 208 (2017) 260–270, https://doi.org/10.1016/j.fuel.2017.07.024.
[410] K.K. Srinivasan, A.K. Agarwal, S.R. Krishnan, V. Mulone, Natural Gas Engines: For Transportation and Power Generation, Springer,, Singapore, 2018.
[411] Y. Li, P. Wang, S. Wang, J. Liu, Y. Xie, W. Li, Quantitative investigation of the effects of CR, EGR and spark timing strategies on performance, combustion and NOx emissions characteristics of a heavy-duty natural gas engine fueled with 99% methane content, Fuel 255 (2019), 115803, https://doi.org/10.1016/j.fuel.2019.115803.
[412] J.A. Miller, C.T. Bowman, Mechanism and Modeling of Nitrogen Chemistry in Combustion, Prog. Energy Combust. Sci. 15 (1989) 287–338, https://doi.org/10.1016/0360-1285(89)90017-8.
[413] M. Abian, M.U. Alzueta, P. Glarborg, Formation of NO from N_2/O_2 Mixtures in a Flow Reactor: Toward an Accurate Prediction of Thermal NO, Int. J. Chem. Kinet. 47 (2015) 518–532, https://doi.org/10.1002/kin.20929.
[414] G.A. Lavoie, J.B. Heywood, J.C. Keck, Experimental and Theoretical Study of Nitric Oxide Formation in Internal Combustion Engines, Combust. Sci. Technol. 1 (1970) 313–326, https://doi.org/10.1080/00102206908952211.
[415] C.P. Fenimore, Formation of nitric oxide in premixed hydrocarbon flames, Symp. (Int.) Combust., 13 (1971) 373–380. https://doi.org/10.1016/S0082–0784(71)80040–1.
[416] A.A. Konnov, Implementation of the NCN pathway of prompt-NO formation in the detailed reaction mechanism, Combust. Flame 156 (2009) 2093–2105, https://doi.org/10.1016/j.combustflame.2009.03.016.
[417] C.P. Fenimore, Formation of nitric oxide from fuel nitrogen in ethylene flames, Combust. Flame 19 (1972) 289–296, https://doi.org/10.1016/S0010-2180(72)80219-0.
[418] G.G.De Soete, Overall reaction rates of NO and N2 formation from fuel nitrogen, Symp. (Int.) Combust., 15 (1975) 1093–1102. https://doi.org/10.1016/S0082–0784(75)80374–2.
[419] C.P. Fenimore, Reactions of fuel-nitrogen in rich flame gases, Combust. Flame 26 (1976) 249–256, https://doi.org/10.1016/0010-2180(76)90075-4.
[420] V. Dupont, M. Pourkashanian, A. Williams, R. Woolley, The reduction of NO_x formation in natural gas burner flames, Fuel 72 (1993) 497–503, https://doi.org/10.1016/0016-2361(93)90108-E.
[421] F.H.V. Coppens, J. De Ruyck, A.A. Konnov, The effects of composition on burning velocity and nitric oxide formation in laminar premixed flames of $CH_4 + H_2 + O_2 + N_2$, Combust. Flame 149 (2007) 409–417, https://doi.org/10.1016/j.combustflame.2007.02.004.
[422] J. Santner, S.F. Ahmed, T. Farouk, F.L. Dryer, Computational Study of NO_x Formation at Conditions Relevant to Gas Turbine Operation: Part 1, Energy Fuels 30 (2016) 6745–6755, https://doi.org/10.1021/acs.energyfuels.6b00420.
[423] H. Chen, J. He, X. Zhong, Engine combustion and emission fuelled with natural gas: A review, J. Energy Inst. 92 (2019) 1123–1136, https://doi.org/10.1016/j.joei.2018.06.005.
[424] G. Löffler, R. Sieber, M. Harasek, H. Hofbauer, R. Hauss, J. Landauf, NO_x formation in natural gas combustion—a new simplified reaction scheme for CFD calculations, Fuel 85 (2006) 513–523, https://doi.org/10.1016/j.fuel.2005.07.012.
[425] D. Deublein, A. Steinhauser, Biogas, Biogas from Waste and Renewable Resources: An Introduction, Wiley-VCH Verlag GmbH & Co,, KGaA, Weinheim, 2008, pp. 49–56.
[426] W.M. Hao, S.C. Wofsy, M.B. Mcelroy, J.M. Beer, M.A. Toqan, Sources of Atmospheric Nitrous-Oxide from Combustion, J. Geophys. Res.: Atmos. 92 (1987) 3098–3104, https://doi.org/10.1029/JD092iD03p03098.
[427] F.P. Qian, C.S. Chyang, K.S. Huang, J. Tso, Combustion and NO emission of high nitrogen content biomass in a pilot-scale vortexing fluidized bed combustor, Bioresour. Technol. 102 (2011) 1892–1898, https://doi.org/10.1016/j.biortech.2010.08.008.
[428] F. Obeid, T.C. Van, E.J. Horchler, Y. Guo, P. Verma, B. Miljevic, R.J. Brown, Z. Ristovski, T.A. Bodisco, T. Rainey, Engine performance and emissions of high nitrogen-containing fuels, Fuel 264 (2020) 116805, https://doi.org/10.1016/j.fuel.2019.116805.
[429] S. Ozgen, S. Cernuschi, S. Caserini, An overview of nitrogen oxides emissions from biomass combustion for domestic heat production, Renew. Sustain. Energy Rev. 135 (2021) 110113, https://doi.org/10.1016/j.rser.2020.110113.
[430] P.G. Kristensen, J.K. Jensen, M. Nielsen, J.B. Illerup, Emission factors for gas fired CHP units < 25 MW, Danish Gas Technology Centre and National Environmental Research Institute, Hørsholm and Roskilde, Denmark, 2004.
[431] J. Das, S. Nolan, P.N.L. Lens, Simultaneous removal of H_2S and NH_3 from raw biogas in hollow fibre membrane bioreactors, Environ. Technol. Innov. 28 (2022), 102777, https://doi.org/10.1016/j.eti.2022.102777.
[432] A.A. Werkneh, Biogas impurities: environmental and health implications, removal technologies and future perspectives, Heliyon 8 (2022), e10929, https://doi.org/10.1016/j.heliyon.2022.e10929.
[433] W. Leitner, J. Klankermayer, S. Pischinger, H. Pitsch, K. Kohse-Höinghaus, Advanced Biofuels and Beyond: Chemistry Solutions for Propulsion and Production, Angew. Chem., Int. Ed. 56 (2017) 5412–5452, https://doi.org/10.1002/anie.201607257.
[434] R.J. Crookes, Comparative bio-fuel performance in internal combustion engines, Biomass Bioenergy 30 (2006) 461–468, https://doi.org/10.1016/j.biombioe.2005.11.022.
[435] Y. Kim, N. Kawahara, K. Tsuboi, E. Tomita, Combustion characteristics and NO_x emissions of biogas fuels with various CO_2 contents in a micro co-generation spark-ignition engine, Appl. Energy 182 (2016) 539–547, https://doi.org/10.1016/j.apenergy.2016.08.152.
[436] K.C. Johnson, Y. Jiang, J. Yang, Ultra-Low NOx Natural Gas Vehicle Evaluation ISL G NZ - Final Report, University of California, Riverside, 2016.
[437] C. Misra, C. Ruehl, J. Collins, D. Chernich, J. Herner, In-Use NOx Emissions from Diesel and Liquefied Natural Gas Refuse Trucks Equipped with SCR and TWC, Respectively, Environ. Sci. Technol. 51 (2017) 6981–6989, https://doi.org/10.1021/acs.est.6b03218.

[438] A. Dimaratos, Z. Toumasatos, G. Triantafyllopoulos, A. Kontses, Z. Samaras, Real-world gaseous and particle emissions of a Bi-fuel gasoline/CNG Euro 6 passenger car, Transp. Res. D: Transp. Environ. 82 (2020) 102307, https://doi.org/10.1016/j.trd.2020.102307.

[439] J. Gong, J. Pihl, D. Wang, M.Y. Kim, W.P. Partridge, J.H. Li, M. Cunningham, K. Kamasamudram, N. Currier, A. Yezerets, O_2 dosage as a descriptor of TWC performance under lean/rich dithering in stoichiometric natural gas engines, Catal. Today 360 (2021) 294–304, https://doi.org/10.1016/j.cattod.2020.02.022.

[440] D. Bounechada, G. Groppi, P. Forzatti, K. Kallinen, T. Kinnunen, Enhanced Methane Conversion Under Periodic Operation Over a Pd/Rh Based TWC in the Exhausts from NGVs, Top. Catal. 56 (2013) 372–377, https://doi.org/10.1007/s11244-013-9982-8.

[441] J.J. Chen, Y. Wu, W. Hu, P.F. Qu, G.C. Zhang, P. Granger, L. Zhong, Y.Q. Chen, New insights into the role of Pd-Ce interface for methane activation on monolithic supported Pd catalysts: A step forward the development of novel PGM Three-Way Catalysts for natural gas fueled engines, Appl. Catal. B 264 (2020) 118475, https://doi.org/10.1016/j.apcatb.2019.118475.

[442] S.B. Kang, K. Karinshak, P.W. Chen, S. Golden, M.P. Harold, Coupled methane and NO_x conversion on Pt + Pd/Al_2O_3 monolith: Conversion enhancement through feed modulation and $Mn_{0.5}Fe_{2.5}O_4$ spinel addition, Catal. Today 360 (2021) 284–293, https://doi.org/10.1016/j.cattod.2020.02.039.

[443] K. Karinshak, P.W. Chen, R.-F. Liu, S.J. Golden, M.P. Harold, Optimizing feed modulation for coupled methane and NO_x conversion over Pd-Pt/$Mn_{0.5}Fe_{2.5}O_4$/Al_2O_3 monolith catalyst, Appl. Catal. B 304 (2022), 120607, https://doi.org/10.1016/j.apcatb.2021.120607.

[444] T.V. Johnson, Review of Selective Catalytic Reduction (SCR) and Related Technologies for Mobile Applications, in: I. Nova, E. Tronconi (Eds.), Urea-SCR Technology for deNOx After Treatment of Diesel Exhausts, Springer, New York, 2014, pp. 3–31.

[445] D. Chatterjee, K. Rusch, S.C.R. Technology, for Off-highway (Large Diesel Engine) Applications, in: I. Nova, E. Tronconi (Eds.), Urea-SCR Technology for deNOx After Treatment of Diesel Exhausts, Springer, New York, 2014, pp. 33–61.

[446] B. Guan, R. Zhan, H. Lin, Z. Huang, Review of state of the art technologies of selective catalytic reduction of NO_x from diesel engine exhaust, Appl. Therm. Eng. 66 (2014) 395–414, https://doi.org/10.1016/j.applthermaleng.2014.02.021.

[447] G. Busca, L. Lietti, G. Ramis, F. Berti, Chemical and mechanistic aspects of the selective catalytic reduction of NO_x by ammonia over oxide catalysts: A review, Appl. Catal. B 18 (1998) 1–36, https://doi.org/10.1016/S0926-3373(98)00040-X.

[448] J. Jansson, Vanadia-Based Catalysts for Mobile SCR, in: I. Nova, E. Tronconi (Eds.), Urea-SCR Technology for deNOx After Treatment of Diesel Exhausts, Springer, New York, 2014, pp. 65–96.

[449] W.P. Shan, H. Song, Catalysts for the selective catalytic reduction of NO_x with NH_3 at low temperature, Catal. Sci. Technol. 5 (2015) 4280–4288, https://doi.org/10.1039/c5cy00737b.

[450] H.-Y. Chen, Cu/Zeolite SCR Catalysts for Automotive Diesel NOx Emission Control, in: I. Nova, E. Tronconi (Eds.), Urea-SCR Technology for deNOx After Treatment of Diesel Exhausts, Springer, New York, 2014, pp. 123–147.

[451] T.J. Toops, J.A. Pihl, W.P. Partridge, Fe-Zeolite Functionality, Durability, and Deactivation Mechanisms in the Selective Catalytic Reduction (SCR) of NO_x with Ammonia, in: I. Nova, E. Tronconi (Eds.), Urea-SCR Technology for deNOx After Treatment of Diesel Exhausts, Springer, New York, 2014, pp. 97–121.

[452] J.H. Baik, S.D. Yim, I.S. Nam, Y.S. Mok, J.H. Lee, B.K. Cho, S.H. Oh, Control of NO_x emissions from diesel engine by selective catalytic reduction (SCR) with urea, Top. Catal., 30 (2004) 37–41, https://doi.org/10.1023/B:Toca.0000029725.88068.97.

[453] B.M. Shakya, M.P. Harold, V. Balakotaiah, Simulations and optimization of combined Fe- and Cu-zeolite SCR monolith catalysts, Chem. Eng. J. 278 (2015) 374–384, https://doi.org/10.1016/j.cej.2014.11.029.

[454] D.B. Olsen, M. Kohls, G. Arney, Impact of Oxidation Catalysts on Exhaust NO_2/NO_x Ratio from Lean-Burn Natural Gas Engines, J. Air Waste Manage. Assoc. 60 (2010) 867–874, https://doi.org/10.3155/1047-3289.60.7.867.

[455] F. Gramigni, U. Iacobone, N.D. Nasello, T. Selleri, N. Usberti, I. Nova, Review of Hydrocarbon Poisoning and Deactivation Effects on Cu-Zeolite, Fe-Zeolite, and Vanadium-Based Selective Catalytic Reduction Catalysts for NOx Removal from Lean Exhausts, Ind. Eng. Chem. Res. 60 (2021) 6403–6420, https://doi.org/10.1021/acs.iecr.0c05894.

[456] K. Lehtoranta, T. Murtonen, H. Vesala, P. Koponen, J. Alanen, P. Simonen, T. Rönkkö, H. Timonen, S. Saarikoski, T. Maunula, K. Kallinen, S. Korhonen, Natural Gas Engine Emission Reduction by Catalysts, Emiss. Control Sci. Technol. 3 (2017) 142–152, https://doi.org/10.1007/s40825-016-0057-8.

[457] R. Villamaina, I. Nova, E. Tronconi, T. Maunula, M. Keenan, The Effect of CH_4 on NH_3-SCR Over Metal-Promoted Zeolite Catalysts for Lean-Burn Natural Gas Vehicles, Top. Catal. 61 (2018) 1974–1982, https://doi.org/10.1007/s11244-018-1004-4.

[458] D. Adouane, S. Capela, P. Da Costa, On the Efficiency of NH_3-SCR Catalysts for Heavy Duty Vehicles Running on Compressed Natural Gas in Synthetic Gas Bench Scale, Top. Catal. 56 (2013) 45–49, https://doi.org/10.1007/s11244-013-9927-2.

[459] J. Wang, H. Gui, Z. Yang, T. Yu, X. Zhang, J. Liu, Real-world gaseous emission characteristics of natural gas heavy-duty sanitation trucks, J. Environ. Sci. 115 (2022) 319–329, https://doi.org/10.1016/j.jes.2021.06.023.

[460] G. Zou, Integrated energy solutions to smart and green shipping, Green Shipping and Technology Summit, Athens, Greece, 2019.

[461] M. Elsener, R.J.G. Nuguid, O. Kröcher, D. Ferri, HCN production from formaldehyde during the selective catalytic reduction of NO_x with NH_3 over V_2O_5/WO_3-TiO_2, Appl. Catal. B 281 (2021) 119462, https://doi.org/10.1016/J.Apcatb.2020.119462.

[462] A.A. Schönberger Alvarez, C. Özyalcin, T. Padeken, P. Mauermann, B. Lehrheuer, S. Sterlepper, A. Abouserie, M. Vennewald, U. Simon, R. Palkovits, S. Pischinger, Impact of unintentionally formed CH_2O in oxygenated fuel exhausts on DeNO$_x$-SCR at different NO_2/NO_x ratios under close to real conditions, Catal. Sci. Technol. 13 (2023) 4069–4081, https://doi.org/10.1039/D2CY01935C.

[463] A.B. Ngo, T.H. Vuong, H. Atia, U. Bentrup, V.A. Kondratenko, E.V. Kondratenko, J. Rabeah, U. Ambruster, A. Brückner, Effect of Formaldehyde in Selective Catalytic Reduction of NO_x by Ammonia (NH_3-SCR) on a Commercial V_2O_5-WO_3/TiO_2 Catalyst under Model Conditions, Environ. Sci. Technol. 54 (2020) 11753–11761, https://doi.org/10.1021/acs.est.0c00884.

[464] F.P. Simeonova, L. Fishbein, Hydrogen cyanide and cyanides: human health aspects, World Health Organization, Genava, 2004.

[465] G.R. Maxwell, V.H. Edwards, M. Robertson, K. Shah, Assuring process safety in the transfer of hydrogen cyanide manufacturing technology, J. Hazard. Mater. 142 (2007) 677–684, https://doi.org/10.1016/j.jhazmat.2006.06.071.

[466] R.J.G. Nuguid, M. Elsener, D. Ferri, O. Kröcher, Operando diffuse reflectance infrared detection of cyanide intermediate species during the reaction of formaldehyde with ammonia over V_2O_5/WO_3-TiO_2, Appl. Catal. B 298 (2021), 120629, https://doi.org/10.1016/j.apcatb.2021.120629.

[467] J. Li, R. Zhu, Y. Cheng, C.K. Lambert, R.T. Yang, Mechanism of Propene Poisoning on Fe-ZSM-5 for Selective Catalytic Reduction of NO_x with Ammonia, Environ. Sci. Technol. 44 (2010) 1799–1805, https://doi.org/10.1021/es903576d.

[468] L. Chmielarz, M. Jabłońska, Advances in selective catalytic oxidation of ammonia to dinitrogen: a review, RSC Adv. 5 (2015) 43408–43431, https://doi.org/10.1039/C5RA03218K.

[469] T. Lan, Y. Zhao, J. Deng, J. Zhang, L. Shi, D. Zhang, Selective catalytic oxidation of NH_3 over noble metal-based catalysts: state of the art and future prospects, Catal. Sci. Technol. 10 (2020) 5792–5810, https://doi.org/10.1039/D0CY01137A.

[470] T. Maunula, M. Tuikka, T. Wolff, The Reactions and Role of Ammonia Slip Catalysts in Modern Urea-SCR Systems, Emiss. Control Sci. Technol. 6 (2020) 390–401, https://doi.org/10.1007/s40825-020-00171-1.

[471] F. Gao, Y. Liu, Z. Sani, X. Tang, H. Yi, S. Zhao, Q. Yu, Y. Zhou, Advances in selective catalytic oxidation of ammonia (NH_3–SCO) to dinitrogen in excess oxygen: A review on typical catalysts, catalytic performances and reaction mechanisms, J. Environ. Chem. Eng. 9 (2021), 104575, https://doi.org/10.1016/j.jece.2020.104575.

[472] H.B. Zhao, R.G. Tonkyn, S.E. Barlow, B.E. Koel, C.H.F. Peden, Catalytic oxidation of HCN over a 0.5% Pt/Al_2O_3 catalyst, Appl. Catal. B 65 (2006) 282–290, https://doi.org/10.1016/j.apcatb.2006.02.009.

[473] O. Kröcher, M. Elsener, Hydrolysis and oxidation of gaseous HCN over heterogeneous catalysts, Appl. Catal. B 92 (2009) 75–89, https://doi.org/10.1016/j.apcatb.2009.07.021.

[474] N. Liu, X.N. Yuan, B.H. Chen, Y.X. Li, R.D. Zhang, Selective catalytic combustion of hydrogen cyanide over metal modified zeolite catalysts: From experiment to theory, Catal. Today 297 (2017) 201–210, https://doi.org/10.1016/j.cattod.2017.03.038.

[475] J. Li, Y. Peng, H. Chang, X. Li, J.C. Crittenden, J. Hao, Chemical poison and regeneration of SCR catalysts for NO_x removal from stationary sources, Front. Environ. Sci. Eng. 10 (2016) 413–427, https://doi.org/10.1007/s11783-016-0832-3.

[476] L. Lisi, S. Cimino, Poisoning of SCR Catalysts by Alkali and Alkaline Earth Metals, Catalysts 10 (2020) 1475, https://doi.org/10.3390/catal10121475.

[477] A. Szymaszek, B. Samojeden, M. Motak, The Deactivation of Industrial SCR Catalysts—A Short Review, Energies 13 (2020) 3870, https://doi.org/10.3390/en13153870.

[478] X. Wang, Y. Xu, Z. Zhao, J. Liao, C. Chen, Q. Li, Recent progress of metal-exchanged zeolites for selective catalytic reduction of NO_x with NH_3 in diesel exhaust, Fuel 305 (2021), 121482, https://doi.org/10.1016/j.fuel.2021.121482.

[479] S. Zhao, J. Peng, R. Ge, K. Yang, S. Wu, Y. Qian, T. Xu, J. Gao, Y. Chen, Z. Sun, Poisoning and regeneration of commercial V_2O_5-WO_3/TiO_2 selective catalytic reduction (SCR) catalyst in coal-fired power plants, Process Saf. Environ. Prot. 168 (2022) 971–992, https://doi.org/10.1016/j.psep.2022.10.066.

[480] Z. Shi, Q. Peng, J. E, B. Xie, J. Wei, R. Yin, G. Fu, Mechanism, performance and modification methods for NH_3-SCR catalysts: A review, Fuel 331 (2023), 125885, https://doi.org/10.1016/j.fuel.2022.125885.

[481] P.S. Hammershøi, Y. Jangjou, W.S. Epling, A.D. Jensen, T.V.W. Janssens, Reversible and irreversible deactivation of Cu-CHA NH_3-SCR catalysts by SO_2 and SO_3, Appl. Catal. B 226 (2018) 38–45, https://doi.org/10.1016/j.apcatb.2017.12.018.

[482] Y. Jangjou, D. Wang, A. Kumar, J. Li, W.S. Epling, SO_2 Poisoning of the NH_3-SCR Reaction over Cu-SAPO-34: Effect of Ammonium Sulfate versus Other S-Containing Species, ACS Catal. 6 (2016) 6612–6622, https://doi.org/10.1021/acscatal.6b01656.

[483] L. Zhang, D. Wang, Y. Liu, K. Kamasamudram, J. Li, W. Epling, SO_2 poisoning impact on the NH_3-SCR reaction over a commercial Cu-SAPO-34 SCR catalyst, Appl. Catal. B 156–157 (2014) 371–377, https://doi.org/10.1016/j.apcatb.2014.03.030.

[484] K. Guo, J. Ji, W. Song, J. Sun, C. Tang, L. Dong, Conquering ammonium bisulfate poison over low-temperature NH_3-SCR catalysts: A critical review, Appl. Catal. B 297 (2021), 120388, https://doi.org/10.1016/j.apcatb.2021.120388.

[485] A. Kumar, K. Kamasamudram, N. Currier, A. Yezerets, Effect of Transition Metal Ion Properties on the Catalytic Functions and Sulfation Behavior of Zeolite-Based

SCR Catalysts, SAE Int. J. Engines 10 (2017) 1604–1612, https://doi.org/10.4271/2017-01-0939.
[486] J.W. Girard, C. Montreuil, J. Kim, G. Cavataio, C. Lambert, Technical Advantages of Vanadium SCR Systems for Diesel NOx Control in Emerging Markets, SAE Int. J. Fuels Lubr. 1 (2008) 488–494, https://doi.org/10.4271/2008-01-1029.
[487] Y. Xi, N.A. Ottinger, Z.G. Liu, New insights into sulfur poisoning on a vanadia SCR catalyst under simulated diesel engine operating conditions, Appl. Catal. B 160–161 (2014) 1–9, https://doi.org/10.1016/j.apcatb.2014.04.037.
[488] P.S. Hammershøi, A.D. Jensen, T.V.W. Janssens, Impact of SO_2-poisoning over the lifetime of a Cu-CHA catalyst for NH_3-SCR, Appl. Catal. B 238 (2018) 104–110, https://doi.org/10.1016/j.apcatb.2018.06.039.
[489] A. Kumar, M.A. Smith, K. Kamasamudram, N.W. Currier, A. Yezerets, Chemical deSOx: An effective way to recover Cu-zeolite SCR catalysts from sulfur poisoning, Catal. Today 267 (2016) 10–16, https://doi.org/10.1016/j.cattod.2016.01.033.
[490] S. Dahlin, J. Englund, H. Malm, M. Feigel, B. Westerberg, F. Regali, M. Skoglundh, L.J. Pettersson, Effect of biofuel- and lube oil-originated sulfur and phosphorus on the performance of Cu-SSZ-13 and V_2O_5-WO_3/TiO_2 SCR catalysts, Catal. Today 360 (2021) 326–339, https://doi.org/10.1016/j.cattod.2020.02.018.
[491] K. Xie, K. Leistner, K. Wijayanti, A. Kumar, K. Kamasamudram, L. Olsson, Influence of phosphorus on Cu-SSZ-13 for selective catalytic reduction of NO_x by ammonia, Catal. Today 297 (2017) 46–52, https://doi.org/10.1016/j.cattod.2017.07.016.
[492] Z. Chen, C. Fan, L. Pang, S. Ming, P. Liu, T. Li, The influence of phosphorus on the catalytic properties, durability, sulfur resistance and kinetics of Cu-SSZ-13 for NO_x reduction by NH_3-SCR, Appl. Catal. B 237 (2018) 116–127, https://doi.org/10.1016/j.apcatb.2018.05.075.
[493] A. Guo, K. Xie, H. Lei, V. Rizzotto, L. Chen, M. Fu, P. Chen, Y. Peng, D. Ye, U. Simon, Inhibition Effect of Phosphorus Poisoning on the Dynamics and Redox of Cu Active Sites in a Cu-SSZ-13 NH_3-SCR Catalyst for NO_x Reduction, Environ. Sci. Technol. 55 (2021) 12619–12629, https://doi.org/10.1021/acs.est.1c03630.
[494] K. Xie, J. Woo, D. Bernin, A. Kumar, K. Kamasamudram, L. Olsson, Insights into hydrothermal aging of phosphorus-poisoned Cu-SSZ-13 for NH_3-SCR, Appl. Catal. B 241 (2019) 205–216, https://doi.org/10.1016/j.apcatb.2018.08.082.
[495] J. Jansson, S. Shwan, M. Skoglundh, Impact of Thermal and Chemical Ageing of Fe-BEA SCR Catalyst on NO_x Conversion Performance, SAE Int. J. Engines 9 (2016) 1305–1313, https://doi.org/10.4271/2016-01-0946.
[496] J. Schobing, V. Tschamber, J.F. Brilhac, A. Auclaire, R. Vonarb, Investigation of the Impact of Calcium, Zinc and Phosphorus on DeNO$_x$ Activity of a Commercial SCR Catalyst, Top. Catal. 59 (2016) 1013–1019, https://doi.org/10.1007/s11244-016-0583-1.
[497] Y. Liu, Z. Liu, B. Mnichowicz, A.V. Harinath, H. Li, B. Bahrami, Chemical deactivation of commercial vanadium SCR catalysts in diesel emission control application, Chem. Eng. J. 287 (2016) 680–690, https://doi.org/10.1016/j.cej.2015.11.043.
[498] Z. Chen, C. Bian, Y. Guo, L. Pang, T. Li, Efficient Strategy to Regenerate Phosphorus-Poisoned Cu-SSZ-13 Catalysts for the NH_3-SCR of NO_x: The Deactivation and Promotion Mechanism of Phosphorus, ACS Catal. 11 (2021) 12963–12976, https://doi.org/10.1021/acscatal.1c03752.
[499] J. Guo, A. Wang, H. Lin, Effect of phosphorus poisoning on the hydrothermal stability of Cu/CHA and Cu/LTA towards NH_3-SCR, Microporous Mesoporous Mater. 346 (2022), 112313, https://doi.org/10.1016/j.micromeso.2022.112313.
[500] P. Wu, X. Tang, Z. He, Y. Liu, Z. Wang, Alkali metal poisoning and regeneration of selective catalytic reduction denitration catalysts: recent advances and future perspectives, Energy Fuels 36 (2022) 5622–5646, https://doi.org/10.1021/acs.energyfuels.2c01036.
[501] F. Gao, Y. Wang, N.M. Washton, M. Kollár, J. Szanyi, C.H.F. Peden, Effects of Alkali and Alkaline Earth Cocations on the Activity and Hydrothermal Stability of Cu/SSZ-13 NH_3–SCR Catalysts, ACS Catal. 5 (2015) 6780–6791, https://doi.org/10.1021/acscatal.5b01621.
[502] Y. Cui, Y. Wang, E.D. Walter, J. Szanyi, Y. Wang, F. Gao, Influences of Na^+ co-cation on the structure and performance of Cu/SSZ-13 selective catalytic reduction catalysts, Catal. Today 339 (2020) 233–240, https://doi.org/10.1016/j.cattod.2019.02.037.
[503] L. Xie, F. Liu, X. Shi, F.-S. Xiao, H. He, Effects of post-treatment method and Na co-cation on the hydrothermal stability of Cu–SSZ-13 catalyst for the selective catalytic reduction of NO_x with NH_3, Appl. Catal. B 179 (2015) 206–212, https://doi.org/10.1016/j.apcatb.2015.05.032.
[504] C. Fan, Z. Chen, L. Pang, S. Ming, C. Dong, K. Brou Albert, P. Liu, J. Wang, D. Zhu, H. Chen, T. Li, Steam and alkali resistant Cu-SSZ-13 catalyst for the selective catalytic reduction of NO_x in diesel exhaust, Chem. Eng. J. 334 (2018) 344–354, https://doi.org/10.1016/j.cej.2017.09.181.
[505] C. Wang, W. Yan, Z. Wang, Z. Chen, J. Wang, J. Wang, J. Wang, M. Shen, X. Kang, The role of alkali metal ions on hydrothermal stability of Cu/SSZ-13 NH3-SCR catalysts, Catal. Today 355 (2020) 482–492, https://doi.org/10.1016/j.cattod.2019.06.074.
[506] S. Shwan, J. Jansson, L. Olsson, M. Skoglundh, Chemical deactivation of H-BEA and Fe-BEA as NH_3-SCR catalysts—effect of potassium, Appl. Catal. B 166–167 (2015) 277–286, https://doi.org/10.1016/j.apcatb.2014.11.042.
[507] P. Kern, M. Klimczak, T. Heinzelmann, M. Lucas, P. Claus, High-throughput study of the effects of inorganic additives and poisons on NH_3-SCR catalysts. Part II: Fe–zeolite catalysts, Appl. Catal. B 95 (2010) 48–56, https://doi.org/10.1016/j.apcatb.2009.12.008.
[508] H. Siaka, C. Dujardin, A. Moissette, P. Granger, Structural Induced Effect of Potassium on the Reactivity of Vanadate Species in V_2O_5–WO_3/TiO_2 SCR-Catalyst, Top. Catal. 62 (2019) 56–62, https://doi.org/10.1007/s11244-018-1103-2.
[509] Y. Tian, J. Yang, C. Yang, F. Lin, G. Hu, M. Kong, Q. Liu, Comparative study of the poisoning effect of NaCl and Na_2O on selective catalytic reduction of NO with NH_3 over V_2O_5-WO_3/TiO_2 catalyst, J. Energy Inst. 92 (2019) 1045–1052, https://doi.org/10.1016/j.joei.2018.07.002.
[510] X. Xie, J. Lu, E. Hums, Q. Huang, Z. Lu, Study on the Deactivation of V_2O_5–WO_3/TiO_2 Selective Catalytic Reduction Catalysts through Transient Kinetics, Energy Fuels 29 (2015) 3890–3896, https://doi.org/10.1021/acs.energyfuels.5b01034.
[511] J. Cao, X. Yao, L. Chen, K. Kang, M. Fu, Y. Chen, Effects of different introduction methods of Ce^{4+} and Zr^{4+} on denitration performance and anti-K poisoning performance of V_2O_5-WO_3/TiO_2 catalyst, J. Rare Earths 38 (2020) 1207–1214, https://doi.org/10.1016/j.jre.2019.11.005.
[512] P. Wang, L. Yan, Y. Gu, S. Kuboon, H. Li, T. Yan, L. Shi, D. Zhang, Poisoning-Resistant NO_x Reduction in the Presence of Alkaline and Heavy Metals over H-SAPO-34-Supported Ce-Promoted Cu-Based Catalysts, Environ. Sci. Technol. 54 (2020) 6396–6405, https://doi.org/10.1021/acs.est.0c00100.
[513] J. Liu, J. Liu, Z. Zhao, Z. Duan, Y. Wei, W. Song, Y. Sun, Fe/Beta@Meso-CeO_2 Nanostructure Core–Shell Catalyst: Remarkable Enhancement of Potassium Poisoning Resistance, Catal. Surv. Asia 22 (2018) 181–194, https://doi.org/10.1007/s10563-018-9251-8.
[514] F. Gao, X. Tang, H. Yi, S. Zhao, T. Zhang, D. Li, D. Ma, The poisoning and regeneration effect of alkali metals deposed over commercial V_2O_5-WO_3/TiO_2 catalysts on SCR of NO by NH_3, Chin. Sci. Bull. 59 (2014) 3966–3972, https://doi.org/10.1007/s11434-014-0496-y.
[515] Y. Peng, J. Li, W. Si, J. Luo, Y. Wang, J. Fu, X. Li, J. Crittenden, J. Hao, Deactivation and regeneration of a commercial SCR catalyst: Comparison with alkali metals and arsenic, Appl. Catal. B 168–169 (2015) 195–202, https://doi.org/10.1016/j.apcatb.2014.12.005.
[516] J. Li, P. Zhang, L. Chen, Y. Zhang, L. Qi, Regeneration of Selective Catalyst Reduction Catalysts Deactivated by Pb, As, and Alkali Metals, ACS Omega 5 (2020) 13886–13893, https://doi.org/10.1021/acsomega.0c01283.
[517] Y. Peng, J. Li, W. Shi, J. Xu, J. Hao, Design Strategies for Development of SCR Catalyst: Improvement of Alkali Poisoning Resistance and Novel Regeneration Method, Environ. Sci. Technol. 46 (2012) 12623–12629, https://doi.org/10.1021/es302857a.
[518] V. Joergl, P. Keller, O. Weber, K. Mueller-Haas, R. Konieczny, Influence of Pre Turbo Catalyst Design on Diesel Engine Performance, Emissions and Fuel Economy, SAE Int. J. Fuels Lubr. 1 (2009) 82–95, https://doi.org/10.4271/2008-01-0071.
[519] O. Kröcher, M. Elsener, M.-R. Bothien, W. Dölling, Pre-Turbo SCR - Influence of Pressure on NO_x Reduction, MTZ Worldw. 75 (2014) 46–51, https://doi.org/10.1007/s38313-014-0140-x.
[520] C.R. Florén, M. Van den Bossche, D. Creaser, H. Grönbeck, P.A. Carlsson, H. Korpi, M. Skoglundh, Modelling complete methane oxidation over palladium oxide in a porous catalyst using first-principles surface kinetics, Catal. Sci. Technol. 8 (2018) 508–520, https://doi.org/10.1039/c7cy02135f.
[521] C.R. Florén, P.A. Carlsson, D. Creaser, H. Grönbeck, M. Skoglundh, Multiscale reactor modelling of total pressure effects on complete methane oxidation over Pd/Al_2O_3, Catal. Sci. Technol. 9 (2019) 3055–3065, https://doi.org/10.1039/c8cy02461h.
[522] C.R. Florén, C. Demirci, P.A. Carlsson, D. Creaser, M. Skoglundh, Total oxidation of methane over Pd/Al_2O_3 at pressures from 1 to 10 atm, Catal. Sci. Technol. 10 (2020) 5480–5486, https://doi.org/10.1039/d0cy00813c.
[523] T. Rammelt, B. Torkashvand, C. Hauck, J. Böhm, R. Gläser, O. Deutschmann, Nitric Oxide Reduction of Heavy-Duty Diesel Off-Gas by NH_3-SCR in Front of the Turbocharger, Emiss. Control Sci. Technol. 3 (2017) 275–288, https://doi.org/10.1007/s40825-017-0078-y.
[524] J.H. Bromly, F.J. Barnes, S. Muris, X. You, B.S. Haynes, Kinetic and thermodynamic sensitivity analysis of the NO-sensitised oxidation of methane, Combust. Sci. Technol. 115 (1996) 259–296, https://doi.org/10.1080/00102209608935532.
[525] K. Otsuka, R. Takahashi, K. Amakawa, I. Yamanaka, Partial oxidation of light alkanes by NO_x in the gas phase, Catal. Today 45 (1998) 23–28, https://doi.org/10.1016/S0920-5861(98)00233-8.
[526] W.T. Chan, S.M. Heck, H.O. Pritchard, Reaction of nitrogen dioxide with hydrocarbons and its influence on spontaneous ignition. A computational study, Phys. Chem. Chem. Phys. 3 (2001) 56–62, https://doi.org/10.1039/B006088g.
[527] A.A. Konnov, J.N. Zhu, J.H. Bromly, D.K. Zhang, The effect of NO and NO2 on the partial oxidation of methane: experiments and modeling, Proc. Combust. Inst., 30 (2005) 1093–1100. https://doi.org/10.1016/j.proci.2004.07.012.
[528] J.M. Zalc, W.H. Green, E. Iglesia, NO_x-mediated homogeneous pathways for the synthesis of formaldehyde from CH_4-O_2 mixtures, Ind. Eng. Chem. Res. 45 (2006) 2677–2688, https://doi.org/10.1021/ie050885t.
[529] C.L. Rasmussen, A.E. Rasmussen, P. Glarborg, Sensitizing effects of NO_x on CH_4 oxidation at high pressure, Combust. Flame 154 (2008) 529–545, https://doi.org/10.1016/j.combustflame.2008.01.012.
[530] Y.L. Chan, F.J. Barnes, J.H. Bromly, A.A. Konnov, D.K. Zhang, The differentiated effect of NO and NO_2 in promoting methane oxidation, Proc. Combust. Inst. 33 (2011) 441–447, https://doi.org/10.1016/j.proci.2010.05.029.
[531] S. Gersen, A.V. Mokhov, J.H. Darmeveil, H.B. Levinsky, P. Glarborg, Ignition-promoting effect of NO_2 on methane, ethane and methane/ethane mixtures in a rapid compression machine, Proc. Combust. Inst. 33 (2011) 433–440, https://doi.org/10.1016/j.proci.2010.05.097.
[532] A.B. Abai, D. Zengel, C. Janzer, L. Maier, J.-D. Grunwaldt, M. Olzmann, O. Deutschmann, Effect of NO_2 on Gas-Phase Reactions in Lean NO_x/NH_3/O_2/H_2O

Mixtures at Conditions Relevant for Exhaust Gas Aftertreatment, SAE Technical Paper 2021–01-5005, (2021). https://doi.org/10.4271/2021–01-5005.
[533] S. Gossler, L. Ruwe, W.H. Yuan, J.Z. Yang, X.M. Chen, S. Schmitt, L. Maier, K. Kohse-Höinghaus, F. Qi, O. Deutschmann, Exploring the interaction kinetics of butene isomers and NO_x at low temperatures and diluted conditions, Combust. Flame 233 (2021) 111557, https://doi.org/10.1016/j.combustflame.2021.111557.
[534] S. Schmitt, S. Schwarz, L. Ruwe, J. Horstmann, F. Sabath, L. Maier, O. Deutschmann, K. Kohse-Höinghaus, Homogeneous conversion of NO_x and NH_3 with CH_4, CO, and C_2H_4 at the diluted conditions of exhaust-gases of lean operated natural gas engines, Int. J. Chem. Kinet. 53 (2021) 213–229, https://doi.org/10.1002/kin.21435.
[535] W.H. Yuan, L. Ruwe, S. Schwarz, C.C. Cao, J.Z. Yang, O. Deutschmann, K. Kohse-Höinghaus, F. Qi, Insights into the interaction kinetics between propene and NO_x at moderate temperatures with experimental and modeling methods, Proc. Combust. Inst. 38 (2021) 795–803, https://doi.org/10.1016/j.proci.2020.07.041.
[536] B. Torkashvand, P. Lott, D. Zengel, L. Maier, M. Hettel, J.-D. Grunwaldt, O. Deutschmann, Homogeneous oxidation of light alkanes in the exhaust of turbocharged lean-burn gas engines, Chem. Eng. J. 377 (2019), 119800, https://doi.org/10.1016/j.cej.2018.08.186.
[537] J. Smith, J. Phillips, A. Graham, R. Steele, A. Redondo, J. Coons, Homogeneous chemistry in lean-burn exhaust mixtures, J. Phys. Chem. A 101 (1997) 9157–9162, https://doi.org/10.1021/Jp9716647.
[538] E.J. Houdry Catalytic structure and composition, Patent No 1956 US2742437A, USA .
[539] N.G. González, Condensation in Exhaust Gas Coolers, in: C. Junior, D. Jänsch, O. Dingel (Eds.), Energy and Thermal Management, Air Conditioning, Waste Heat Recovery, Springer International Publishing, Cham, 2017, pp. 97–105.
[540] N. Garrido Gonzalez, R. Baar, J. Drueckhammer, C. Kaeppner, The Thermodynamics of Exhaust Gas Condensation, SAE Int. J. Engines 10 (2017) 1411–1421, https://doi.org/10.4271/2017-01-9281.
[541] J.-D. Grunwaldt, J.B. Wagner, R.E. Dunin-Borkowski, Imaging Catalysts at Work: A Hierarchical Approach from the Macro- to the Meso- and Nano-scale, ChemCatChem 5 (2013) 62–80, https://doi.org/10.1002/cctc.201200356.
[542] J. Becher, D.F. Sanchez, D.E. Doronkin, D. Zengel, D.M. Meira, S. Pascarelli, J.-D. Grunwaldt, T.L. Sheppard, Chemical gradients in automotive Cu-SSZ-13 catalysts for NO_x removal revealed by operando X-ray spectrotomography, Nat. Catal. 4 (2021) 46–53, https://doi.org/10.1038/s41929-020-00552-3.
[543] J. Becher, T. Sheppard, J.-D. Grunwaldt, X-Ray Microscopy and Tomography, in: I.E. Wachs, M.A. Bañares (Eds.), Springer Handbook of Advanced Catalyst Characterization, Springer International Publishing, Cham, 2023, pp. 689–738.
[544] R. Chacko, K. Keller, S. Tischer, A.B. Shirsath, P. Lott, S. Angeli, O. Deutschmann, Automating the optimization of catalytic reaction mechanism parameters using Basin-Hopping: A proof of concept, J. Phys. Chem. C 127 (2023) 7628–7639, https://doi.org/10.1021/acs.jpcc.2c08179.
[545] B. Kreitz, P. Lott, J. Bae, K. Blöndal, S. Angeli, Z.W. Ulissi, F. Studt, C. F. Goldsmith, O. Deutschmann, Detailed microkinetics for the oxidation of exhaust gas emissions through automated mechanism generation, ACS Catal. 12 (2022) 11137–11151, https://doi.org/10.1021/acscatal.2c03378.
[546] B. Kreitz, P. Lott, F. Studt, A.J. Medford, O. Deutschmann, C.F. Goldsmith, Automated generation of microkinetics for heterogeneously catalyzed reactions considering correlated uncertainties, Angew. Chem., Int. Ed. (2023), e202306514, https://doi.org/10.1002/anie.202306514.
[547] H. Gossler, L. Maier, S. Angeli, S. Tischer, O. Deutschmann, CaRMeN: a tool for analysing and deriving kinetics in the real world, Phys. Chem. Chem. Phys. 20 (2018) 10857–10876, https://doi.org/10.1039/c7cp07777g.
[548] H. Gossler, L. Maier, S. Angeli, S. Tischer, O. Deutschmann, CaRMeN: An improved computer-aided method for developing catalytic reaction mechanisms, Catalysts (2019).
[549] C. Wulf, M. Beller, T. Boenisch, O. Deutschmann, S. Hanf, N. Kockmann, R. Kraehnert, M. Oezaslan, S. Palkovits, S. Schimmler, S.A. Schunk, K. Wagemann, D. Linke, A unified research data infrastructure for catalysis research - challenges and concepts, ChemCatChem 13 (2021) 3223–3236, https://doi.org/10.1002/cctc.202001974.
[550] R.X. Yang, C.A. McCandler, O. Andriuc, M. Siron, R. Woods-Robinson, M. K. Horton, K.A. Persson, Big data in a nano world: a review on computational, data-driven design of nanomaterials structures, properties, and synthesis, ACS Nano 16 (2022) 19873–19891, https://doi.org/10.1021/acsnano.2c08411.
[551] L. Grajciar, C.J. Heard, A.A. Bondarenko, M.V. Polynski, J. Meeprasert, E. A. Pidko, P. Nachtigall, Towards operando computational modeling in heterogeneous catalysis, Chem. Soc. Rev. 47 (2018) 8307–8348, https://doi.org/10.1039/c8cs00398j.
[552] S. Matera, W.F. Schneider, A. Heyden, A. Savara, Progress in accurate chemical kinetic modeling, simulations, and parameter estimation for heterogeneous catalysis, ACS Catal. 9 (2019) 6624–6647, https://doi.org/10.1021/acscatal.9b01234.
[553] G.D. Wehinger, M. Ambrosetti, R. Cheula, Z.-B. Ding, M. Isoz, B. Kreitz, K. Kuhlmann, M. Kutscherauer, K. Niyogi, J. Poissonnier, R. Réocreux, D. Rudolf, J. Wagner, R. Zimmermann, M. Bracconi, H. Freund, U. Krewer, M. Maestri, Quo vadis multiscale modeling in reaction engineering? - A perspective, Chem. Eng. Res. Des. 184 (2022) 39–58, https://doi.org/10.1016/j.cherd.2022.05.030.